



BRNO UNIVERSITY OF TECHNOLOGY

VYSOKÉ UČENÍ TECHNICKÉ V BRNĚ

FACULTY OF MECHANICAL ENGINEERING

FAKULTA STROJNÍHO INŽENÝRSTVÍ

INSTITUTE OF PROCESS ENGINEERING

ÚSTAV PROCESNÍHO INŽENÝRSTVÍ

DESIGN OF AN AUTONOMOUS DESALINATION UNIT

NÁVRH AUTONOMNÍ ODSOLOVACÍ JEDNOTKY

MASTER'S THESIS

DIPLOMOVÁ PRÁCE

AUTHOR

AUTOR PRÁCE

Bc. Michael Kijanica

SUPERVISOR

VEDOUCÍ PRÁCE

M.Phil. Yee Van Fan, Ph.D.

BRNO 2023

Assignment Master's Thesis

Institut: Institute of Process Engineering
Student: **Bc. Michael Kijanica**
Degree programm: Process Engineering
Branch: no specialisation
Supervisor: **M.Phil. Yee Van Fan, Ph.D.**
Academic year: 2022/23

As provided for by the Act No. 111/98 Coll. on higher education institutions and the BUT Study and Examination Regulations, the director of the Institute hereby assigns the following topic of Master's Thesis:

Design of an autonomous desalination unit

Brief Description:

Water is one of the most important resources on the planet. According to the UN, its scarcity already affects more than 40 % of the world's population. Desalination is one of the promising sources of drinking or technological water for many dry coastal areas. Approximately 16,000 operational desalination plants are located across 177 countries, generating an estimated 95 million m³/day of freshwater. The mineral salts dissolved in seawater can be removed using thermal and membrane technologies. Both of these technologies have their specifics and energy requirements. With the growing demand for smaller distributed sources, there is a growing interest in smaller units that can supply small and medium-sized companies or even households with fresh water. It would be a great advantage for remote locations if the units were adapted for autonomous island operation and portable. Energy intensive is one of the main drawbacks of desalination. It is essential to assess the energy efficiency and environmental impact of the proposed desalination system or unit to understand its sustainability from a different perspective beyond the technical feasibility and economic aspects.

Master's Thesis goals:

- Introduction of the current state of the art and trends in the field of water desalination
- Basic design of a small autonomous solar-powered desalination unit
- Environmental impact assessment of the production and operation of this unit

Recommended bibliography:

ZHENG, Hongfei. Solar Energy Desalination Technology. Amsterdam: Elsevier, [2017]. ISBN 978-0-12-805411-6.

JONES, Edward, Manzoor QADIR, Michelle T.H. VAN VLIET, Vladimir SMAKHTIN a Seong-mu KANG. The state of desalination and brine production: A global outlook. Science of The Total Environment [online]. 2019, 657, 1343-1356 [cit. 2022-10-18]. ISSN 00489697. Dostupné z: doi:10.1016/j.scitotenv.2018.12.076

ALHAJ, Mohamed, Furqan TAHIR a Sami G. AL-GHAMDI. Life-cycle environmental assessment of solar-driven Multi-Effect Desalination (MED) plant. Desalination [online]. 2022, 524 [cit. 2022-10-19]. ISSN 00119164. Dostupné z: doi:10.1016/j.desal.2021.115451

Deadline for submission Master's Thesis is given by the Schedule of the Academic year 2022/23

In Brno,

L. S.

prof. Ing. Petr Stehlík, CSc., dr. h. c.
Director of the Institute

doc. Ing. Jiří Hlinka, Ph.D.
FME dean

Abstract

Water scarcity has evolved into a global issue beyond the concern of deserts and arid areas. Seawater desalination gained prominence as a means of producing drinking water in coastal areas facing long-term water scarcity. However, desalination is known for its technical complexity, energy intensive and incurring economic cost. The operation of desalination plants raised concerns about their environmental impact, particularly regarding energy consumption and the generation of high concentration brine waste. This master's thesis focuses on designing an autonomous desalination unit that operates using solar energy with the economic feasibility and environmental impact assessment being evaluated. Two desalination units (Variant A: reverse osmosis, Variant B: Mechanical vapor compression) and their photovoltaic systems were designed based on insights from a thorough literature review. The reverse osmosis unit was selected for environmental evaluation based on technical and economic parameters – specifically because of lower energy intensity and lower investment cost. The designed Variant A has a daily production capacity of 22.1 m³ with a specific electricity consumption is 5.6 kWh/m³, which is comparable to units of similar capacity. The photovoltaic system has an electrical output of 209 kW_p and consists of 36 panels covering a surface area of 95 m². The investment cost for this reverse osmosis system amount to \$146,550 with a calculated payback period of 5.6 years compared to Variant B, which has a payback period of 18.8 years. Out of the 11 assessed environmental impacts, the global warming potential impact of Variant A is identified as 335 kgCO₂eq/1000m³, with 42 % contributed by material manufacturing and 58 % contributed by energy consumption. The environmental performance of solar-powered reverse osmosis desalination unit was assessed in comparison to the environmental impact of electricity supplied by the European and Czech grid mixes. Further research should focus on investigating the environmental impact of the autonomous desalination unit by expanding the scope to include the end-of-life management and transportation activities. Potential improvement could also be identified by optimizing the photovoltaic system and comparing this unit with emerging desalination technologies that are being researched.

Abstrakt

Nedostatek vody se rozvinul v globální problém, který se již netýká jen pouštních a suchých oblastí. Odsolování mořské vody se rozvinulo jakožto způsob výroby pitné vody v přímořských oblastech, které se zároveň potýkají s dlouhodobým nedostatkem vody. Ale odsolování mořské vody je známé svou technickou komplexností, energetickou náročností a nutnými investičními náklady. Provoz odsolovacích zařízení vzbudil obavy ohledně jejich dopadu na životní prostředí, konkrétně kvůli vysoké spotřebě energie a produkce vysoce koncentrované odpadní solanky. Tato diplomová práce se zaměřuje na návrh malé autonomní odsolovací jednotky, která k provozu využívá solární energii a vyhodnocením její ekonomické proveditelnosti a dopadů na životní prostředí. Dvě odsolovací jednotky (Varianta A: reverzní osmóza, Varianta B: mechanická parní komprese) a jejich fotovoltaické systémy byly navrženy na základě rešerše literatury. Jednotka s reverzní osmózou byla zvolena na základě technických a ekonomických parametrů – konkrétně kvůli nižší spotřebě energie a nižším investičním nákladům. Navržená varianta A má denní kapacitu produkce $22,14 \text{ m}^3$ a jednotkovou spotřebu elektřiny $5,6 \text{ kWh/m}^3$, což je srovnatelné s jinými jednotkami obdobné kapacity. Fotovoltaický systém má výkon 209 kWp a skládá se z 36 panelů, které zaujímají plochu 95 m^2 . Investiční náklady systému s reverzní osmózou činí 146 550 dolarů a prostá doba návratnosti je 5,6 let, oproti variant B, která má prostou dobu návratnosti 18,8 let. Z celkem 11 posuzovaných environmentálních vlivů, potenciál globálního oteplení varianty A byl vyhodnocen na $335 \text{ kg CO}_2\text{eq}/1000 \text{ m}^3$, kde celkem 42 % zaujímal vliv výroby a zpracování materiálů a 58 % zaujímá vliv výroby energie. Environmentální profil této solární odsolovací jednotky s reverzní osmózou byl hodnocen v porovnání s environmentálními vlivy dodávky elektřiny z evropských a českých energetických mixů. Další výzkum by se měl zaměřit na prozkoumání environmentálních vlivů této odsolovací jednotky a zahrnout management zpracování po konci životnosti a transport. Potenciál zlepšení byl shledán v optimalizaci fotovoltaického systému a porovnání této jednotky s nově se rozvíjejícími jednotkami, které jsou momentálně ve fázi výzkumu.

Keywords

desalination, photovoltaic panels, renewable energy, LCA, reverse osmosis

Klíčová slova

odsolování, fotovoltaické panely, obnovitelná energie, LCA, reverzní osmóza

Bibliographic Citation

KIJANICA, Michael. *Design of an autonomous desalination unit*. Brno, 2023. Available also at: <https://www.vut.cz/studenti/zav-prace/detail/149944>. Master's Thesis. Vysoké učení technické v Brně, Fakulta strojního inženýrství, Institute of Process Engineering. Supervisor Yee Van Fan.

Statement of Originality

I certify that this thesis “Basic Design of an Autonomous Desalination Unit” is my own work that I have written with the supervision of M.Phil. Yee Van Fan, Ph.D. Additionally, I certify that all resources and literature used are listed in the list of references.

In Brno 26th May 2023

Bc. Michael Kijanica

Acknowledgments

By this statement I would like to thank my supervisor M.Phil. Yee Van Fan, Ph.D. for her time and valuable advice and insights, which she has given me during the process of writing this thesis. Also, I would like to thank my entire family and friends for their support and patience during my studies.

Contents

1	Introduction	12
1.1	Problem Statement	12
1.2	Objective	12
1.3	Scope of Study	12
2	Water Scarcity	14
2.1	Influencing Factors	14
2.1.1	Geographical Location and Climate	14
2.1.2	Population Density	15
2.1.3	Water-Intensive Agriculture	15
2.2	Potential Solutions	15
2.2.1	Environmental Policy	16
2.2.2	Economic Solutions	16
2.2.3	Engineering Solutions.....	16
3	Desalination of Seawater.....	17
3.1	The Role of Desalination in Solving Water Scarcity.....	17
3.1.1	Overview	17
3.1.2	Challenges and Problems.....	19
3.2	Basic Principles & Classification.....	20
3.3	Evaporation & Condensation Technologies	22
3.3.1	Multi-Effect Distillation	22
3.3.2	Multi-Stage Flash	24
3.3.3	Vapor Compression	27
3.4	Membrane Technologies.....	28
3.4.1	Reverse Osmosis.....	28
3.4.2	Nanofiltration.....	33
3.5	General Trends in Research & Development	34
3.5.1	Renewable Energy Sources	35
3.5.2	Decentralization.....	37
3.5.3	Environmental Impact of Desalination.....	37
4	Methodology	39
4.1	Process Selection	39
4.2	Basic Design Methodology.....	41
4.2.1	Variant A – RO Unit.....	41
4.2.2	Variant B – MVC Unit with NF Pretreatment.....	45
4.3	PV System Design	52
4.3.1	PV Module Selection & Field Sizing	52
4.3.2	Inverter Selection.....	53
4.3.3	Battery Selection.....	54
4.4	Techno-Economic Study.....	54
4.4.1	Capital Costs.....	54
4.4.2	Operating Cost & Revenue Streams.....	56
4.5	Environmental Impact Assessment Methodology	56

5	Results & Discussion	59
5.1	Basic Design Calculations	59
5.1.1	Variant A	59
5.1.2	Variant B.....	61
5.2	Economic Analysis	63
5.2.1	Variant A	63
5.2.2	Variant B.....	64
5.2.3	Cashflow Evaluation & Summary	65
5.3	Basic Design & Economic Analysis Conclusion.....	68
5.4	Environmental Impact Assessment Results	69
6	Conclusions	75
	List of Symbols & Abbreviations.....	77
	List of Figures	78
	List of Appendices	79
	List of References.....	80

1 Introduction

Water scarcity is a growing concern worldwide. It can broadly be understood as the lack of access to adequate quantities of water for human and environmental uses [1]. Simply put, it is a phenomenon when water demand exceeds water supply in a certain area. It is estimated that the freshwater demand per capita per year is approximately 1,500-1,800 m³ on average (including industrial and agricultural water), which is extremely difficult to meet in water-deficient areas – many countries facing difficulty finding potable water or meeting the water quality requirements set by the World Health Organization (WHO) [2]. The water quality requirements set the standards for permissible impurity contents of <500 ppm for drinking purposes, 1-3000 ppm for industrial use, and approximately 3000 ppm for agricultural use [2].

There are several technologies and measures for addressing water scarcity, including water conservation measures, rainwater harvesting, groundwater management, wastewater reusing, desalination and water transfer by moving water from one area to an area that is experiencing water scarcity. Diversification of water sources is one of the effective approaches to dealing with water scarcity. Desalination provides an alternative water source (e.g. seawater) that does not depend on rainfall or surface water availability and reduces reliance on traditional water sources. It is relatively reliable as it can be operated continuously regardless of weather conditions or other external factors, with water free from impurities, minerals, and contaminants being produced, making it suitable for various uses.

1.1 Problem Statement

Several desalination technologies have been proposed and established, however, with different benefits and drawbacks. Desalination is known for its high energy consumption, representing the major drawbacks on top of high costs, brine waste production and the potential impact on marine life. The integration of renewable energy via an autonomous desalination unit could mitigate the environmental impact of this energy-intensive process which contributes to the increase of greenhouse gas emissions.

1.2 Objective

The aim of the study is to assess the current state of the art in the waste desalination field with the goal of proposing a basic design of a small autonomous solar-powered desalination unit, supported by environmental impact assessment to ensure environmental performance.

1.3 Scope of Study

The research scopes of this thesis are as follows:

- I. To investigate the existing desalination technologies, the strength as well as the potential for improvement from the economic, environmental and efficiency perspective, reflected from the current research and development.
- II. To propose a basic design of a small autonomous solar-powered desalination unit, aiming for the features of reducing reliance on traditional energy sources, reducing the environmental impact, increasing resilience or flexibility in terms of location and installation without compromising the desalination efficiency.

- III. To assess the environmental performance of the proposed unit, particularly the greenhouse gas emission, compared to the existing study, by referring to the functional unit of CO₂eq per 1000 m³ water.

2 Water Scarcity

The objective of this chapter is to explain the problematics of water scarcity and related environmental issues.

Water Scarcity can have negative effects on populations, the state of society, ecosystems, industry, and agriculture in concerned areas. High water scarcity usually occurs in areas with high population density, with the presence of much irrigated agriculture, areas with very low natural water availability, and areas with polluted water resources (often it is the combination of these factors) [1]. Mekonnen and Hoekstra [1] investigated the aspects of water scarcity in detail and created a table, which displays the number of people facing low, moderate, significant, and severe water scarcity during a given number of months per year (see *Table 1*).

Table 1 Percentages of people facing different levels of water scarcity – edited from [1]

Number of months per year (<i>n</i>)	Percentage of people facing low, moderate, significant, and severe water scarcity during <i>n</i> months per year [%]			
	Low water scarcity	Moderate water scarcity	Significant water scarcity	Severe water scarcity
0	9.0	82.5	86.4	34.3
1	2.0	13.4	10.9	5.1
2	2.0	3.1	2.2	6.1
3	5.8	0.8	0.5	6.1
4	5.5	0.2	0.0	9.8
5	5.0	0.0	0.0	9.1
6	5.5	0.0	0.0	4.5
7	7.8	0.0	0.0	3.5
8	9.8	0.0	0.0	4.8
9	6.8	0.0	0.0	5.0
10	6.6	0.0	0.0	2.0
11	5.0	0.0	0.0	1.5
12	29.5	0.0	0.0	8.3

They found that 71% of the global population lives under conditions of moderate to severe water scarcity at least 1 month of the year (nearly half of those people live in China and India) and about 66% lives under severe water scarcity at least 1 month of the year [1]. These percentages are likely to increase due to climate change, population growth, land use changes and economic activities.

2.1 Influencing Factors

2.1.1 Geographical Location and Climate

Geographical location has been proven to be one of the factors significantly correlated with water scarcity [1]. As mentioned above, areas suffering from low natural water availability tend to suffer from long-term high water scarcity levels as well. These are the world's arid areas – Sahara, Gobi, Central Australia and Arabian desert [1]. Although water scarcity is a big concern mainly in arid areas, it has started to become a growing issue also in southern European countries which were experiencing more frequent drought periods during the 1990s – mainly

Greece, Spain, Portugal and France [2]. A survey done by the European Union (EU) has indicated that up to 33 river basins are affected by water scarcity – that represents 11 % of the EU territory and 17 % of the EU population [3]. Other countries concerned by water scarcity due to its location or climate are India, China, Pakistan, United States, Mexico etc. [1]. In Libya and Somalia 80% to 90% of the population experiences severe water scarcity year-round. [1]

World map with indicated areas suffering from water scarcity is presented in *Figure 1*.

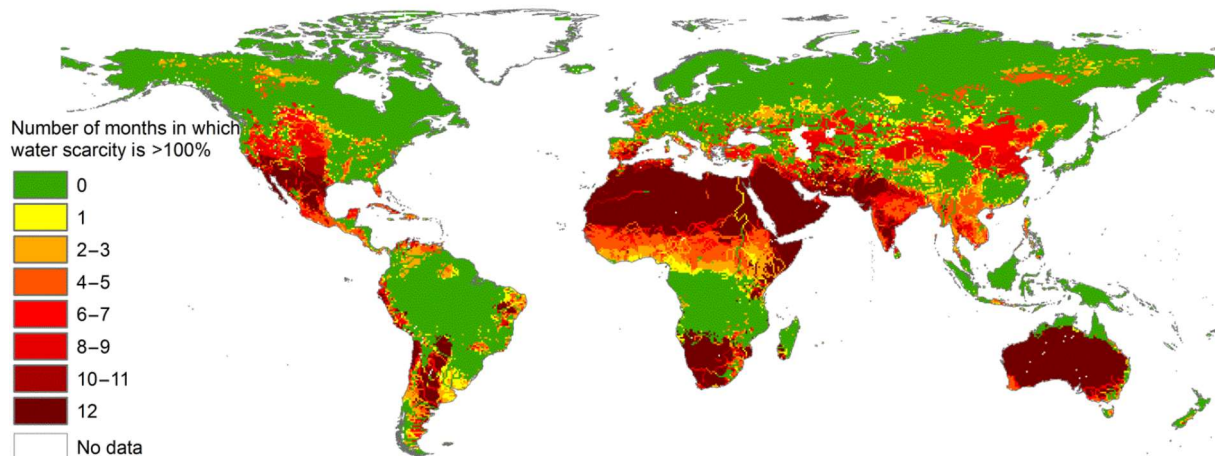


Figure 1 World map of blue water scarcity (Period: 1996-2005) [1]

2.1.2 Population Density

Population density is another factor at play as far as water scarcity is concerned [1]. The key principle is that when a population grows on a limited area (growing water demand), the average volume of water naturally supplied to the area usually stays constant¹. This means that at some point of steadily increasing population density the supply does not meet the demand for water. This phenomenon usually occurs in densely populated areas such as cities (greater London area) [1]. Rising levels of water scarcity have become a trend that goes hand in hand with increased population growth and urbanization. Urban residential and industrial water demand is expected to increase by 50-80% over the next 30 years [4].

2.1.3 Water-Intensive Agriculture

Water scarcity might be an issue in areas with heavily irrigated agriculture. Agriculture consumes 70-86% of the world's available water resources [5], [6]. One of the factors of rising water scarcity in agriculture is unsustainable irrigation utilization which accounts to 52% of total global irrigation [7]. Irrigation-heavy agriculture only exacerbates an existing problem in regions already water scarce due to their climate or location (countries mentioned in *2.1.1 Geographical Location and Climate* such as China, India, Pakistan, Mexico). Crops considered as water intensive are cotton, sugar cane, certain fruits and vegetables [7].

2.2 Potential Solutions

Water scarcity could be mitigated or prevented via different channels, including environmental policy to protect the water resources from being degraded or depleted, economic instruments to reduce the water demand, and engineering solutions to treat or recover the water quality for

¹ Rivers usually do not increase their average inflow, water reservoirs have constant capacity etc.

a certain purpose. The sub-section further discussed the potential solutions from these three aspects.

2.2.1 Environmental Policy

One of possible solutions to prevent water deficits could be governmental (or private) projects focused on restoring natural freshwater ecosystems such as wetlands or forests² [8]. Another measure could be protecting existing important water resources from pollution (for example from agriculture or industry) by imposing stricter regulations. Conservation agriculture practices are one of the approaches to reduce water use in agriculture.

2.2.2 Economic Solutions

Another possibility could be usage of economic instruments to discourage wasteful water management in both residential and commercial sectors. Mekonnen and Hoekstra [1] propose putting caps to water consumption by river basin. Another solution could be increasing the price of freshwater, in other words taxation [8]. Water-saving behavior can be also achieved by subsidizing efficient water use [8]. Some authors believe that decentralization and privatization of water management institutions could have a positive impact on reducing water scarcity by implementing free-market demand principles and improving water allocation [9] [10]. These measures might have significant impacts on societies and economies, therefore thorough analysis must take place before implementing such interventions on a practical level.

2.2.3 Engineering Solutions

Suitable engineering solutions could be beneficial for tackling water scarcity. The list of engineering measures is long and depends on factors specific to the application. One of the most straightforward is infrastructure repair (or building new infrastructure), especially in less-developed countries. Other engineering solutions could be usage of better irrigation technologies in agriculture, diversification of water resources such as reuse of wastewater (or treated water) for non-potable purposes, rainwater harvesting for certain applications and desalination of seawater (or brackish water) in coastal areas [8]. Desalination, on the other hand, is the alternative for a region with traditional water sources are limited.

² Applicable only to certain locations with suitable climate.

3 Desalination of Seawater

3.1 The Role of Desalination in Solving Water Scarcity

3.1.1 Overview

Desalination (or desalting) refers to a water treatment process that removes salts from saltwater or brackish water (seawater is often the raw water source for this process) [11] [12]. The desired product is freshwater which can be utilized as drinking water or other applications. The first type of desalination unit was built by the G. and J. Weir in 1885 in Glasgow (Scotland) [13] and their company practically had a monopoly as a desalination unit builder until the 1940s [12]. A major step in development came during World War II, when military establishments in arid areas needed water to supply their troops [11]. In the late 1950s the first desalination plants were installed – typically thermally driven [14]. The first reverse-osmosis-based desalination plant for a municipality was realized 1977 in the USA³ [12]. Since then, as the cost of energy has progressively increased and properties of membrane materials have developed, membrane-based desalination has become a more popular variant and currently is the most widespread technology for desalination [12]. A timeline showing the development of desalination is shown in *Figure 2*.

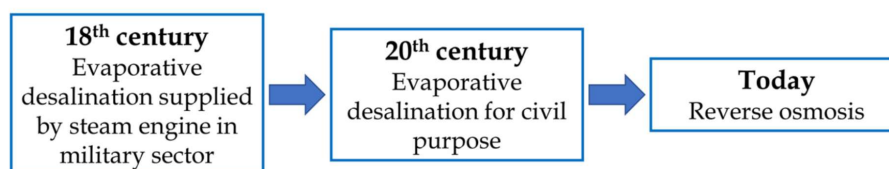


Figure 2 The timeline of desalination technologies [12]

Desalination has grown to be one of the most important water scarcity adaptation and mitigation options, predominantly in the Middle East, North Africa, North and Central America, South East Asia and Australia and has become an essential part of drinking water supply in these regions [15]. The number and capacity of desalination plants by geographic region and sectoral use is displayed in *Table 2*.

Table 2 Global desalination statistics – edited [16]

	Number of desalination plants	Desalination capacity	
		[million m ³ /day]	[%]
Global	15,906	95.37	100
<i>Geographic region</i>			
Middle East and North Africa	4826	45.32	47.5
East Asia and North Africa	3505	17.52	18.4
North America	2341	11.34	11.9
Western Europe	2337	8.75	9.2
Latin America and Caribbean	1373	5.46	5.7
Southern Asia	655	2.94	3.1
Eastern Europe and Central Asia	566	2.26	2.4
Sub-Saharan Africa	303	1.78	1.9
<i>Sector use</i>			
Municipal	6055	59.39	62.3

³ The installed capacity of this desalination plant was 11,350 m³/day [12].

Industrial	7757	28.80	30.2
Power	1096	4.56	4.8
Irrigation	395	1.69	1.8
Military	412	0.59	0.6
Other	191	0.90	0.4

There are approximately 15,906 operational desalination plants globally with a total desalination capacity of approx. 95.37 million m³/day (34.81 billion m³/year) [16]. Customer-type breakdown of global desalination capacity is shown in *Figure 3*⁴. It indicates that approximately 60% of the global capacity is being used in municipalities as drinking water and approx. 30% is being utilized in industrial applications [16] [17]. Map of global distribution of operational desalination facilities and capacities (>1000 m³/day) by sector of produced water is displayed in *Figure 4*.

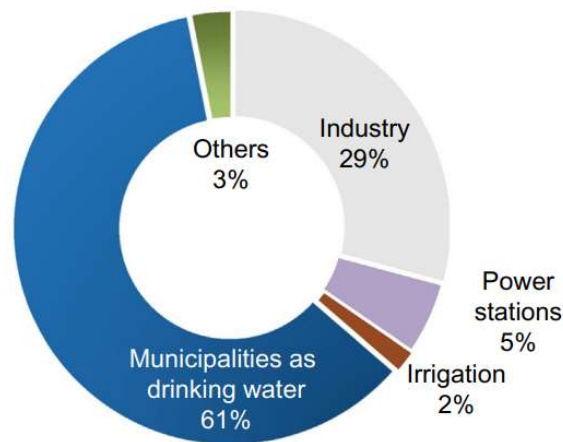


Figure 3 Customer-type breakdown on the basis of global desalination capacity [17]

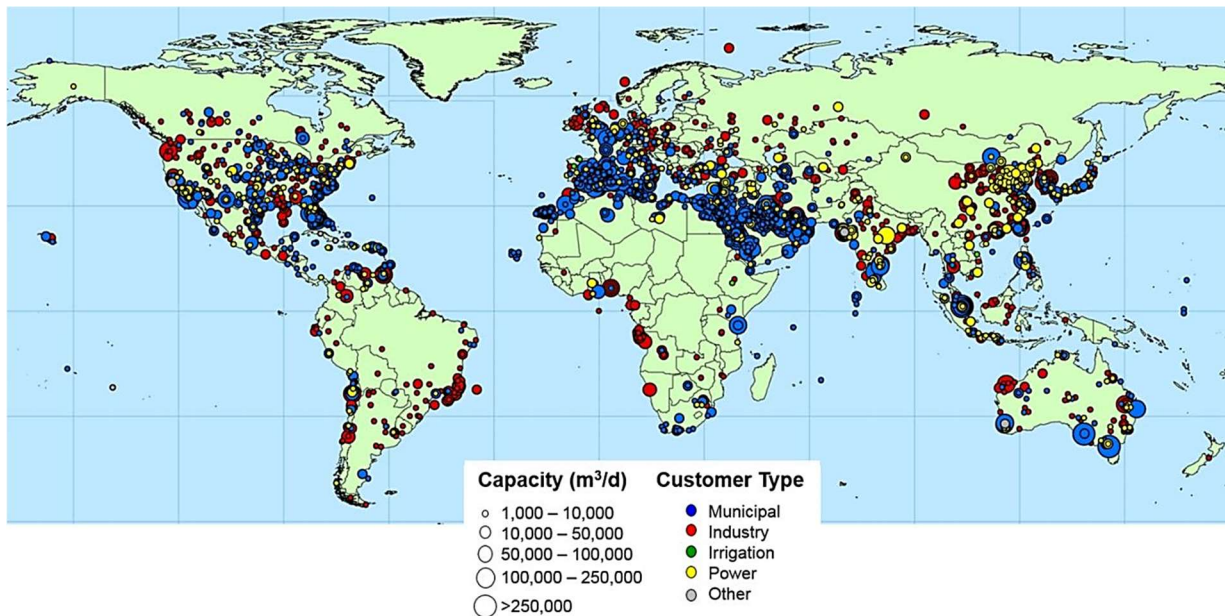


Figure 4 Global distribution of operational desalination plants [16]

With accelerating water stress levels (and awareness of water scarcity) desalination may start playing a more strategic role in national security of water scarce countries. In this context it is often referred to so called water-energy-food security nexus and desalination plays an

⁴ The segment “others” includes plants for military purposes, units used in tourist facilities for drinking water production, discharge, demonstration, process, and water injection [17].

increasingly significant role in finding a sustainable solution to water crisis and possible food insecurities [17]. In order to prevent such crises, it is important to find solutions to problems that make it difficult or problematic to increase desalination capacity. These challenges are described in the next chapter.

3.1.2 Challenges and Problems

Even though the development of new desalination plants has become a growing trend in the last decades [17], there are challenges related to the process itself that must be addressed. These challenges are mostly environmental (energy demand, water intake and brine discharge) and economic (capital and operating costs) [16]. Even though these challenges slow down or complicate developments of new desalination facilities, they could be the driving force behind innovation and research of new more efficient and environmentally friendly desalination methods. The main environmental challenges are briefly described in this chapter.

Increasing Energy Demand

The energy consumption (and efficiency) of desalination is dependent on individual plant, but in general desalination is considered to be an energy-intensive process. Energy demand of desalination is considered to be the most serious problem for developing new desalination facilities [18]. It has been estimated that production of 13×10^6 million m^3/day of desalinated water consumes 130 million tons/year of fuel (oil) [19]. Apart from economic aspects of fossil-fuel-powered desalination, another related aspect to rising energy consumption is the increase of CO_2 emissions, which is why renewable energy desalination (RES) will be an attractive opportunity to tackle all these issues (environmental and economic) at once. Another problem with fossil-fuel powered desalination could be the lack of necessary energy infrastructure, such as electricity, oil or gas, mainly in remote areas.

Water Intake

Studies have reported that by extracting water (for desalination plants) directly from the ocean by open water intakes, marine fauna is inadvertently killed by impingement on intake screens or are killed eventually during saltwater processing [20] [21].

Brine Discharge

Another major environmental challenge is the discharge of brine. Brine is a highly concentrated waste stream (typically almost twice as saline as the intake seawater [17]) which may also contain heavy metals, antifouling substances and other toxic chemicals [17] [20] [21]. Brine released to the ocean tends to sink due to higher density and spread around the bottom of the ocean and affect marine ecosystems [17].

In 2018, the global brine production was 141.5 million m^3/day (51.7 billion m^3/year), which is approx. 50% higher than the total volume of desalinated water produced globally [16].

3.2 Basic Principles & Classification

Currently, desalination can be installed using several technologies, but a desalination plant typically includes [22]:

- Intake – consisting of pumps and pipes to take water from the source,
- Pre-treatment – consisting of the filtration of raw source water to separate solid particles and the addition of chemicals to reduce corrosion inside the unit,
- Desalination – where freshwater is extracted from saltwater,
- Post-treatment – to correct pH levels by adding selected salts.

Desalination technologies (or plants) are generally evaluated (or designed) with respect to these main parameters:

- Total capacity – the total volume of freshwater produced in certain time [m^3/day , m^3/year]. Based on this parameter, desalination plants can be divided into large-scale, mid-scale, and small-scale facilities.
- Recovery ratio – the ratio of the amount of freshwater produced relative to the amount of seawater taken in [%],
- Energy consumption – the energy (thermal or electrical) necessary to produce one cubic meter of freshwater [m^3/kWh , kWh/m^3]

Desalination technologies can be classified into three main categories by Alkaisi et al. [23]: Evaporation & Condensation, Filtration and Crystallization. *Figure 5* shows a detailed classification.

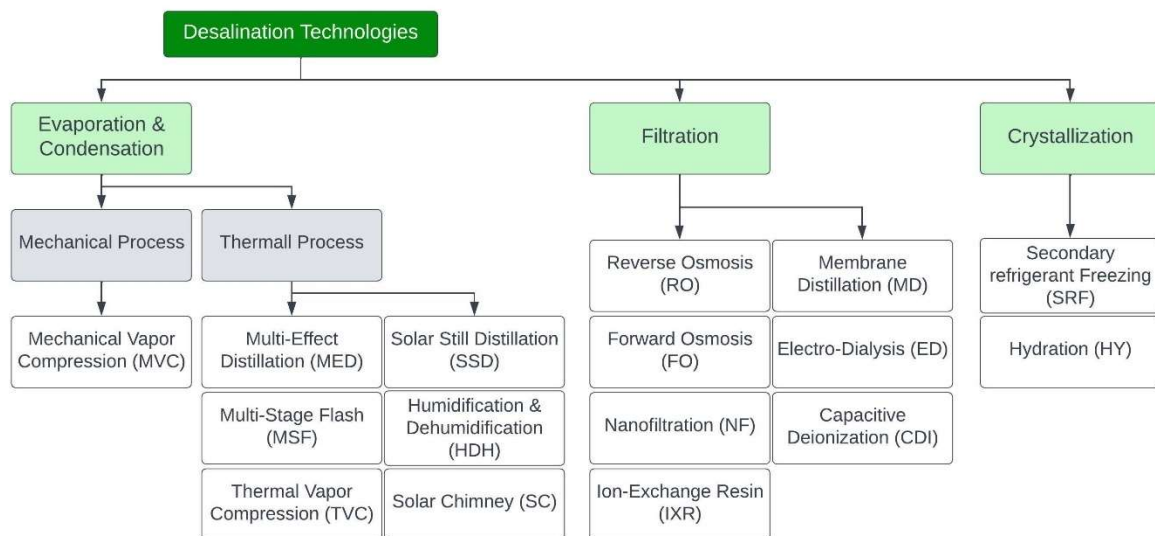


Figure 5 Classification of Desalination Technologies - adopted from [12]

Evaporation & Condensation (also known as Phase-Change) technologies can be further divided by the main energy source into mechanical processes and thermal processes. Thermal technologies were the first desalination technologies to be historically utilized for civil freshwater production [12] (also in 3.1.1 Overview). The main principle is to produce vapor utilizing thermal energy and then condensate it. Most thermal processes involve heating water to its boiling temperature to produce the maximum amount of vapor. Typically, the pressure of

the system is reduced in order to lower the boiling temperature. The most common technologies (usually for large-scale application) are Multiple-Effect Distillation (MED), Multi-Stage Flash (MSF), Thermal Vapor Compression (TVC) [12]. The main method to produce freshwater by evaporation and condensation while utilizing mechanical energy is Mechanical Vapor Compression (MVC) [24].

Most filtration (also called membrane) technologies are essentially based on semi-permeable membranes that permit or limit the passage of certain ions by three types of driving forces: pressure, electric potential, and concentration gradient. Reverse Osmosis (RO) is the most used technology for desalination [12]. Electrodialysis (ED) and Ion Exchange Resin (IXR) are used to produce water with very low concentrations of salts [12]. Other techniques such as Forward Osmosis (FO), Nanofiltration (NF) and Capacitive Deionization (CDI) are in development stage [25] [26].

The Crystallization category comprises of that extract freshwater producing ice as intermediate product. The main techniques are Secondary Refrigerant Freezing (SRF), Hydration (HY), and Vacuum Freezing (VF) desalination. All these methods are currently in the research phase. [12]

The breakdown of current capacity by different desalination technologies (shown in *Figure 6*) is: RO (67%), MSF (21%), MED (7%), ED/EDR (3%) and Emerging⁵ (2%) [27]. As stated above RO is the most used technology has been gaining momentum even in the traditionally thermal market of the Persian Gulf [28].

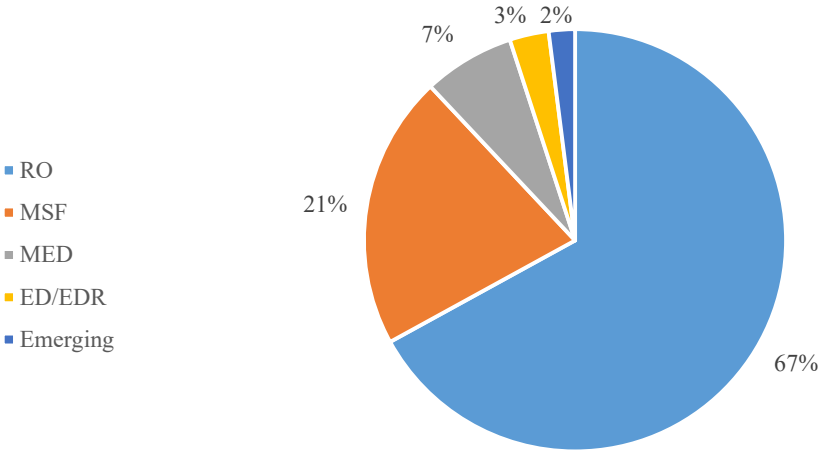


Figure 6 Graph of technology breakdown of installed global desalination - data from [27]

⁵ These emerging technologies are: Nanofiltration (57%), Electrodeionization (17%), Vapor Compression (3%) and Other/Unknown (23%) [27].

3.3 Evaporation & Condensation Technologies

Evaporation & Condensation (E&C) methods was already briefly introduced. In this chapter, this type of desalination is further described and specific E&C processes are covered.

Commercially available evaporation desalination systems are mostly designed to boil water multiple times in a series of vessels that operate at successively lower temperatures and pressures [25]. When designing or modeling a thermal desalination plant (for example MSF or MED), it is important to evaluate the optimal number of stages. Adding stages increases the total surface area, therefore increases robustness of the system and therefore capital cost. This effect is graphically illustrated in *Figure 7*.

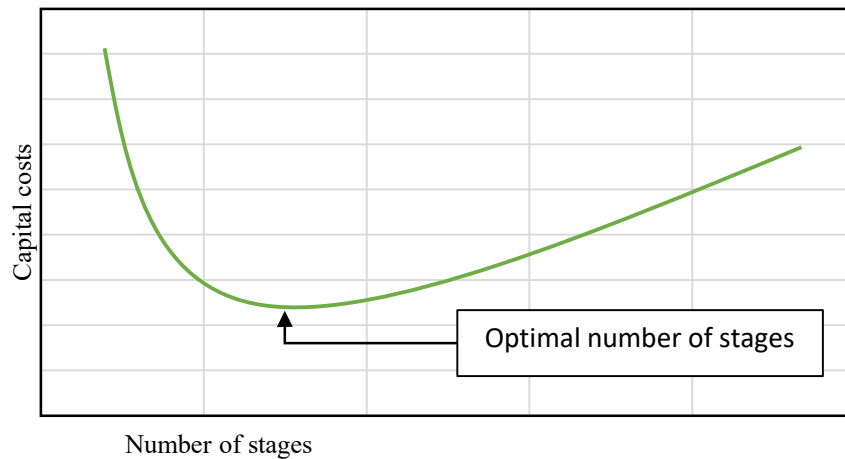


Figure 7 Graph of the relationship between number of evaporation stages and capital costs

3.3.1 Multi-Effect Distillation

The first MED plant was built in Kuwait in the 1950s and used a triple-effect submerged tube evaporator [12]. Even though it was the first technology used for large-scale desalination, MED did not spread due to fouling (scaling) problems on the pipes and corrosion compared to other thermally driven desalination processes [29]. This problem has been partially resolved in the 1980s by building around the concept of operating at lower temperatures to prevent corrosion and minimizing fouling (scaling) [11]. Based on Top Brine Temperature (TBT), MED can be classified as Low Temperature (below 90 °C) or High Temperature (over 90 °C) [12]. MED is currently used also in food industries to extract juice from sugarcane, and to produce salts from seawater [30].

MED uses multiple vessels (effects) arranged in a series with reduced pressure in each subsequent effect – 8 to 16 effects are used typically [25]. The feed water is sprayed on the outside of the evaporator tubes in a thin film to promote rapid boiling and evaporation. The surfaces in the first effect are usually heated by steam from turbines (in case of a power plant) or a boiler [11]. Steam is condensed on the colder inside surface. Vapor produced by evaporation in one effect is condensed and the heat is used to boil the feed water in the next effect, thus allowing water to undergo multiple boiling without supplying additional heat (with the exception of the first effect). This lowers thermal energy consumption and electrical power consumption [12]. In *Figure 8* is shown a diagram of a MED plant with horizontal tubes, which is also the most common heat-exchanger in MED applications [11] [12].

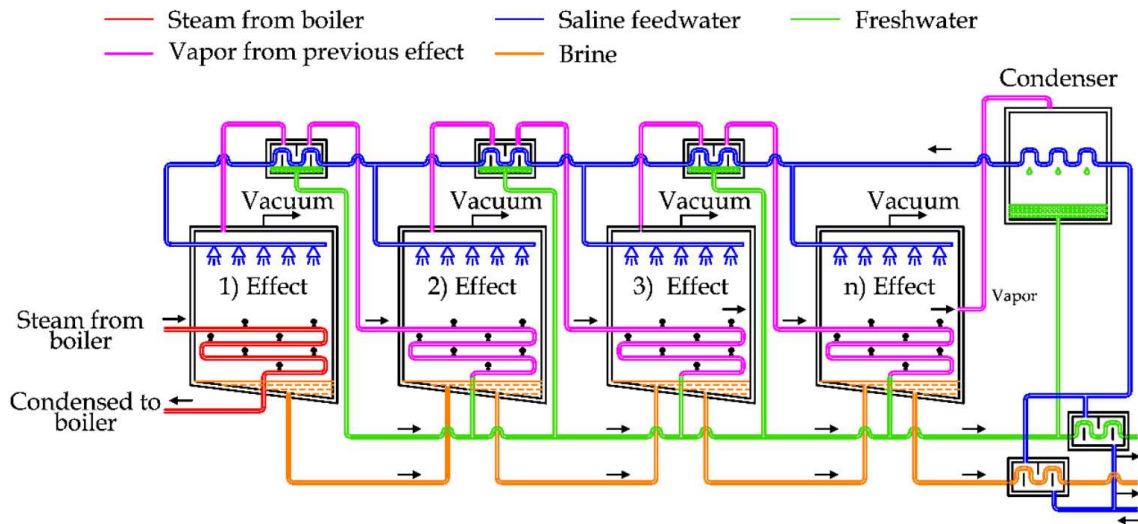


Figure 8 Scheme of the MED process [12]

The Classification of MED Process

The multi-effect distillation has three configurations of the process including normal flow, reversed flow, and parallel flow [18].

Normal Flow

Normal flow means that the feed water is going from the first effect to the last effect in a sequence. The characteristics of this arrangement are [18]:

- 1) Since the vacuum degree increases gradually, the pressure of each effect is decreased successively. Thus, there is no need for additional pump to get the feedwater from the last effect to the next.
- 2) Since there is a temperature difference between the effects and it is decreasing by sequence, the feedwater turns to superheated water at a relatively low pressure, as it flows through the effects. This will create a little extra amount of steam and produce more freshwater.
- 3) Considering the high-concentrated feedwater with high viscosity in the latter effects, the heat transfer coefficient is relatively low as the boiling point of the water is increasing. This makes it hard to maintain the temperature difference between two adjacent effects. Although for seawater desalination, this is not a serious issue because the concentrations among the effects are not high enough.

Reversed Flow

Reversed flow means that the flowing direction of feedwater is reversed to the flowing direction of heated steam. The pressure of the front effect is higher than the latter effect, that is why there needs to be a pump to get the feedwater through the system. As the temperature is increasing with the feedwater flowing through the effects, there is no flash evaporation between the effects and there is a need to preheat to the boiling point. Thus, contra flow is suitable for high-concentration and high-viscosity feedwater and is often used in chemical processes. [18]

Parallel flow

Parallel flow means that each effect has an independent feedwater inlet. The heated steam-flow into the first effect flows also to the rest of the effects. This arrangement is suitable for applications with easily crystallizing feeds such as salt manufacturing. [18]

As for the seawater desalination process, the main objective is to obtain pure freshwater. Thus, normal flow arrangement is the more suitable option than the latter two (also considering higher heat utility efficiency of normal flow variant).

Advantages & Disadvantages

The main advantages of MED desalination are [12] [31]:

- low energy consumption,
- less critical levels of operating temperature and pressure equilibrium,
- high water quality.

The main disadvantages are [12] [31]:

- more complicated circuit equipment,
- tendency to scaling of the pipes.

In conclusion, since the MED process has lower operating temperature and pressure, it is suitable for solar energy utilization (if equipped with the Multi-Effect Stack Evaporator⁶) [31]. Also, the MED system does not require a lot of energy (compared to other thermal desalination systems) – it is a once-only process, which means that there is less liquid required to flow through the system [18].

3.3.2 Multi-Stage Flash

Multi-Stage Flash (shorter version of Multiple Stage Flash Distillation) process has quickly displaced early MED plants in the 1950s due to better resistance to scaling and currently is the most widespread thermal desalination process globally [11] [16]. MSF is mostly used in countries where costs of thermal energy are low – Saudi Arabia, the United Arab Emirates and Kuwait [30].

MSF plants can be divided into two sections. The first section is the brine heater section, and the second section is the heat recovery [12]. The principle behind MSF process is as follows [18]:

- 1) Seawater is heated in a vessel called the brine heater by steam (spilled from a power plant, typically).
- 2) Seawater is then pumped into a vessel – the flash room (also called a stage [11]) and is then heated to certain temperature, as the pressure is controlled at lower than the heated seawater saturated vapor pressure⁷.

⁶ The Multi-Effect Stack Evaporator (MES) is a type of evaporator, in which the effects are stacked on top of each other. It provides stable operation even when sudden changes are made. [31]

⁷ The vacuum is obtained by the utilization of steam ejectors or vacuum pumps [22].

- 3) The heated seawater becomes superheated water, the vaporization is fast, causing the “flash effect”, and the temperature of seawater decreases.
- 4) The water vapor condenses on the wall of the exchanger pipe and becomes pure water.
- 5) Meanwhile, the incoming seawater is preheated in the exchanger.

Seawater flows into several flash rooms where pressure declines one by one. The temperature of the seawater decreases as the concentration of seawater increases, until the temperature is approaching the natural seawater temperature [18]. Typically, a MSF plant operates at the top brine temperatures (see also 3.3.1). Operating a plant at the higher temperature limits (above 110 °C) increases efficiency, but also increases the potential for scale formation and accelerated corrosion [11]. Usually, a MSF plant contains from 15 to 25 stages, and is built in units producing from 4,000 to 57,000 m³/d [11].

The Classification of MSF Process

The process of MSF can be classified as a tubular and circular type [18].

Tubular

In the tubular type the seawater is heated to the highest temperature and then goes through the heat exchanger. Then stage by stage process evaporation takes place until the last stage, when the concentrated seawater is discharged out. A diagram of tubular (also through-flow) MSF plant is displayed in *Figure 9* and its temperature profile is displayed in *Figure 10*. [18]

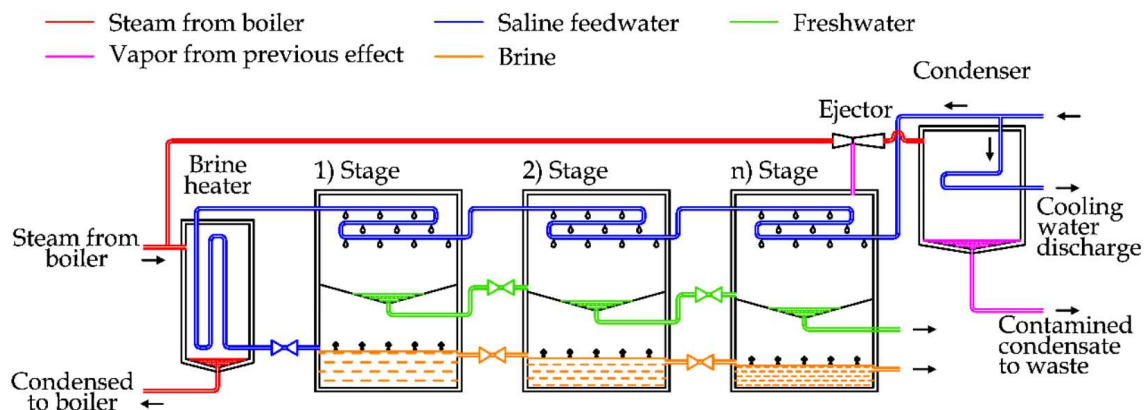


Figure 9 Scheme of the through-flow MSF process [12]

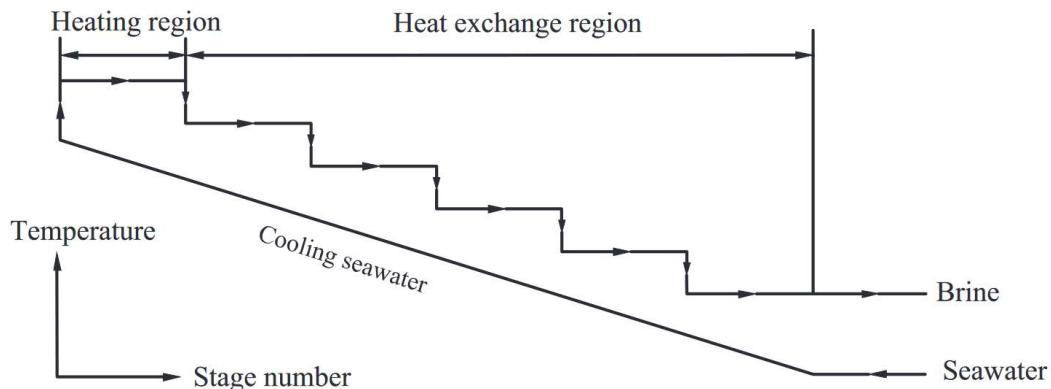


Figure 10 The temperature profile of through-flow MSF process [18]

Circular

In the circular type the concentrated seawater from the last stage is not discharged out completely. Instead of a condenser, a heat rejection section is added and a large portion of concentrated seawater is recycled and mixed with new feedwater [18]. This technique adds 2-3 heat rejection stages to the process and is applied to increase the energy efficiency of big desalination plants, composed of 19-40 flash stages [22] [32]. This type of MSF is used in more recently built plants [12]. A diagram of circular (also recycling) MSF plant is displayed in *Figure 11* and its temperature profile in *Figure 12*.

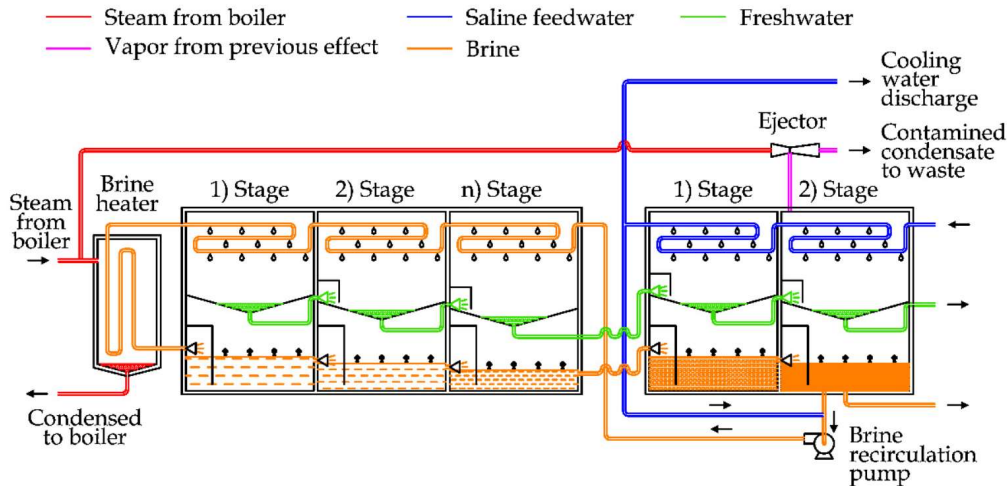


Figure 11 Scheme of the recycling MSF process [12]

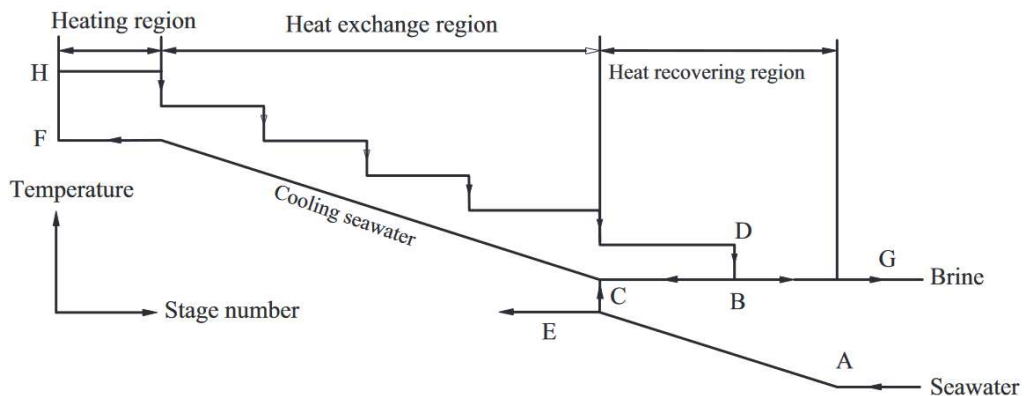


Figure 12 Temperature profile of a recycling MSF process [18]

Advantages & Disadvantages

The main advantages of MSF desalination are [12] [19]:

- simplicity of the process,
- high water quality,
- suitable for high-capacity plants,
- scale control and relatively simple maintenance.

The main disadvantages of MSF desalination are [12] [31]:

- high energy demand,

- precise pressure levels in different stages are required – some transient time is required to establish the normal running operation,
- high investment cost.

In conclusion, since the MSF process requires some transient time to establish the normal running operation, it has slow start up times and is therefore relatively unsuitable for solar energy applications unless a storage tank is used for thermal buffering [31]. Due to the robustness and reliable performance characteristics of the MSF process, it is suitable for large-scale operations in locations with low fossil fuel prices.

3.3.3 Vapor Compression

Vapor compression (VC) is a technique based on liquid-vapor phase change. The process generally is as follows:

- 1) Seawater is under environmental pressure and temperature is introduced into the evaporation chamber and heated to saturation temperature.
- 2) Then the saturated steam is compressed by a compressor and is turned into superheated steam in the cooling coil.
- 3) This superheated steam releases heat and turns into a new saturated steam and a part of saturated water in the cooling coil.
- 4) This saturated water from the last stage exchanges heat with new incoming seawater.
- 5) Finally, the saturated steam condenses and is discharged from the system.

The Classification of VC Process

There are two types of vapor compression technology based on the type of energy used to evaporate the feedwater: Mechanical Vapor Compression (MVC), which increases vapor pressure using a mechanical compressor (powered by electricity), and Thermal Vapor Compression (TVC), which uses thermal compressor supplied by high pressure steam (usually spilled from a power plant) [12]. The diagrams of the MVC and TVC processes are displayed in *Figure 13* and *Figure 14* respectively.

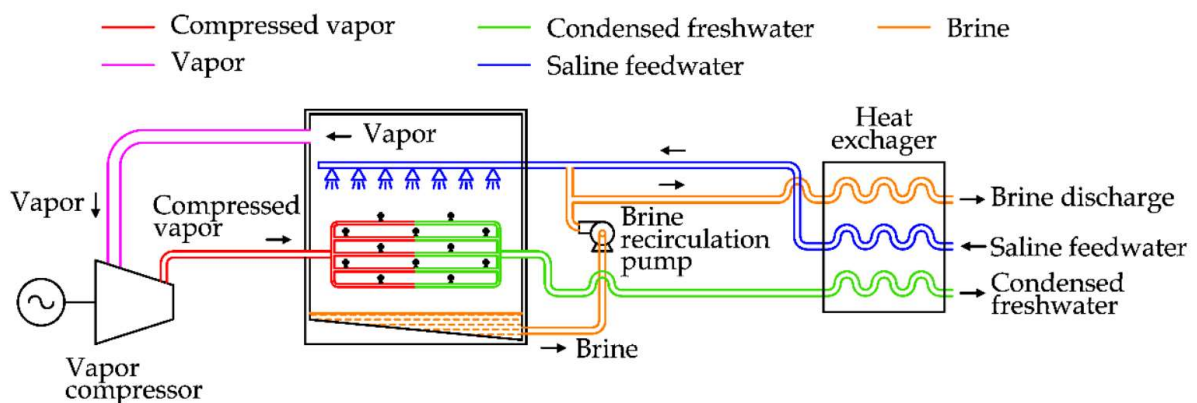


Figure 13 Scheme of the MVC process [12]

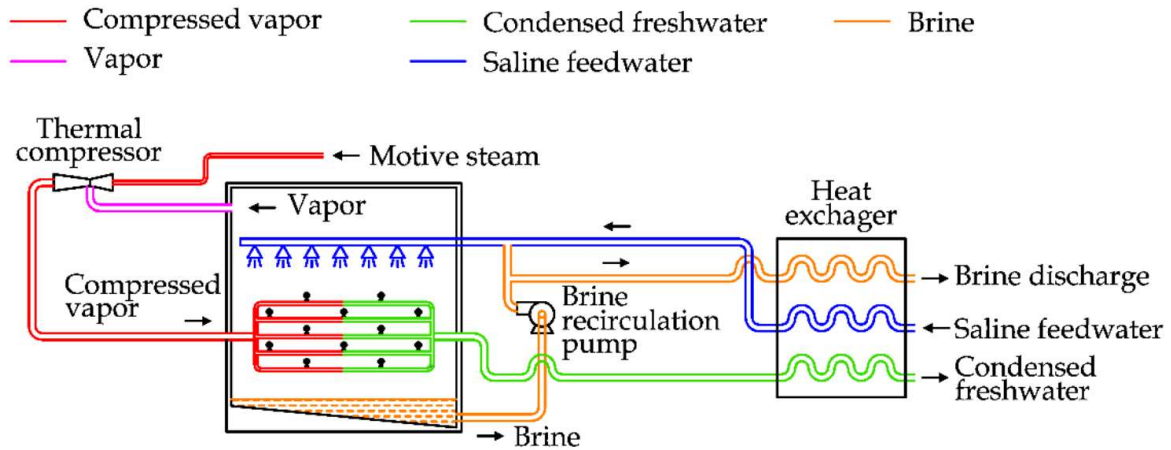


Figure 14 Scheme of the TVC process [12]

Advantages & Disadvantages

In this chapter, only the MVC process is discussed, because the TVC process is mostly used coupled with large energy sources or as an additional technology for other thermal desalination system [31]. The main advantages of the MVC process are [12] [18]:

- high water quality,
- low energy consumption (high efficiency),
- small volumes – no need for large energy sources.

The main disadvantages of the process are [18]:

- low production capacity – not suitable for large-scale operations,
- vapor-containing brine is carried over to the compressor, which leads to corrosion of the compressor blades,
- susceptible to serious scaling on the boiler walls.

In conclusion, the MVC process is suitable for low or mid-scale applications, since it is limited by the vapor compressor size, which is also the main energy-consuming element. Especially, decentralized small-scale MVC units coupled with centrifugal compression distillation is a promising method [18]. Additionally, it is not suitable for applications with low-grade energy (heat).

3.4 Membrane Technologies

As stated at the beginning of this chapter (*3 Desalination*), membrane desalination processes rely on semi-permeable membranes to separate salts from the seawater, imitating the function of similar membranes in nature (for example in the human body).

3.4.1 Reverse Osmosis

RO is a process in which the seawater flows through a semi-permeable membrane under high pressure and the dissolved material (salts) are separated without heating or phase change. In comparison to other conventional desalination processes, RO is relatively new and has been commercially successful since the early 1970s [11].

This process is based on overcoming the natural phenomenon of osmotic pressure, which naturally occurs (also in human body) when a semi-permeable membrane separates (is between) two solutions with different concentrations of ions. Naturally, these two solutions are driven by osmotic pressure to establish chemical equilibrium – one solution with the same concentration. This phenomenon can be reversed by applying enough hydraulic pressure (higher than the osmotic pressure), thus increasing the concentration gradient between the two solutions. Therefore, most of the energy necessary to power this process is used for pressurizing the feedwater. This concept is illustrated in *Figure 15*.

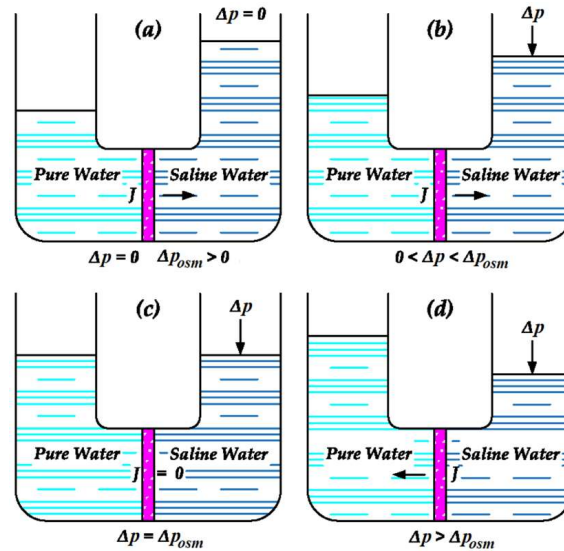


Figure 15 The principle of osmotic pressure [12]

In the figure above are shown two solutions (pure and saline water) separated by a semi-permeable membrane under four different scenarios. In scenario (a), the external pressure is zero and the osmotic pressure naturally induces the flow of pure water solution to saline water solution in order to create the concentration equilibrium. In scenario (b), the external pressure is higher than zero, but not higher than the osmotic pressure. The flow of pure water into saline water is not as high as in case (a) but is still present. In scenario (c), the external pressure is equal to the osmotic pressure and no flow through the membrane occurs. In scenario (d), the external pressure is higher than the osmotic pressure – the saline water flows through the membrane (the natural flow is reversed).

The process in a RO desalination plant generally works as follows:

- 1) Feedwater is pumped from the seawater water source at the intake into the pretreatment device.
- 2) During pretreatment, the feed water is removed from suspended solids by fine filtration and acids or other chemicals are added to prevent salt precipitation and microbial growth on the membrane surface [11].
- 3) The water flows into the high-pressure pump which pressurizes the feedwater and is further pumped into a pressure vessel.
- 4) From the pressure vessel, the feedwater is pumped through the membrane into the post-treatment device.
- 5) Post-treatment generally consists of preparing the water for distribution. Specifically, it might consist of removing gases (such as hydrogen sulfide) and adjusting the pH [11].

The RO desalination (without pre-treatment and post-treatment) is displayed in *Figure 16*.

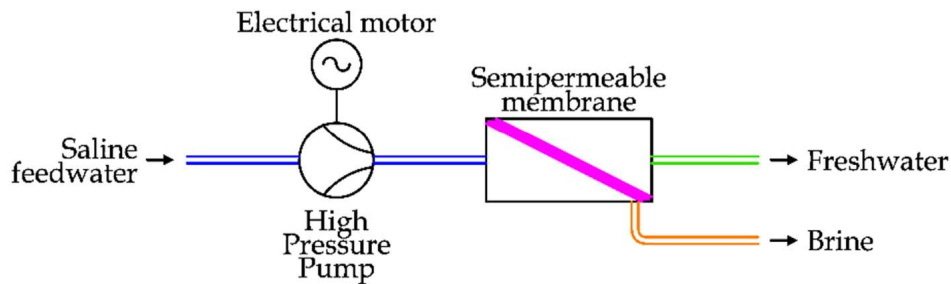


Figure 16 Scheme of the RO desalination process [12]

Membrane Materials

The early membranes, developed in the 1960s, have been made out of asymmetric cellulose acetate (CA) and were less permeable and had worse salt rejection ability. The membranes required pressures exceeding 8.3 MPa at typical operating fluxes. CA membranes utilized an asymmetric structure, in which the membrane consists of the same material throughout with a dense layer on top and porous layer beneath. Modern CA membranes are still used in the desalination industry, since they can tolerate low concentrations of chlorine, which is beneficial for biofouling control. Although, they are susceptible to hydrolysis (especially if the operating pH is less than approx. 4 or greater than approx. 7 and temperatures are higher than 30 °C), which compromises the membrane's salt rejection performance.

The more widespread types of membranes currently are thin-film composite (TFC) membranes which provide greater salt rejection and higher water production per unit membrane area. TFC membranes contain multiple layers made of different materials (thin – dense film, and porous underlying material). The thin film usually consists of aromatic polyamide (PA) and the bottom support layer is typically polysulfone. TFC membranes are stable over a broad pH range (2-11) and can withstand temperatures higher than 45 °C. However, unlike CA membranes, they are sensitive to strong oxidants such as free chlorine. Therefore, TFC membrane materials degrade upon exposure to chlorine. Membranes used for desalination typically operate at feed pressures of 5.5 to 6.9 MPa. [25]

Membrane Configurations

RO membranes are usually arranged in four configurations: plate-and-frame, tubular, spiral-wound, and hollow fiber, although the construction of the membrane varies depending on the manufacturer [11] [33].

Plate-and-Frame

These modules are among the first RO membrane modules, a flat sheet membrane is attached to the two sides of a rigid plate. A number of plates are used that are stacked within a pressurized support framework. The plates contain a grooved structure providing a path for the permeate flow. The permeate leaves the module from one end, the brine (concentrate) leaves from the other end. The illustration of plate-and-frame module is shown in *Figure 17*. [33]

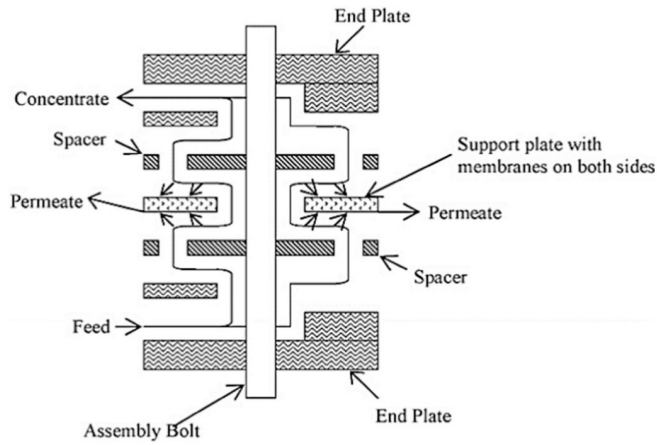


Figure 17 Plate-and-Frame membrane configuration [34]

Tubular Modules

A typical tubular module, shown in Figure 18, consists of a porous tube with an inserted or surface-coated RO membrane. The tubes are made of ceramic, carbon, paper, plastic, or fiberglass. Pressurized feedwater enters the tube from one end, water molecules permeate radially through the membrane. Brine leaves from the other end of the tube. [33]

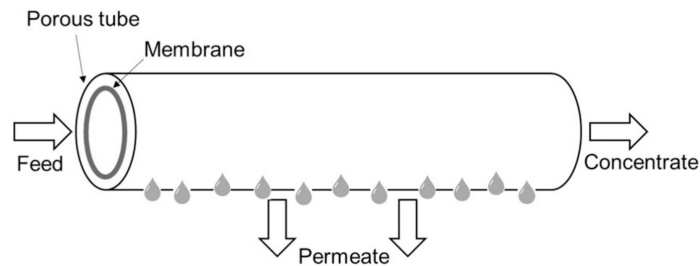


Figure 18 Tubular membrane module [33]

Hollow Fiber

A hollow fiber module (displayed in Figure 19) is composed of numerous small-diameter fibers contained within a pressure vessel. On one side, the module consists of an epoxy tube sheet where the fibers ends are potted in epoxy while keeping them open for permeate flow. On the other side, the fiber ends are sealed in epoxy to prevent bypassing of the feed to the concentrate outlet. Pressurized feedwater enters the module through a core tube and the water molecules permeate radially into the fibers and exit through the open fiber ends in the epoxy tube sheet while the concentrate leaves the module at the same end as the feed inlet. [33]

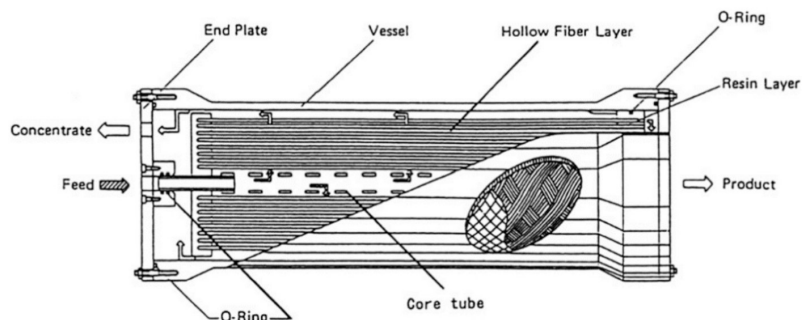


Figure 19 Hollow Fiber membrane configuration [33]

Spiral-Wound

Spiral-wound (displayed in *Figure 20*) is currently the most common type of module used for RO desalination. In this module two membrane sheets are placed together with a permeate spacer (made of nylon or dacron) in between. These layers are wrapped around the permeate collector tube to create a spiral configuration and placed inside a pressure vessel (also called housing). Feed water flows axially along the length of the module. Spiral wound modules are cost-effective, possess high packing density, and allow for high mass transfer rates due to the presence of feed spacers. However, they are difficult to clean and are susceptible to fouling if pre-treatment is inadequate. [33]

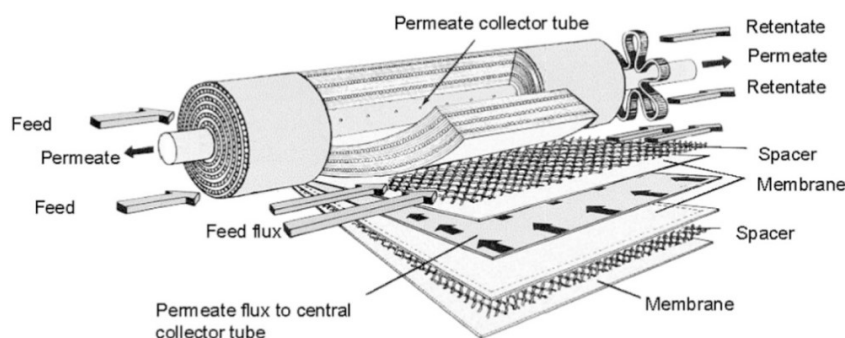


Figure 20 Spiral-wound membrane module [33]

Energy Recovery

To minimize energy losses of RO plants, an Energy Recovery Device (ERD) has been introduced. The ERDs utilize energy of the brine stream or the feedwater stream (the pressure of brine stream is practically the same as the saline input water). The ERDs can be classified as centrifugal and isobaric devices [35].

There are two main centrifugal devices, the first one is a hydro turbine (Pelton) which extracts energy from the brine stream and transfers it to the high-pressure pump. The pressure drop inside the brine circuit is about 2-3 bar and the efficiency of the energy conversion is approx. 70% [12]. The second centrifugal device is the turbocharger, which uses a turbine to extract energy from the brine stream and converts the energy to rotational energy which turns an impeller that pumps another fluid stream. If the turbocharger is positioned properly between two stages, it can reduce the need or even replace the interstage boost pump. [35]

The isobaric devices are more recent solutions that transfer energy without intermediate energy conversions. They function by directly hydraulically pressurizing the feed stream via exposure to the brine stream. One isobaric ERD is the rotary isobaric device also known as the rotary pressure exchanger (RPX). The device is displayed in *Figure 21*.

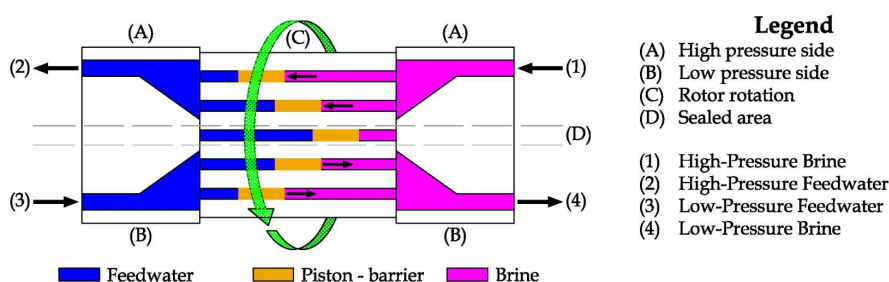


Figure 21 Rotary Pressure Exchanger scheme [12]

In the device a ceramic matrix is taken into rotation by the brine flow, which enters the matrix with a tangential speed component. The channels inside the matrix are connected by pipes with pistons inside. High pressure brine pushes the pistons, which transfer the pressure and pressurizes the feedwater as it leaves the device. Simultaneously, the feedwater flowing into the device pushes the brine out of the channel on the low-pressure side. The process is practically continuous because of the high rotary speed of the matrix and the number of internal channels. [12]

Advantages & Disadvantages

The main advantages of RO desalination are [12]:

- uses only electrical energy,
- coupleable with many renewable energy sources,
- low investment costs.

The main disadvantages of RO desalination are [12]:

- lower product water quality,
- tendency to biofouling (and non-biological fouling as well [31]),
- high costs of membranes and chemicals.

In conclusion, the RO desalination is suitable for small-scale as well as large-scale applications. RO is also compatible with multiple renewable energy sources. Compared to other desalination technologies, RO generally offers lower capital costs [12]. Although, the operating costs can be relatively high. Since the membranes are susceptible to biofouling, they should be changed regularly (approx. every 4-5 years) [18] [31]. To prevent biofouling, chemicals are added to pretreat the feedwater, but the chemicals also tend to disintegrate the material of the membrane, adding to the problem of operating costs. Another disadvantage of RO systems is lower water quality of the product, which generally has a concentration of salts (NaCl) approx. 300 ppm, which still meets the standards of 500 ppm (set by the WHO for drinking water), but still is one order of magnitude higher than water produced by thermal processes [31]. High salinity of feedwater is problematic for RO technology [31].

3.4.2 Nanofiltration

Nanofiltration is a membrane filtration process used to remove dissolved ions or organic matter to produce soft water – water with a limited number of ions that cause scaling (Ca^{2+} , Mg^{2+} etc.) [12]. As the prefix “Nano” suggests, this technology removes particles through pores, ranging from 1 to 10 nm. NF technology is used in applications such as water and wastewater treatment, pharmaceutical industry, textile industry, and food processing, but it has found its way into the desalination industry [36]. The saline feedwater is pushed through a semipermeable membrane and disallow passage of divalent ions mostly, with an efficiency of 90-98% [12]. The principle and scheme of nanofiltration technology is illustrated in *Figure 22*. The soft water produced by NF has greater ion concentration than RO, therefore a lower pressure gradient must be applied to the membrane (between 38 and 48 bar) [25].

Wafi et al. [37] have tested and compared nanofiltration with RO and found that the electrical energy consumption (per m^3 of product water) of the nanofiltration plant was 29% lower than RO plants. They also found that the quality of water from nanofiltration is equally comparable to RO in respect of TDS, pH, cations, and anions. Although NF is still in the development

phase, studies suggest that is going to compete on the desalination market, especially with RO in brackish water applications [37].

Turek et al. [38] modelled a pilot-scale three-stage (RO-evaporator-crystallizer) desalination system for brackish water from a coal mine. NF was used as a pretreatment method. The results show that adding a two-pass NF can decrease the energy consumption by 21% (therefore cut operating costs), increase salt recovery from 58.8% to 76.1%, and could also create economic potential by using magnesium-rich waste stream for magnesium hydroxide recovery.

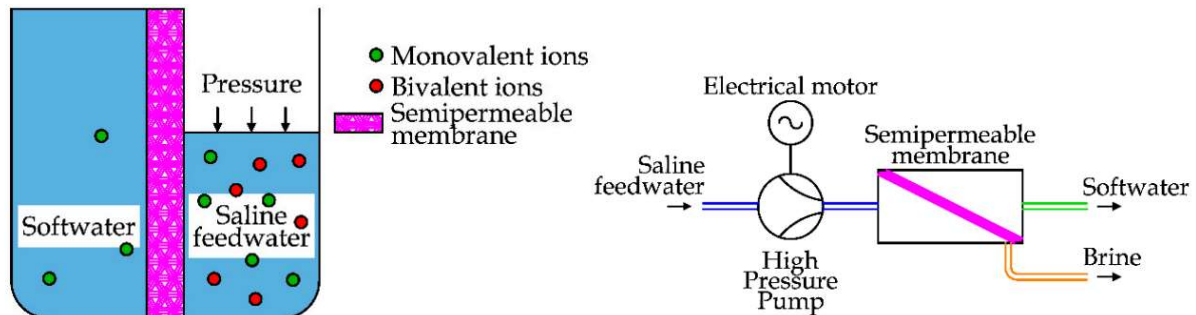


Figure 22 The working principle and scheme of nanofiltration technology [12]

Advantages & Disadvantages

The main advantages of NF desalination are [12] [37]:

- low energy consumption (lower than RO),
- water quality comparable to RO,
- variability of applications.

The main disadvantages of NF desalination are [12] [37]:

- produces soft water (a dilute saline solution),
- commercially unavailable for seawater applications,
- susceptibility to fouling.

In conclusion, even though NF desalination is still in the development phase with smaller pilot-scale projects in operation, it is a promising technology that has proved itself as a cost-effective alternative to RO (due to lower energy consumption and comparable water quality) [37] or as pretreatment to other desalination technology [38].

3.5 General Trends in Research & Development

The trends and history since 1980 in research of desalination were documented by Jones et al. [16] and are illustrated in Figure 23, which displays the historical development of published literature on desalination.

On the right-hand side is a graph of the number of publications by desalination technology. The exponential increase in publications can be also seen in RO research (which also complements the data from Figure 6, as it shows RO being the most widespread technology currently), followed by emerging technologies. The research of conventional thermal technologies has also been growing, although at a lower rate – MSF is the least popular technology in research. [16]

On the left-hand side is a graph of the number of publications on the topic of desalination by categorization – since 1980, approximately 16,500 publications have been found in total. Based on this graph, the exponential increase in technological aspects of desalination is the main driver of desalination research, followed by the economic and energy aspects. The environmental impacts of desalination were severely neglected with just 118 publications before 2000. However, the number publications in this category are increasing at the fastest rate. [16]

One of the aforementioned environmental aspects of desalination – the production of brine in particular – has been also studied by Jones et al. [16]. It has been found that the large volume of produced brine poses a major environmental concern that requires better management. Even though there are economic opportunities associated with brine in fish and halophyte production systems, there is need to translate such environmental problem into an economic opportunity. [16]

3.5.1 Renewable Energy Sources

Research and development of desalination has also shifted from conventional fossil fuel powered plants towards renewable energy powered solutions. As previously discussed, energy

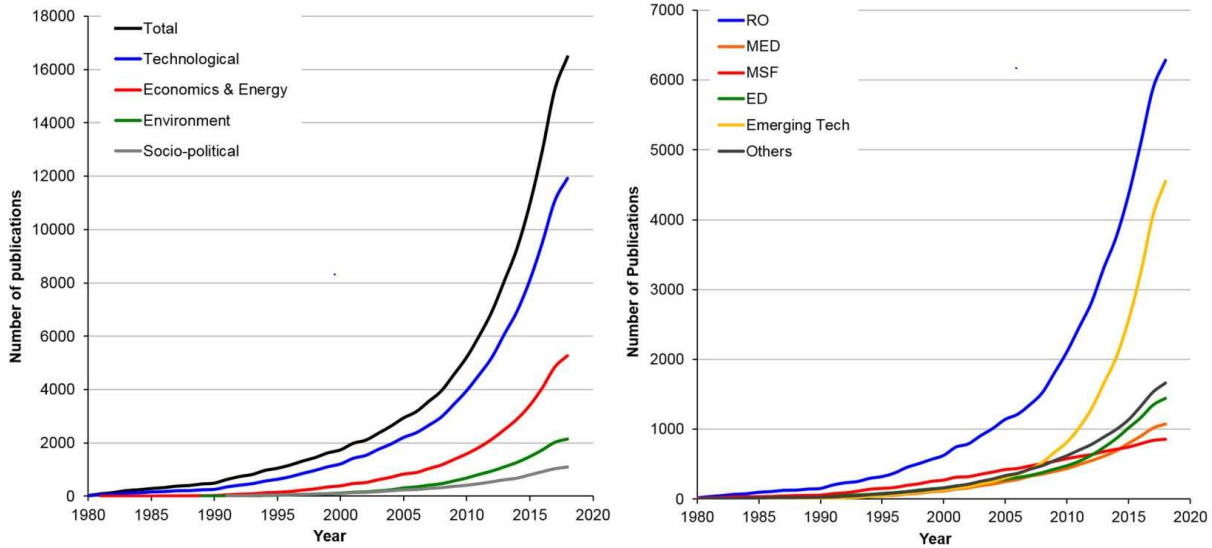


Figure 23 Graphs of trends and history in desalination research [18]

consumption is a big problem in the desalination industry, thus coupling desalination with renewable energy sources that supply at least a part of the necessary consumption is a more attractive solution. Bundschuh et al. [39] found that renewable technologies can be successfully combined with many desalination methods (based on global experience), although optimization of some techno-economic aspects is necessary to make such systems effective in the long-term. Possible combinations of renewable energy sources and available desalination technologies are displayed in Figure 24. Mostly used renewable energy sources in the industry are solar thermal energy, photovoltaics (PV), wind, and geothermal energy [40].

Above mentioned renewable energy technologies will be described further in this chapter.

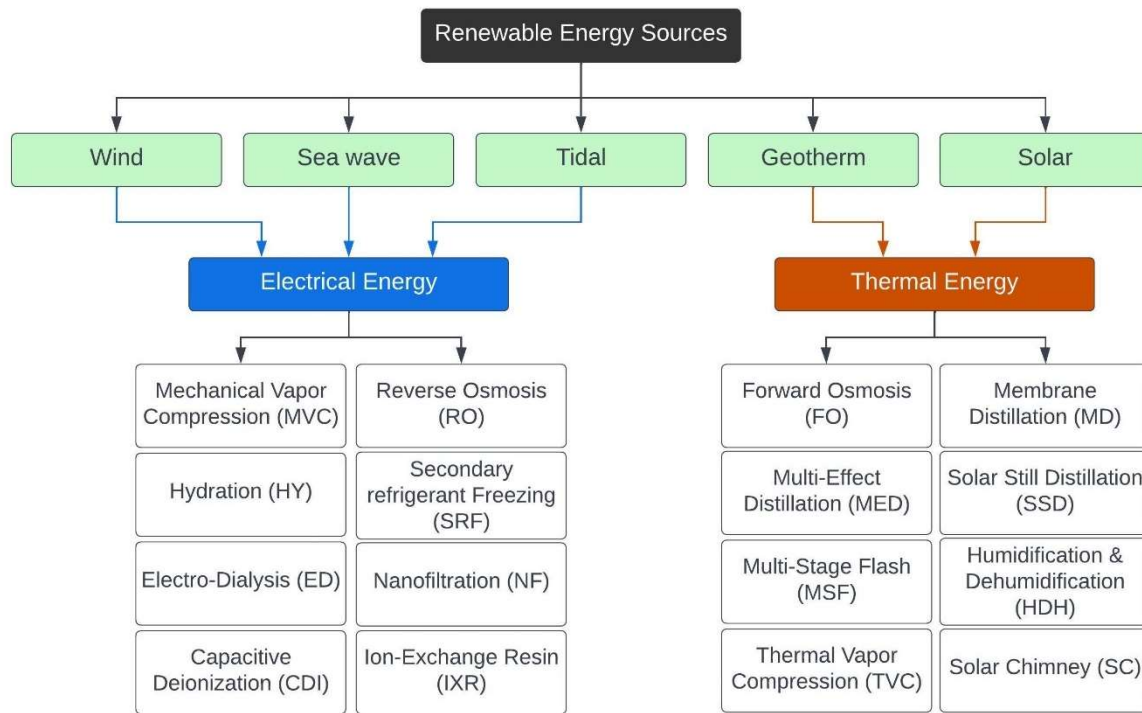


Figure 24 Combinations of RES with Desalination Technologies – adopted from [12]

Solar Energy

Solar desalination has made a breakthrough in the 20th century, as the first completely PV-powered RO desalination plant was built in 1982 in Saudi Arabia on the eastern shore of the Red Sea - it provided drinking water to a settlement of 250 people and the power source was an array of 210 modules producing 8 kWp⁸ [41] [42]. The solar energy option (thermal and PV) has been experiencing big growth especially in the last decade, mainly because of improved performance and efficiency characteristics, governmental subsidies, and decreasing costs of the equipment material. The advantage of solar energy is the ability to generate thermal and electrical energy. [39]

Solar thermal technologies extract thermal energy from the sun's radiation using solar collector or concentrated solar power technologies (CSP). These technologies are one of the most popular and most common RES applications globally, especially used for energy-intensive processes such as MSF, MED and VC. [39]

Solar electricity technologies are classified as photovoltaic or concentrator photovoltaics (CPV), which are modules used to harness solar energy carried by photons into electricity via photoelectric effect. [39]

Wind Energy

Apart from solar energy, wind energy is the most popular RES used and investigated in the context of being coupled with desalination technology. However, the majority of publications considers wind energy desalination used in combination with other RES (mostly solar power). Nevertheless, in recent years the research of desalination processes powered exclusively by wind energy has been gaining popularity. [39]

⁸ Unit kWp (kilowatt-peak) is a unit of maximum available power produced in reference (laboratory) conditions.

3.5.2 Decentralization

Decentralization of desalination plants has been found to be an effective way to supply water to remote areas. Additionally, small and medium-size decentralized water production systems could eliminate the need to construct large water transmission infrastructure, which could reduce the water levelized cost and environmental impact. However, when proposing a decentralized system of desalination plants, it is important to consider the applicability of decentralization regarding installation cost. RO has been found to be the most suitable technology for decentralized installations. On the other hand, MSF and MED have been found to be not suitable, since these technologies are not economically viable in small and medium scale applications. [43]

3.5.3 Environmental Impact of Desalination

As has been stated earlier, the research of environmental impacts of desalination processes has been gaining popularity in recent years. Lee and Jepson [44] have divided the available literature into three main topics: 1) facility life cycle, 2) water cycle, 3) energy, chemicals and materials.

The facility life cycle consists of three main subcategories: construction, operation and maintenance (O&M), and disposal. O&M has been found to be the biggest contributor (operation specifically) to negative environmental impacts of desalination regardless of technology (MSF, MED, RO). The operation of desalination facility is the largest contributor in most of the impact categories. These include acidification potential (AP), eutrophication potential (EP), global warming potential (GWP), human toxicity potential (HTP), energy use and others⁹. [44]

Water treatment is also a major contributor to environmental impacts, regardless of technology. The environmental impact in the water cycle is mainly due to electricity consumption of the treatment. Factors that play a role in environmental impact of water cycle can be also chemical and membrane usage, raw water quality (the higher the salinity of feed water, the higher the energy consumption), distribution of the water (mostly the distance between the plant and the consumer), and state of the water infrastructure. Water treatment in the desalination process is a major contributor to all the environmental impact categories, including AP, GWP, EP, photochemical oxidation (PHO), depletion of abiotic resources (DAR), ETP (ecotoxicity potential), cumulative energy demand (CED), freshwater use (FWU). [44]

As far as components (energy, chemical and materials) are concerned, the biggest environmental burden is due to energy consumption. Chemical manufacturing contributes only 10% of greenhouse gas emissions (GHG), mostly from electricity used during the manufacturing process [45]. A connection has been found between the rise in adoption of renewable energy used to supply desalination plants and increased usage of chemicals. As the desalination industry attempts to reduce the energy use and carbon footprint, the tradeoff is reliance on new chemicals, thus increasing the negative environmental impacts of chemicals in certain renewable energy desalination applications. The environmental impact caused by materials is negligible compared to energy use and chemical manufacturing. [44]

⁹ Marine aquatic ecotoxicity potential (MAETP), terrestrial ecotoxicity potential (TETP), photochemical oxidant formation potential (POCP), freshwater ecosystem impact (FEI).

As implied above, energy demand is the largest contributor to negative environmental impacts of desalination. Several studies have been conducted to compare the LCA results of different energy sources for desalination, including renewable energy sources. Among fossil fuels, natural gas showed lower environmental burden and coal caused the highest negative environmental impact. Renewable energy sources reduce the environmental burden. Solar thermal reports better environmental performance than photovoltaic panels because PV panels requires special raw materials. Studies show that RES are not equal across the different desalination technologies. For example thermal methods such as MED and MSF generate more benefits than RO when they adopt RES. [44]

4 Methodology

As stated earlier in this thesis, the main outcome of this thesis is a basic design of a small autonomous solar-powered desalination unit supported by environmental impact assessment.

This will be done by selecting suitable desalination technologies and performing basic designs of desalination systems. These designed systems will be later compared and evaluated in regard to their parameters and characteristics. Based on these criteria, one desalination system will be selected for solar system design and sizing with an environmental impact assessment being conducted. *Figure 25* shows the flowchart illustrating the overall framework or methodology.

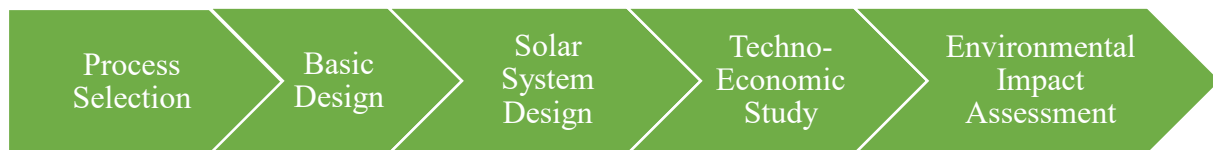


Figure 25 Thesis Methodology

4.1 Process Selection

In this chapter suitable desalination processes (technologies) will be selected for the next step – basic design. In regard to process selection, Kalogirou [46] proposed these factors to be considered:

- 1) The suitability of the process for renewable energy application,
- 2) The effectiveness of the process with respect to energy consumption,
- 3) The amount of freshwater required in a particular application, in combination with the range of applicability of the various desalination processes,
- 4) The seawater treatment requirements,
- 5) The capital cost of the equipment,
- 6) The land area required or that could be made available for the installation of the equipment.

The first factor (suitability of the process for renewable energy application) is also one of the obligatory objectives of this thesis. Regarding the second factor (effectiveness of the process with respect to energy consumption), the energy necessary to produce the desired capacity of freshwater of the proposed unit should be as low as possible, thus reducing overall energy consumption and capital cost. The third factor concerns the capacity of the unit. The objective of this thesis is to design a small-scale unit; thus, the unit is designed primarily for communities with approx. 220 population equivalents (PE) and a total freshwater production capacity of 20 m³ per day. The fourth factor concerns the quality of water produced. The WHO requirements for concentration of impurity content are <500 ppm for drinking water. The objective is of course to produce water as pure as possible. The fifth factor concerns the capital cost of equipment but also labor. The design of the proposed unit should not be too complex as the material cost, land cost, and labor costs tend to increase with size and complexity. The sixth factor concerns the land area required to install the unit. This goes hand in hand with all the other factors. The required land area is related to energy consumption (more solar panels required increases the necessary area of installation), the capacity of the unit, and capital cost (cost of land).

Additional factors that should be considered are:

- salinity of the source seawater – higher salinity results in higher susceptibility to scaling,
- operating costs – different processes require different compounds for pretreatment or post-treatment,
- maintenance complexity – some technologies require knowledgeable and trained staff to operate and maintain the unit,
- reinvestment costs.

From the factors above and available literature an evaluation table (*Table 3*) has been created.

Table 3 Evaluation of different desalination processes [12] [31]

Criteria	MED	MSF	MVC	TVC	RO	NF
Suitability for small-scale applications	No	No	Yes	No	Yes	Yes
Suitability for solar energy	Yes	No	Yes	No	Yes	Yes
Thermal energy consumption [kJ/kg]	230-390	190-390	-	145-390	-	-
Electrical energy consumption [kWh/m ³]	1.5-2.5	4-6	6-12	1.5-2.5	3-6	2-4
Exergy efficiency	< 6%	< 3%	< 8.5%	< 20%	< 32%	< 45%
Water quality	High	High	High	High	Low	Low
Capital costs	High	High	Medium	High	Low	Low

Note: MED = multiple effect distillation, MMSF = multi-stage flash, MVC = mechanical vapor compression, TVC = thermal vapor compression, RO = reverse osmosis, NF = nanofiltration

The technologies suitable for small-scale desalination are MVC, RO and NF. Even though implementing other methods, such as MED and MSF, for small-scale applications is feasible, the relative cost of equipment deems these methods not suitable, as reflected in *Table 3*. With regard to energy consumption, one big advantage of MVC, RO and NF is that there is no necessity for thermal energy supply to run the process. The exergy efficiency tends to be higher in membrane processes and vapor compression methods. The water quality is high in all thermal processes reaching concentration below 10 ppm of impurity content. On the other hand, membrane processes tend to produce water with lower quality, although still under the WHO limit.

The considered technologies proposed for basic autonomous desalination design powered by solar energy and later environmental impact assessment that are consistent with the objectives of this thesis are:

- mechanical vapor compression,
- reverse osmosis,
- nanofiltration.

The first selected process for basic design is RO (variant A), because of its simplicity, efficient energy utilization and the overall capital expenditures (CAPEX) are relatively low compared to other methods. The disadvantages are lower water quality, operating expenditures (OPEX), and the necessity for trained maintenance personnel.

The second selected process for basic design is MVC with NF as pretreatment (variant B). This combination has been proven to be a good option for small-scale remote applications. Even though it is estimated that CAPEX will be relatively higher, the nanofiltration pretreatment will mitigate the scaling problem of the MVC evaporator, therefore increasing the service life of the equipment and lowering the necessary reinvestment. Additionally, the water quality of the produced water is higher since it is treated thermally.

4.2 Basic Design Methodology

In this chapter, two desalination systems will be designed, which is one of the main objectives of this thesis. The design methods include calculations, estimations, or direct selection of specific products from the market. The design does not include the design of piping, seawater intake part, and control of the system.

For calculations of both desalination units there are the same following boundary conditions and assumptions:

- total production capacity: 20 m³/day,
- time of production per day: 12 hours of continuous operation,
- total days of operation per year: approximately 355 days with 10 days left for larger maintenance works,
- calculation model: steady state
- the only salt in seawater is sodium chloride (NaCl),
- seawater intake temperature: 25 °C,
- seawater intake salinity: 35,000 ppm,
- seawater density is 1023 kg/m³, freshwater density is 996 kg/m³, brine density is 1045 kg/m³,
- maximum drinking water salinity: 500 ppm.

4.2.1 Variant A – RO Unit

The scheme of the proposed unit is in *Figure 26* with the labeled streams being specified in *chapter 5*. In this variant, the system works as follows: the feed seawater is pumped through a particulate filter to filter out larger solid particles, and the pressure of the filtered water is increased through a high-pressure pump. The pressure must be higher than the osmotic pressure in order to get through the membrane effectively, filtered water leaves the RO module and is ready to get post-treatment. Additionally, the brine leaving the RO module flows into an ERD to recover some of the energy in the stream. This energy is transmitted to the seawater entering the process.

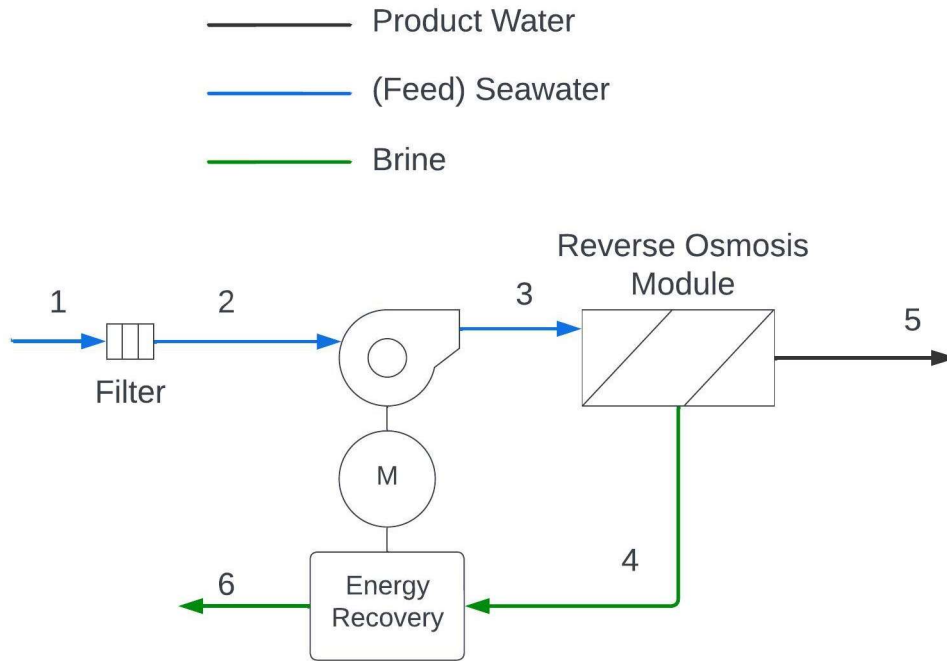


Figure 26 Variant A scheme

Material Balance

The first step is the material balance calculation of the desalination system. The calculations follow assumptions and boundaries listed at the beginning of this chapter. The mass balance can be described by the following system of equations (Eq. 1-11).

$$\dot{M}_1 = \dot{M}_2 \quad (\text{Eq. 1})$$

$$\dot{M}_2 = \dot{M}_3 \quad (\text{Eq. 2})$$

$$\dot{M}_3 = \frac{\dot{M}_5}{RR_{RO}} \quad (\text{Eq. 3})$$

$$\dot{M}_4 = \dot{M}_3 - \dot{M}_5 \quad (\text{Eq. 4})$$

$$\dot{M}_5 = \dot{V}_p \cdot \frac{\rho_P}{OT} \quad (\text{Eq. 5})$$

$$\dot{M}_6 = \dot{M}_4 \quad (\text{Eq. 6})$$

In equations above, $\dot{M}_{1...n} \left[\frac{kg}{h} \right]$ is the mass flow rate in 1 to n-stream (the numbering is the same as in *Figure 26*, $RR_{RO} [-]$ is the reverse osmosis recovery ratio, $\dot{V}_p \left[\frac{m^3}{day} \right]$ is the daily production capacity of the system, $\rho_P \left[\frac{kg}{m^3} \right]$ is the density of the produced water, and $OT \left[\frac{h}{day} \right]$ is the operating time per day.

$$X_1 = X_2 \quad (\text{Eq. 7})$$

$$X_2 = X_3 \quad (\text{Eq. 8})$$

$$X_4 = \frac{M_3 \cdot X_3 - M_5 \cdot X_5}{M_4} \quad (\text{Eq. 9})$$

$$X_5 = 0.03 \frac{g}{kg} \quad (\text{Eq. 10})$$

$$X_6 = X_4 \quad (\text{Eq. 11})$$

In the equations above $X_{1...n} \left[\frac{g}{kg} \right]$ is the concentration of salt in 1 to n-stream (the numbering is the same as in *Figure 26*).

To be able to solve this system of equations, it is necessary to determine the recovery rate of the reverse osmosis membrane RR_{RO} . The recovery rate is calculated in segment *Reverse Osmosis Membrane* in this chapter. The system now contains 11 unknown parameters and 11 equations, therefore it is possible to solve this system.

Pretreatment

In the pretreatment section the intake seawater goes through a sequence of smaller procedures. The first procedure is chlorination (dosing). Chlorine added to the seawater stream reacts with water and creates hydrochloric acid, which dissociates and oxidizes the microorganism present in the seawater. Then, the chlorinated water is dechlorinated by adding bisulfite to prevent destroying the membrane. The second procedure is filtration, where larger particles are filtered out. The third procedure is the addition of antiscalants to prevent formation of scales. This part of the process is not included in the design.

Reverse Osmosis Membrane

Regarding the type of RO module, single-stage unit was selected with 3 parallel elements (branches). The selected membrane is spiral-wound vessel M-S4040A shown in *Figure 27* (the datasheet can be found in *Appendix 1*). The dimensions of the membrane are 4 inches in diameter and 40 inches in length by the company Applied Membranes Inc. The biggest advantage of this membrane element is that it offers high salt rejection rates of 99.4% at minimum.



Figure 27 Single element membrane AMI M-S4040A (taken from Appendix 1)

The membrane has a permeate flow rate of $7.38 \text{ m}^3/\text{day}$, the recovery ratio of a single element is 8% at 55 bar pressure. The maximum pressure drop across the element is 1 bar. The minimum recovery rate has been selected at 40%. The number of passes is calculated using *equations 12 and 14*.

$$\dot{V}_F = \frac{\dot{V}_P}{RR_{total}} \quad (\text{Eq. 12})$$

Where $\dot{V}_P \left[\frac{\text{m}^3}{\text{h}} \right]$ is the permeate flow which is determined by the permeate flow of a single element and the number of parallel elements, and $RR_{total} [-]$ is the total recovery rate of the unit which is calculated *equation 13* defined by Vince et al. [47]:

$$RR_{tot} = RR_1 + \sum_{k=2}^{np} RR_k \cdot \prod_{l=1}^{k-1} (1 - RR_l) \quad (\text{Eq. 13})$$

Where RR_k is the recovery rate of element number k , $np [-]$ is the number of passes.

The number of passes was determined by incrementing the np parameter in the equation until the total recovery rate parameter was above the minimal desired value of 40%.

High-Pressure Pump

The selection of a HPP is determined by the necessary input pressure of the membrane which is around 55 bar in this case. After market research it has been decided that the proper HPP for this application is APP (W) 5.1 by the company Danfoss A/S (the datasheet is shown in *Appendix 2*). The pump is able to create a maximum outlet pressure of 83 bar_g and has an electrical power input of 15 kW at maximum speed and pressure. Another advantage of this pump is the possibility of easy installation of energy recovery device. For that the HPP must be equipped with a dual shaft electrical motor.

The selected HPP is shown in *Figure 28*.



Figure 28 Danfoss APP (W) 5.1 high pressure pump [48]

Energy Recovery

To reduce the necessary energy input of the HPP, the system highly benefits from installation of an ERD. Danfoss A/S offers ERDs that are compatible with the APP pump series and are suitable for lower flow rates. In this case, the hydraulic motor APM 2.5 has been selected (the datasheet is shown in *Appendix 3*). The maximum volumetric flow rate up is 2.69 m³/h and the

maximum recovered power is 5.3 kW at max. speed and pressure. The installation schematics of the APM energy recovery (ER) motor coupled with the APP pump is displayed in *Figure 29*.

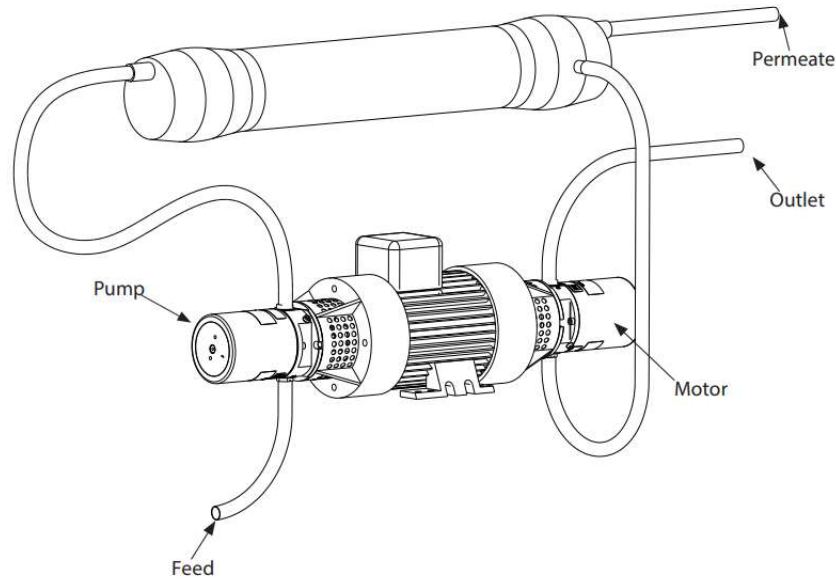


Figure 29 Installation of the APM motor and the APP pump (reference to Appendix 3)

The APP pump and APM ER motor are mounted on the dual shaft motor. The brine line is connected to the ERD device, which utilizes the brine flow to recover energy.

Post-Treatment

In the post-treatment phase, calcium and magnesium are added to the produced water as well as disinfection. The produced water is stored in two 5 m³ water storage tanks. The total water storage capacity is 10 m³, which is approx. one half of the total daily water production.

4.2.2 Variant B – MVC Unit with NF Pretreatment

The scheme of proposed variant is displayed in *Figure 30*. In this variant, the system works as follows: the feed seawater is pumped through a particulate filter to filter out larger solid particles, the filtered water flows through a pump, which increases the pressure of the water up to get through the membrane. The required pressure of 50 bar has been selected in order to achieve salt rejection rate high enough to prolong the service life of the evaporator as well as prolong the time between membrane changes. Then, the stream is divided into two separate streams in 50/50 ratio. Both streams are preheated in parallel heat exchangers (first by newly produced water from the evaporator, second by brine from the evaporator). The preheated streams then enter the single-stage evaporator where they evaporate below atmospheric pressure. The vapor is compressed by a centrifugal vapor compressor which turns said vapor into superheated vapor which later condensates and releases heat to newly incoming feedwater. Temperature and pressure values of streams 11, 12, 13 were taken from [49]. For other streams they were estimated or calculated from energy balance equations.

The calculation considers heat losses to be negligible.

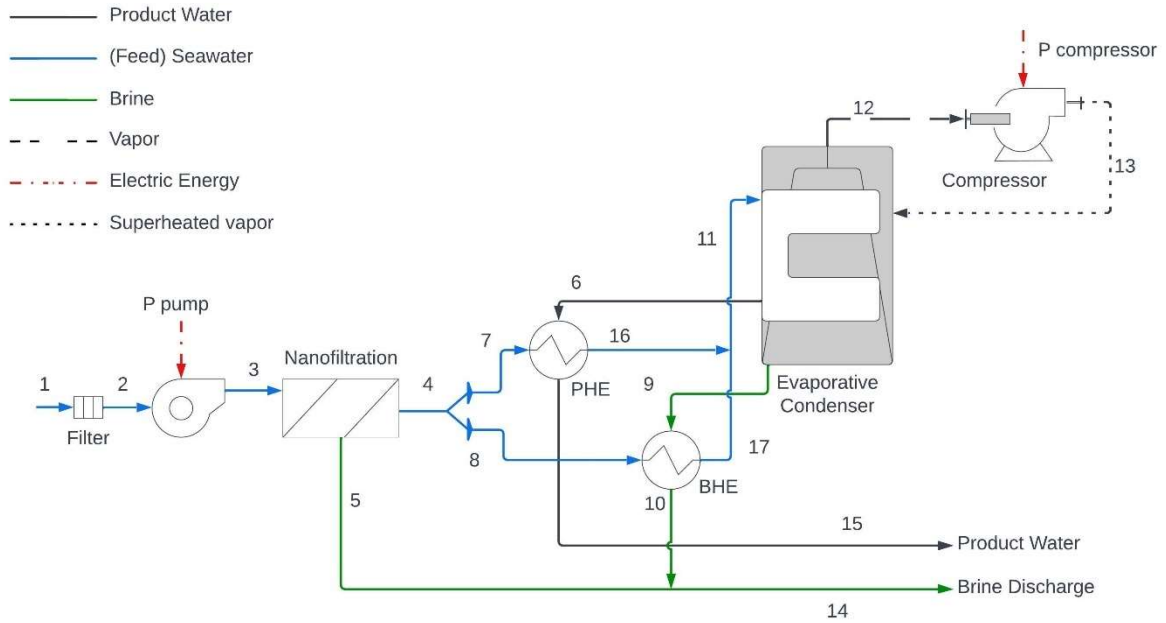


Figure 30 Variant B scheme

Material Balance

The first step in designing this variant is the material balance of the system. The balance follows the assumptions and boundary conditions listed at the beginning of this chapter 4.2. The balance has been calculated in steady state conditions and can be described by the following system of equations (Eq. 14-46):

$$\dot{M}_1 = \dot{M}_3 \quad (\text{Eq. 14})$$

$$\dot{M}_2 = \dot{M}_1 \quad (\text{Eq. 15})$$

$$\dot{M}_3 = \frac{\dot{M}_4}{RR_{NF}} \quad (\text{Eq. 16})$$

$$\dot{M}_4 = \dot{M}_7 + \dot{M}_8 \quad (\text{Eq. 17})$$

$$\dot{M}_5 = \dot{M}_3 - \dot{M}_4 \quad (\text{Eq. 18})$$

$$\dot{M}_6 = \dot{M}_{15} \quad (\text{Eq. 19})$$

$$\dot{M}_7 = \frac{\dot{M}_{11}}{2} \quad (\text{Eq. 20})$$

$$\dot{M}_8 = \frac{\dot{M}_{11}}{2} \quad (\text{Eq. 21})$$

$$\dot{M}_9 = \dot{M}_{11} - \dot{M}_6 \quad (\text{Eq. 22})$$

$$\dot{M}_{10} = \dot{M}_9 \quad (\text{Eq. 23})$$

$$\dot{M}_{11} = \frac{\dot{M}_6}{RR_{MVC}} \quad (\text{Eq. 24})$$

$$\dot{M}_{12} = \dot{M}_{13} \quad (\text{Eq. 25})$$

$$\dot{M}_{13} = \dot{M}_6 \quad (\text{Eq. 26})$$

$$\dot{M}_{14} = \dot{M}_{10} + \dot{M}_5 \quad (\text{Eq. 27})$$

$$\dot{M}_{15} = \dot{V}_P \cdot \frac{\rho_P}{OT} \quad (\text{Eq. 28})$$

$$\dot{M}_{16} = \dot{M}_7 \quad (\text{Eq. 29})$$

$$\dot{M}_{17} = \dot{M}_8 \quad (\text{Eq. 30})$$

In equations above, $\dot{M}_{1...n} \left[\frac{kg}{h} \right]$ is the mass flow rate in 1 to n-stream from *Figure 30*, $RR_{NF} [-]$ is the recovery ratio of the nanofiltration module, $RR_{MVC} [-]$ is the recovery ratio of the evaporation and condensation module (MVC section), $\dot{V}_P \left[\frac{m^3}{day} \right]$ is the daily production capacity of the system, $\rho_P \left[\frac{kg}{m^3} \right]$ is the density of the produced water, and $OT \left[\frac{h}{day} \right]$ is the operating time per day.

$$X_1 = X_2 \quad (\text{Eq. 31})$$

$$X_2 = X_3 \quad (\text{Eq. 32})$$

$$X_4 = X_5 \cdot (1 - SR) \quad (\text{Eq. 33})$$

$$X_5 = \frac{M_3 \cdot X_3 - M_4 \cdot X_4}{M_5} \quad (\text{Eq. 34})$$

$$X_6 = X_{15} \quad (\text{Eq. 35})$$

$$X_7 = X_4 \quad (\text{Eq. 36})$$

$$X_8 = X_6 \quad (\text{Eq. 37})$$

$$X_9 = \frac{M_{11} \cdot X_{11} - M_6 \cdot X_6}{M_9} \quad (\text{Eq. 38})$$

$$X_{10} = X_9 \quad (\text{Eq. 39})$$

$$X_{11} = X_4 \quad (\text{Eq. 40})$$

$$X_{12} = X_6 \quad (\text{Eq. 41})$$

$$X_{13} = X_{12} \quad (\text{Eq. 42})$$

$$X_{14} = \frac{M_{10} \cdot X_{10} + M_5 \cdot X_5}{M_{14}} \quad (\text{Eq. 43})$$

$$X_{15} = 0.03 \frac{g}{kg} \quad (\text{Eq. 44})$$

$$X_{16} = X_7 \quad (\text{Eq. 45})$$

$$X_{17} = X_8 \quad (\text{Eq. 46})$$

In the equations above $X_{1...n} \left[\frac{g}{kg} \right]$ is the concentration of salt in 1 to n-stream from *Figure 30*; and $SR [-]$ is the salt rejection rate.

To be able to solve this system of equations, it is necessary to define some of the parameters of the system such as: the recovery ratio of mechanical vapor compression RR_{MVC} of 40% based on literature [50], the recovery ratio of nanofiltration RR_{NF} of 90 % and salt rejection rate SR of 40%, which have been both selected based on literature [51]. That means that the system of equations now contains 34 unknown parameters and can be described by 34 equations, thus this system of equations has a solution.

Preheater

In order to start the MVC process, it requires an external thermal energy source. The selected energy source is electric water heater Model ME by the company Hubell Heaters. The water heater is specifically designed for marine use in a remote or offshore environment and has a heating power output of 12 kW.

This water heater is only used when turning on the desalination unit. After the unit generates enough flow rate of distilled water to create the necessary temperature difference in the heat exchangers to recover the thermal energy, the heater is turned off. The necessary electricity required to run this heater is supplied by the PV system.

Nanofiltration Pretreatment

The first part of the design is the selection of the nanofiltration membrane and the high-pressure pump. The purpose of this pump is to create enough pressure to get the seawater through the nanofiltration module and achieve the desired salt rejection rate of 40%.

The NF pretreatment consists of a single-stage one pass module. The selected membrane is FilmTec™ NF-3838/30-FF by the company DuPont, which offers a maximum cross-flow of 6.8 m³/h, maximum operating pressure of 54.8 bar and a pressure drop of 1 bar.

The NF module is equipped with a high-pressure pump CRN 5-16 A-FGJ-A-E-HQQE (see *Figure 31*) by the company Grundfos, which is able to pressurize the feed water up to 9.8 bar at the flowrate calculated in the material balance. Using the Grundfos pump curve tool it was calculated that the necessary power input of the pump is approx. 2 kW (see charts in *Appendix 4*).



Figure 31 Grundfos CRN 5-16 A-FGJ-A-E-HQQE pump [52]

Compressor

The next step in designing this system is the calculation of the compressors performance and power consumption. The purpose of the compressor is to increase the pressure of incoming steam, thus creating superheated steam. The performance of the compressor is calculated in *equation 47* below:

$$W_c = \dot{M}_{12} \cdot (h_{13} - h_{12}) \quad (\text{Eq. 47})$$

In this equation, $\dot{M}_{13} \left[\frac{kg}{s} \right]$ is the mass flow rate of the steam through the compressor, $h_{13} [kJ/kg]$ is the specific enthalpy of the steam feed, $h_{14} [kJ/kg]$ is the specific enthalpy of the superheated steam. Values of both enthalpies were obtained from steam tables and are based on temperatures of vapor and superheated vapor of a typical MVC system from [49].

The power consumption of the compressor is calculated in *equation 48*:

$$P_c = \frac{W_c}{\eta_c} \quad (\text{Eq. 48})$$

In this equation, $W_c [kW]$ is the performance of the compressor, $\eta_c [-]$ is the efficiency of the compressor, which was assumed to be 80%.

Evaporator

The next step is to calculate the heat transfer area. The reason why this parameter is important in this design is that it affects the size and overall cost of the device.

The heat transfer area can be calculated using the *equation 49*:

$$A_e = \frac{\dot{M}_6 \cdot L_6 + \dot{M}_6 \cdot c_{pv} \cdot (T_{13} - T_6)}{U_e \cdot (T_6 - T_9)} \quad (\text{Eq. 49})$$

In this equation, $L_6 \left[\frac{kJ}{kg} \right]$ is the latent heat of stream 6, $c_{pv} \left[\frac{kJ}{kg \cdot K} \right]$ is specific heat capacity of the vapor, $T_{13} [^{\circ}C]$ is the temperature of the superheated steam, $T_6 [^{\circ}C]$ is the temperature of the stream 6 (distilled water), $U_e \left[\frac{kW}{m^2 K} \right]$ is the overall heat transfer coefficient of the evaporator, which has been assumed to be $5 \text{ kW}/(m^2 K)$.

Energy Recovery Section

The energy recovery section consists of two heat exchangers (HE). Plate-and-frame type of HEs was selected in both cases. The performance of distilled water heat exchanger (PHE) can be calculated using either *eq. 50* or *eq. 51* (energy balance):

$$P_{PHE} = \dot{M}_6 \cdot c_{pP} \cdot (T_6 - T_{15}) \quad (\text{Eq. 50})$$

$$P_{PHE} = \dot{M}_7 \cdot c_{pSW} \cdot (T_{16} - T_7) \quad (\text{Eq. 51})$$

In these equations, $\dot{M}_6 \left[\frac{kg}{s} \right]$ is the mass flow rate of the distilled water, $\dot{M}_7 \left[\frac{kg}{s} \right]$ is the mass flow rate of the seawater entering the heat exchanger, $c_{pP} \left[\frac{kJ}{kg K} \right]$ is the specific heat capacity at isobaric conditions of the distilled water, $c_{pSW} \left[\frac{kJ}{kg K} \right]$ is the specific heat capacity at isobaric conditions of seawater, $T_{15} [^{\circ}C]$ is the temperature of distilled water leaving the heat exchanger (stream 15), $T_7 [^{\circ}C]$ is the temperature of seawater entering the heat exchanger (stream 7), $T_{16} [^{\circ}C]$ is the temperature of preheated seawater (stream 16).

The performance of brine water heat exchanger (BHE) can be calculated using either *eq.52* or *eq. 53* (energy balance):

$$P_{BHE} = \dot{M}_8 \cdot c_{pSW} \cdot (T_{17} - T_8) \quad (\text{Eq. 52})$$

$$P_{BHE} = \dot{M}_9 \cdot c_{pB} \cdot (T_9 - T_{10}) \quad (\text{Eq. 53})$$

In these equations, $\dot{M}_8 \left[\frac{kg}{s} \right]$ is the mass flow rate of seawater entering the heat exchanger (stream 8), $\dot{M}_9 \left[\frac{kg}{s} \right]$ is the mass flow rate of brine entering the heat exchanger, $c_{pB} \left[\frac{kJ}{kg K} \right]$ is the specific heat capacity at isobaric conditions of the brine, $T_8 [^{\circ}C]$ is the temperature of seawater entering the heat exchanger (stream 8), $T_9 [^{\circ}C]$ is the temperature of brine entering the heat exchanger (this temperature is calculated through specific enthalpy of the brine stream, which can be obtained from brine tables [53], also shown in *Appendix 5*), $T_{10} [^{\circ}C]$ is the temperature of brine leaving the heat exchanger (stream 10), $T_{17} [^{\circ}C]$ is the temperature of preheated seawater leaving the heat exchanger (stream 17).

The heat transfer area affects the size and capital cost of these heat exchangers (cost of the heat recovery section). The heat transfer area of both HEs is calculated using *equations 54* and *55*:

$$A_{PHE} = \frac{P_{PHE}}{U_{PHE} \cdot \Delta T_{lm,PHE}} [m^2] \quad (\text{Eq. 54})$$

$$A_{PHE} = \frac{P_{BHE}}{U_{BHE} \cdot \Delta T_{lm,BHE}} [m^2] \quad (\text{Eq. 55})$$

In these equations, $U_{PHE} \left[\frac{kW}{m^2K} \right]$ is the overall heat transfer coefficient of the distilled water heat exchanger, $U_{BHE} \left[\frac{kW}{m^2K} \right]$ is the overall heat transfer coefficient of the brine heat exchanger, $\Delta T_{lm,PHE} [K]$ is the logarithmic mean of the temperature difference of the distilled water heat exchanger, $\Delta T_{lm,BHE} [K]$ is the logarithmic mean of the temperature difference of the brine heat exchanger. Since the HEs are in plate-and-frame configuration, the selected overall heat transfer area was selected to be $4 \text{ kW}/(\text{m}^2\text{K})$.

The above-mentioned logarithmic means can be obtained from *equations 56 and 57*:

$$\Delta T_{lm,PHE} = \frac{(T_6 - T_{16}) - (T_{15} - T_7)}{\ln \frac{T_6 - T_{16}}{T_{15} - T_7}} [K] \quad (\text{Eq. 56})$$

$$\Delta T_{lm,BHE} = \frac{(T_9 - T_{17}) - (T_{10} - T_8)}{\ln \frac{T_9 - T_{17}}{T_{10} - T_8}} [K] \quad (\text{Eq. 57})$$

Where $T_i [K]$ is the temperature of i -stream.

Post-treatment

In the post-treatment phase calcium and magnesium are added to the produced water, which is then stored in two 5 m^3 water storage tanks. The total water storage capacity is 10 m^3 , which is approx. one half of the total daily water production.

4.3 PV System Design

The design of the PV system consists of three main steps: PV field design (module selection and field sizing), selection of inverters, and battery selection.

The time of operation was assumed to be 12 hours per day, 355 days of the year.

4.3.1 PV Module Selection & Field Sizing

The idea behind selecting the right type of panels is that the panels should have high efficiency as well as high power output and size. High efficiency of PV panels reduces the total number of panels necessary and higher power output and panel size reduces costs related to frames and mounting.

The reference panel used for designing the PV system is Q.PEAK DUO XL-G11S 580 (shown in *Figure 32*) by the company Qcells USA Corp. with performance 580 kWp and surface area of 2.64 m² (reference to datasheet in *Appendix 6*).



Figure 32 PV panel Q.PEAK DUO XL-G11S 580 (edited from Appendix 6)

The design of the PV system must take into account the location of the desalination unit, since it directly affects the electrical energy output of the panels. The properties of the PV systems of both variants were calculated using values of total solar irradiance (TSI) ranging from 1,500 to 2,150 kWh/m². The value of TSI used for the purposes of the techno-economic study is set at 2,150 kWh/m², since the proposed desalination unit is likely to be implemented in locations with similar TSI values¹⁰.

Total annual consumption of electrical energy of the unit is calculated in *eq. 58*:

$$E_{total} = \frac{P_{total} \cdot OT \cdot ODA}{1000} [MWh] \quad (\text{Eq. 58})$$

¹⁰ Countries with high levels of long-term water scarcity (f.e. Egypt, Saudi Arabia, Turkey) also have high solar irradiation levels as well (ranging from approx. 2000-2500 kWh/m²) [54].

Where P_{total} [kW] is the total necessary input power of the unit (necessary electrical power input minus energy recovered)¹¹, OT $\left[\frac{h}{day}\right]$ is the operating time per day in hours per day, ODA $\left[\frac{days}{year}\right]$ is the number of days of operation annually.

The total electrical input is calculated in eq. 59:

$$E_{PV} = \frac{E_{total}}{\eta_{PV}} [MWh] \quad (\text{Eq. 59})$$

Where η_{PV} [-] is the efficiency of the photovoltaic module.

The total surface area of the PV field is calculated in eq. 60:

$$A_{PV} = \frac{1000 \cdot E_{PV}}{TSI} [m^2] \quad (\text{Eq. 60})$$

Where TSI $\left[\frac{kWh}{m^2}\right]$ is the total solar irradiance.

The number of PV modules is calculated in eq. 61:

$$N_{PV} \doteq \frac{A_{PV}}{A_{PVM}} [-] \quad (\text{Eq. 61})$$

Where A_{PVM} [m²] is the surface area of one PV module.

Since the unit itself is expected to have smaller proportions, the PV panels could be put around the unit with consideration to the fact that the unit could shield the immediate surroundings from direct sunlight.

4.3.2 Inverter Selection

The next important component of the PV system is the selection of the inverter. The inverter is selected so that the DC power input of the inverter is 20-30% bigger than the power output of the PV modules.

For the PV system of variant A two SE100K (shown in *Figure 33*) and one SE66.6K inverters by the company SolarEdge are selected. The maximum inverter efficiency stated by the manufacturer is 98.3% (see *Appendix 7*).

For the PV system of variant B a combination of five SE100K inverters (as in variant A above) and one SE90K inverter are selected.

¹¹ In calculations of variant A, the values used were taken from the datasheets.



Figure 33 SE100K inverter by SolarEdge [55]

4.3.3 Battery Selection

For both desalination units, the set requirement for battery sizing is that the battery would be able to supply at least 10% of the daily energy consumption of both units. The selected batteries are Battery-Box Premium LVS 12.0 for variant A and a combination of Premium LVS 24.0 and Premium LVS 8.0 for variant B. The Battery-Box Premium batteries are all made by BYD Company Limited. The datasheet page is in *Appendix 8*.

4.4 Techno-Economic Study

In this section of the thesis, the economic aspect of both designed units is discussed. In order to evaluate and compare the units, it is important to determine for both designed units the capital cost, the operating cost, and the potential profit. Based on these numbers, it is possible to calculate basic economic parameters such as the return of investment (ROI) from *equation 62*, payback time from *equation 63*.

$$ROI = \frac{C_{total}}{AC_{AP}} [\%] \quad (\text{Eq. 62})$$

In the equation above, C_{total} [\$] is the total initial investment, AC_{AP} [\$] is total accumulated cash after economic assessment period.

$$PP = \frac{C_{total}}{CF} \quad (\text{Eq. 63})$$

In the equation above, $CF \left[\frac{\$}{year} \right]$ is cash flow per year. In other words, the difference between annual profits and operating costs.

Discount rate and inflation factors are not considered in this study.

4.4.1 Capital Costs

The capital costs (CC) consist of two main categories: cost of equipment (desalination technology), cost of the PV system, cost of labor, and other costs. Cost of land is not considered. The cost of equipment is determined by summarizing the purchase prices of all the equipment – the purchase prices can be either calculated or estimated. The cost of the PV system is

calculated separately from the equipment cost. For the purposes of this techno-economic study the labor cost is calculated as 150% of equipment cost in evaluations of both variants. Other costs have been estimated.

Variant A

Capital cost of variant A can be divided into the following sections:

- reverse osmosis,
- energy recovery,
- pretreatment,
- post-treatment.

The selected price of one RO membrane is \$440 taken from [56].

Equipment costs of other sections have been estimated.

Variant B

CC of variant B can be divided into the following sections:

- mechanical vapor compression,
- energy recovery,
- preheating,
- nanofiltration pretreatment,
- post-treatment.

The cost of MVC section consists of two components (price of evaporator and the compressor). The price of the evaporator has been estimated based on market research and the price of the vapor compressor has been estimated by calculating *eq. 64* [50].

$$CC_c = 7364 \cdot M_v \cdot \left(\frac{p_{out}}{p_{in}} \right) \cdot \left(\frac{\eta_c}{1 - \eta_c} \right)^{0.7} \quad (\text{Eq. 64})$$

In this equation, $M_v \left[\frac{kg}{s} \right]$ is the mass flow rate of vapor, $p_{out} [bar]$ is the pressure of superheated steam (leaving the compressor), $p_{in} [bar]$ is the pressure of steam (entering the compressor), $\eta_c [-]$ is the efficiency of the vapor compressor.

The cost of energy recovery section consists of two components (price of PHE and BHE). Prices of both components have been estimated by calculating *equations 65 and 66* respectively [50].

$$CC_{PHE} = 1000 \cdot (12.86 - A_{PHE}^{0.8}) \quad (\text{Eq. 65})$$

$$CC_{BHE} = 1000 \cdot (12.86 - A_{BHE}^{0.8}) \quad (\text{Eq. 66})$$

In these equations, $A_{PHE} [m^2]$ is the heat transfer area of the PHE, $A_{BHE} [m^2]$ is the heat transfer area of the brine.

The cost of NF pretreatment consists of two components (price of the high-pressure pump and nanofiltration module). The price of the HPP was estimated to be approx. \$3,780 [57]. The price

of nanofiltration is based on a price of similar membranes on the market was chosen to be \$450 [58]. The capital cost of the nanofiltration module has therefore been estimated to be \$600.

Equipment costs of other sections have been estimated.

PV System

Capital cost of the PV system is determined by the unit price per module, number of modules, price of the inverter, price of a battery, and cost of additional equipment such as a controller, cables and wiring etc. The price range of a single PV panel proposed in 4.3.1 is approx. \$305 to \$529 [59] [60], the selected price based on this range for one PV panel is \$350. The number of modules was also determined in chapter 4.3.1. The total price of the PV field is calculated in equation 67:

$$CC_{PVF} = N_{PV} \cdot UP_{PVM} \quad (\text{Eq. 67})$$

Where UP_{PVM} [\$] is the unit price per PV module.

The prices of inverters CC_{INV} [\$] are taken from [55]. The prices of batteries are taken from mg-solar-shop website [61].

4.4.2 Operating Cost & Revenue Streams

The operating cost consists primarily of the maintenance cost, which has been estimated to be \$5,000/year, and the cost of chemicals, which can be calculated as approx. \$0.25/m³ of product water [62]. Another expense associated with the operation is the membrane replacement – every 5 years for membranes in variant A and every 6 years for nanofiltration membrane in variant B. The calculation also considers the replacement of the PV system after 20 years.

The revenue of the desalination unit is generated by selling the water produced. The typical price of water for units of similar capacity is \$5.6-\$12.9/m³ [63]. The unit price of freshwater was set to be \$5/m³ for both units to compare the key economic parameters.

4.5 Environmental Impact Assessment Methodology

In this chapter, the methodology of the environmental impact assessment of the designed unit is presented. As stated in the theoretical part of this thesis, desalination is a very environmentally impactful process and that is why the environmental factor should be taken into account before manufacturing and installation. Therefore, the objective of the assessment is to analyze the impacts of the manufacturing and operation of the designed unit.

The scope of the assessment is illustrated in *Figure 34* and contains two parts. The first part of the assessment encompasses impacts of the manufacturing of unit's equipment materials. In order to conduct this part of the assessment, it was necessary to obtain data and information about the materials of each component of the unit – mostly from manufacturer datasheets and published scientific literature. The second part of the assessment concerns impacts of the unit's energy consumption. In the second part, the impacts of the energy produced by the PV panels is compared to two scenarios: 1) the energy consumed by the unit is produced by the European energy market – RER energy mix, 2) the energy consumed by the unit is produced by the Czech energy market – CZ energy mix. The reason for including the additional two energy supply

scenarios is to compare the impacts of PV energy (renewable energy) production to other energy sources. Comparing the energy sources between each other offers a broader context and better illustrates the contrast between environmental impacts of renewable energy sources and conventional sources, which is important to understand, since the energy consumption of desalination processes is high.

Since the design of the desalination unit does not consider any specific location, the impacts of transportation and construction are not a part of this assessment. Pretreatment and post-treatment chemicals were also not included as these parts of the desalination unit were not dealt with in detail in this design.

The functional unit used in this assessment is 1000 m³ of desalinated water.

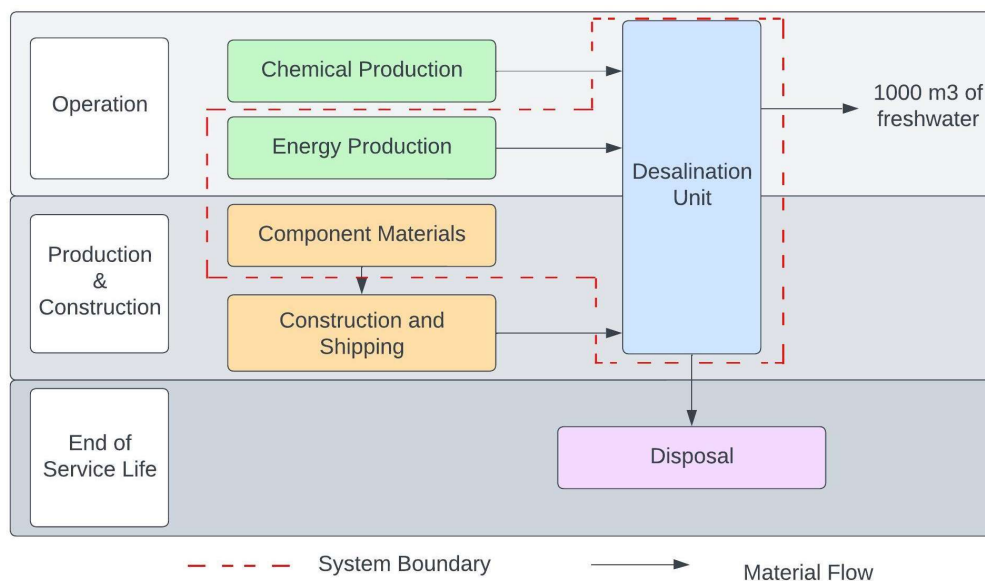


Figure 34 Environmental Assessment Boundaries

The assessment has been conducted using openLCA software (version 1.11.0) and EcoInvent 3.8 database, which contains data about different materials, emissions, methods and processes. The used impact assessment method was the CML method, which classifies environmental impacts into 11 impact categories:

- abiotic depletion – depletion of natural non-fossil resources such as ores or minerals (the reference unit is the equivalent to 1 kg of extracted antimony)
- abiotic depletion (fossil fuels) – depletion of abiotic fossil fuels (the reference unit is MJ)
- acidification – indicator the potential acidification of soils and waters by gases (the reference unit is kg SO₂ equivalent)
- eutrophication – indicates the potential enrichment of surface waters by nutrients (the reference unit is kg PO₄ equivalent),
- freshwater aquatic ecotoxicity – impact of toxic chemicals released into the environment on freshwater organisms (the reference unit is kg 1,4-dichlorobenzene (1,4-DB) equivalent),
- global warming (global warming potential) – indicates the potential global warming due to emissions of greenhouse gases (the reference unit is kg CO₂ equivalent),
- human toxicity – the impact of toxic chemicals on humans (the reference unit is kg 1,4-DB equivalent),

- marine aquatic ecotoxicity – the impact of toxic chemicals released into marine environments on marine ecosystems (the reference unit is kg 1,4-DB equivalent),
- ozone layer depletion – indicates emissions of chemicals that cause the destruction of ozone layer (measured in kg trichlorofluoromethane (CFC-11) equivalent),
- photochemical oxidation – indicates the emissions of gases that cause the creation of photochemical ozone in the lower atmosphere (the reference unit is kg ethene (C₂H₄) equivalents),
- terrestrial ecotoxicity – indicates the release of toxic chemicals (like pesticides) into terrestrial ecosystems (the reference unit is kg 1,4-DB equivalent).

Regarding the assessment results, it had been expected that the comparison between various energy sources would show a significant difference between the impacts of solar energy and electric grid mixes – the CZ energy mix in particular, since fossil fuels amount to 54% of the energy mix (data from 2021)¹² [64].

¹² The fossil fuel representation in the CZ energy mix ranged from 52.5-59.5% annually since 2013 [64].

5 Results & Discussion

In this chapter, the basic design results of both units are summarized and presented. The design mainly focused on desalination technology equipment and PV system. The results are also supplemented by economic analysis, which evaluates basic economic parameters. At the end of the chapter, the environmental impact assessment results are presented and discussed.

5.1 Basic Design Calculations

5.1.1 Variant A

The first step in the basic design of variant A was the material balance calculation. The table material balance and RO parameters (*Table 4*) is based on the scheme in *Figure 26*. The mass flow rate of intake seawater is 4,213 kg/h and has a salinity of 35,000 ppm. This stream flows into the RO membranes which divide it into two streams (permeate and brine). The total permeate flow rate is 1,837.6 kg/h.

Table 4 Material Balance and general desalination properties – variant A

Material Balance				
Stream	M [kg/h]	X _c [g/kg]	X [ppm]	Stream type
1	4,213.0	35.0	35,000	raw seawater
2	4,213.0	35.0	35,000	filtered seawater
3	4,213.0	35.0	35,000	high pressure (HP) seawater
4	2,375.4	61.8	61,844	HP brine
5	1,837.6	0.3	300	permeate
6	2,375.4	61.8	61,844	brine to discharge
General Desalination Properties				
daily desalination capacity				22.1 m ³
number of parallel branches				3
number of passes				6
total feed seawater flow rate				4.1 m ³ /h
total permeate flow rate				1.8 m ³ /h
total brine flow rate				2.3 m ³ /h
recovery ratio				44.8%
minimum salt rejection rate				99.4%

Note: The ratio of the unit conversion of salt concentrations is 1000 g/kg = 1 ppm.

The energy requirements and parameters of the designed unit are shown in *Table 5*. To achieve these results, the electrical power inputs had to be determined based on the total operating time. As per *Table 5* Energy demand parameters – variant A, the HPP has the highest electrical power input of 15 kW, which is relatively high, since the design considers the maximum power input from the datasheet. The expected power input would be lower. Some of the energy (approx. 5.3 kW) is recovered by the ER motor. The item “other” takes into account additional energy demand caused by the unit such as the control unit, other electronics or energy losses.

Table 5 Energy demand parameters – variant A

Electrical Power Requirements	
Device	Electrical Power Input
high pressure pump	15.0 kW
energy recovery	-5.3 kW
other	0.3 kW
Total	10.0 kW
Energy Requirements	
specific energy consumption	5.6 kWh/m ³
daily consumption	120 kWh/day
annual consumption	42,600 kWh/year

Based on calculated results, the required power input is 10 kW. Needless to say, the calculated power input is higher than it would be in reality, since the assumed power input of the HPP which was taken from the datasheet is the maximum energy input at maximum speed and pressure. This assumption increases the specific energy consumption, which is 5.6 kWh/m³ and is still within the range of similar RO plants – the typical energy consumption per m³ of water produced of a RO desalination plant is 2-6 kWh/m³ [12] [65]. The total annual consumption is 42.6 MWh considering the afore-mentioned 355 days of operation.

The results of energy demand obtained above have been used in calculation and sizing of the PV system. The results of PV system sizing are shown in *Table 6*, which also puts into context the relationship between the PV field surface area and the total solar irradiance.

Table 6 PV system parameters – variant A

Total Solar Irradiance [kWh/m²]	Number of panels [-]	PV Field Surface Area [m²]	EE Power Output [kW_p]	PV Field Cost [USD]
1,500	51	134.6	295.8	17,850
1,750	44	116.2	255.2	15,400
2,000	38	100.3	220.4	13,300
2,150	36	95.0	208.8	12,600
inverters – maximum DC power input				269.2 kW
battery capacity				12 kWh

Since it is assumed that the unit would be operating in an area with low freshwater availability and higher sunlight exposure, the design takes into account the results with the highest total solar irradiance. Therefore, the calculated PV system consists of 36 panels with a total power output of 208.8 kW_p, which is higher than typical RO units of similar capacity, although not uncommon. The typical range of the kW_p-to-daily capacity ratio is between 0.2-14.6 kW_p/m³ [63]. In this case, the ratio is equal to 9.3 kW_p/m³. The surface area of the PV field is 95 m².

The power from the PV panels is distributed to the inverters with a maximum DC power input of 269.2 kW, which is approx. 28.9% higher than the power output of the PV panels.

5.1.2 Variant B

The results of material balance of variant B are displayed in *Table 7*. The mass flow rate of intake seawater is 3,689 kg/h and has a salinity of 35,000 ppm. This stream flows first into the NF pretreatment. Then the pretreated seawater at the total flow rate of 3,320 kg/h flows into two heat exchangers where it is preheated before entering the evaporator. The total distilled water (produced water) flow rate is 1.7 m³/h, while discharging 1.9 m³/h of brine.

Table 7 Material Balance and general desalination properties– variant B

Stream number	M [kg/h]	X _c [g/kg]	X [ppm]	Stream type
1	3,688.9	35.0	35,000	raw seawater
2	3,688.9	35.0	35,000	filtered seawater
3	3,688.9	35.0	35,000	pressurized seawater
4	3,320.0	21.0	21,000	pretreated seawater
5	368.9	161.0	161,000	high concentration (HC) brine
6	1,660.0	0.01	10	distilled water
7	1,660.0	21.0	21,000	pretreated seawater
8	1,660.0	21.0	21,000	pretreated seawater
9	1,660.0	42.0	41,990	high temperature (HT) brine
10	1,660.0	42.0	41,990	low temperature (LT) brine
11	3,320.0	21.0	21,000	HT seawater
12	1,660.0	0.01	10	vapor
13	1,660.0	0.01	10	superheated vapor
14	2,028.9	63.6	63,628	brine to discharge
15	1,660.0	0.01	10	chilled distilled water
16	1,660.0	21.0	21,000	HT seawater
17	1,660.0	21.0	21,000	HT seawater
General Desalination Properties				
daily desalination capacity				20 m ³
total feed seawater flow rate				3.6 m ³ /h
total flow rate of produced water				1.7 m ³ /h
total brine flow rate				1.9 m ³ /h
nanofiltration recovery rate				90%
mechanical vapor compression recovery rate				50%
total recovery rate				45%

Note: The ratio of the unit conversion of salt concentrations is 1000 g/kg = 1 ppm.

The energy demand parameters and calculated equipment properties are shown in *Table 8*. After assuming the heat transfer coefficients of the evaporator and both heat exchangers it was possible to calculate the heat transfer surface area and heating power of all three thermal devices. As far as the electrical devices are concerned, the compressor has the highest electrical power input of 20.8 kW. Since the power input is based on theoretical calculation and assumed total efficiency of 80%, it is likely that a custom-built compressor with higher efficiency and compression ratio would have a lower input power.

Table 8 Energy demand parameters – variant B

MVC & ER			
Device	Heat Transfer Coefficient	Heat Transfer Surface Area	Heating Power
evaporator	5 kW/m ² K	35.8 m ²	1,075 kW
PHE	4 kW/m ² K	1.7 m ²	118 kW
BHE	4 kW/m ² K	4.5 m ²	103 kW
Electrical Power Requirements			
Device	Electrical Power Input		
compressor	20.8 kW		
high pressure pump	2.0 kW		
other	0.2 kW		
Total	23.0 kW		
Energy Requirements			
specific electric energy consumption	13.8 kWh/m ³		
daily electric energy consumption	275.4 kWh/day		
annual electric energy consumption	97,767 kWh/year		

The total electric power input required was calculated to be 23 kW and the largest energy consuming device is the compressor and it accounts for 90.4% of the total power requirements. The specific electric energy consumption is 13.8 kWh/m³, which is within the typical range for smaller MVC plants (9-15 kWh/m³) [12] [66].

The results of energy demand obtained above have been used in calculation and sizing of the PV system. The results of PV system sizing are shown in *Table 9*, which also puts into context the relationship between the PV field surface area and the total solar irradiance, similarly to variant A. Since the specific electric energy consumption of this variant is higher than variant A, the total size of the PV system is larger.

Table 9 PV system parameters - variant B

Solar Irradiance [kWh/m²]	Number of panels [-]	PV Field Surface Area [m²]	EE Power Output [kW_p]	PV Field Cost [\$]
1,500	116	306.2	672.8	40,600
1,750	99	261.4	574.2	34,650
2,000	87	229.7	504.2	30,450
2,150	81	213.8	469.8	28,350
inverters – maximum DC power input				595.7 kW
battery capacity				32.3 kWh

The expected solar irradiance was chosen 2,150 kWh/m² (for reasoning see chapter 5.1.1). The PV system consists of 81 PV panels with a total power output of 469.8 kW_p. The total surface area of the PV field is 213.8 m². The selected inverters have a total maximum DC power input of 595.7 kW, which is approx. 26.8% higher than the power output of the PV panels.

5.2 Economic Analysis

In this chapter the results of the techno-economic study are summarized and discussed. Analysis of the capital costs, operating costs, cashflow and economic parameters needs to be done to select the desalination unit variant for the environmental impact assessment. The total investment cost, operating costs and revenue streams of each unit are then used in calculations of cashflow and cumulative cashflow.

Equipment prices are mostly estimations and could change if the units were to be built practically. The price of labor makes up 60% of the total investment and is the biggest expense in both cases regarding the capital cost. The assembly and commissioning costs are dependent on specific pricing details that are negotiated between the customer and the contractor.

5.2.1 Variant A

Overview of capital costs of unit variant A (RO) and variant B (MVC) is shown in *Table 10*. The inventory consists of specific products or items with estimated cost.

Table 10 Capital costs – variant A

Section	Equipment	Cost [\$]	Note
Reverse Osmosis	AMI M-S4040A membranes	7,920	membrane price from [56]
	Danfoss APP 5.1 high-pressure pump	3,000	estimated
	Dual shaft electric motor	1,000	estimated
Energy Recovery	Danfoss APM 2.5 motor	3,000	estimated
Pretreatment	Pretreatment equipment	1,000	estimated
Post-treatment	Water storage tanks	1,000	estimated
PV System	Panels Q.PEAK DUO XL-G11S 580	12,600	panel price based on [59] [60]
	Inverters SolarEdge	14,790	price from [55]
	Battery-Box Premium LVS 12.0	9,310	price from [61]
	Cables and wiring	1,000	estimated
Other	Valves and piping	2,000	estimated
	Sensory and control devices	2,000	estimated
Labor	Assembly and commissioning	87,930	150% of the equipment cost
Total		146,550	-

The total investment cost regarding the variant A desalination unit (reverse osmosis) is approximately \$146,550. The total cost of the desalination technology (sections: reverse osmosis, energy recovery, pretreatment and post-treatment) is \$16,920 and makes up approximately 11.6% of the total investment. The total cost of the PV system is \$36,700 and makes up approx. 25% of the total investment. The most expensive items are the inverters which make up 12% of the total investment. The potential for decreasing the investment costs is mainly in finding equipment sold at a lower price (or locally manufactured and distributed). Another way of lowering the investment cost is by lowering the cost of labor.

The operating costs and revenue streams of variant A are shown in *Table 11*. Annual costs associated with the operation are mainly general maintenance costs and the cost of chemicals used for pretreatment of seawater. The replacement of membranes is also counted as part of the operating costs. The reinvestment into the PV system is also taken into account after 20 years

of operation. The main and only income stream is the sale of drinking water which is \$35,500 per year if the considered price of drinking water is \$5/m³.

Table 11 Operating Costs and Revenue Streams of Variant A

Type	Value	Frequency	Note
General Maintenance & Operation	\$5,000	per year	estimated
Pretreatment Chemicals	\$1,775	per year	calculated based on [62]
Membranes Replacement	\$7,920	every 5 years	calculated based on [56]
HPP and ERD Replacement	\$6,000	after 10 years	based on chapter 4.4.1
Battery Replacement	\$36,700	after 10 years	based on chapter 4.4.1
Revenue Streams			
Drinking Water Sale	\$35,500	per year	calculated
Balance			
Average revenue ¹³	\$26,376	per year	-

The average net revenue (not considering the initial investment) is \$26,376 per year, which is approximately 18% of the initial investment. The total generated income after the assessed period (20 years) is \$527,510. The potential for increasing the average revenue is in lowering the price of maintenance, finding cheaper (or more efficient) membranes for replacement on the market, or increasing the unit price of drinking water. Another income stream could be added by adding fixed fees such as distribution fees, reserved capacity fees, etc.

5.2.2 Variant B

Overview of capital costs of unit variant B (MVC) is shown in *Table 12*. The inventory consists of specific products and products with calculated and estimated costs.

Table 12 Capital costs – variant B

Section	Equipment	Cost [\$]	Note
MVC	Evaporator	53,786	calculated in chapter 4.4.1
	Compressor	11,201	calculated in chapter 4.4.1
Energy Recovery	Distilled water heat exchanger	14,398	calculated in chapter 4.4.1
	Brine heat exchanger	16,199	calculated in chapter 4.4.1
Preheating	Marine electric water heater	1,400	estimated
NF Pretreatment	Seawater pump	3,783	estimated based on [57]
	Nanofiltration module	600	estimated
Post-treatment	Water storage tanks	1,000	estimated
PV System	Panels Q.PEAK DUO XL-G11S 580	28,350	panel price based on [59] [60]
	Inverters SolarEdge	29,100	price from [55]
	BYD batteries	23,521	price from [61]
	Cables and wiring	1,000	estimated
Other	Valves and piping	2,000	estimated
	Sensory and control devices	2,000	estimated
Labor	Assembly and commissioning	282,509	150% of the equipment cost
Total		470,848	-

¹³ Costs with payment frequency longer than one year are divided by their payment frequency [number of years] to obtain the cost per year.

The total investment cost regarding the variant B desalination unit (mechanical vapor compression with nanofiltration pretreatment) is approximately \$470,848. The total cost of the desalination technology (sections: mechanical vapor compression, energy recovery, preheating, nanofiltration pretreatment and post-treatment) is \$102,368 and makes up about 21.7% of the total investment. The total cost of the PV system is \$81,971 and makes up about 17.4% of the total investment. The expenses for the desalination technology equipment (MVC) are higher compared to variant A – mainly because of the complexness due to the usage of thermal technology. The most expensive item is the evaporator, which makes up approx. 11.4% of the total investment. The potential for decreasing the capital cost is mainly in optimizing the PV system. For the purposes of this thesis, the PV system was designed to be more robust to assure enough electric energy generation for the designed unit. Another way of lowering the capital cost could be by lowering the price of labor.

The operating costs and revenue streams of variant B are shown in *Table 13*. In comparison to operating costs of variant A, there is a difference in the cost of PV system replacement and membrane replacement. There is also another cost added and that is the cost of evaporator and the heat exchangers cleaning. The main and only revenue stream is the sale of drinking water which is \$35,500 per year if the considered price of drinking water is \$5/m³.

Table 13 Operating Costs and Revenue Streams of Variant B

Type	Value	Frequency	Note
General Maintenance & Operation	\$5,000	per year	estimated
Pretreatment Chemicals	\$1,775	per year	calculated based on [62]
Evaporator & HE cleaning	\$2,000	every 2 years	estimated
Membrane Replacement	\$450	every 6 years	calculated based on [56]
HPP Replacement	\$3,783	after 10 years	calculated based on 4.4.1
Battery Replacement	\$23,521	after 10 years	calculated based on 4.4.1
Revenue Streams			
Drinking Water Sale	\$35,500	per year	calculated
Balance			
Average revenue ¹⁴	\$26,292	per year	-

The average revenue (not considering the initial investment) is \$26,292 per year, which is approximately 5.6% of the initial investment. The total generated income after the assessed period (20 years) is \$525,846. The potential for increasing the average revenue is in lowering the maintenance cost and optimization of the PV system replacement, which has been stated above. Similarly to variant A, more cost-effective membranes would also help to increase the revenue.

5.2.3 Cashflow Evaluation & Summary

As stated in the methodology chapter 4.4 the economic parameters considered are the payback period, total cumulative cash after the assessed period, and the return on investment. The values of these parameters were determined by calculating (and estimating) the capital cost, identifying the operating cost and income. By putting the determined costs and income together in relation to time, the cashflow table was obtained (shown in *Table 14*).

¹⁴ Costs with payment frequency longer than one year are divided by their payment frequency [number of years] to obtain the cost per year.

Table 14 Cashflow table – comparison

Year	Variant A				Variant B			
	Cumulative Cashflow [\$]	Cashflow [\$]	Income [\$]	Expenses [\$]	Cumulative Cashflow [\$]	Cashflow [\$]	Income [\$]	Expenses [\$]
1	-117,825	-117,825	35,500	-153,325	-442,123	-442,123	35,500	-477,623
2	-89,100	28,725	35,500	-6,775	-415,398	26,725	35,500	-8,775
3	-60,375	28,725	35,500	-6,775	-386,673	28,725	35,500	-6,775
4	-31,650	28,725	35,500	-6,775	-359,948	26,725	35,500	-8,775
5	-10,845	20,805	35,500	-14,695	-331,223	28,725	35,500	-6,775
6	17,880	28,725	35,500	-6,775	-304,948	26,275	35,500	-9,225
7	46,605	28,725	35,500	-6,775	-276,223	28,725	35,500	-6,775
8	75,330	28,725	35,500	-6,775	-249,498	26,725	35,500	-8,775
9	104,055	28,725	35,500	-6,775	-220,773	28,725	35,500	-6,775
10	109,550	5,495	35,500	-30,005	-221,352	-579	35,500	-36,079
11	138,275	28,725	35,500	-6,775	-192,627	28,725	35,500	-6,775
12	167,000	28,725	35,500	-6,775	-166,352	26,275	35,500	-9,225
13	195,725	28,725	35,500	-6,775	-137,627	28,725	35,500	-6,775
14	224,450	28,725	35,500	-6,775	-110,902	26,725	35,500	-8,775
15	245,255	20,805	35,500	-14,695	-82,177	28,725	35,500	-6,775
16	273,980	28,725	35,500	-6,775	-55,452	26,725	35,500	-8,775
17	302,705	28,725	35,500	-6,775	-26,727	28,725	35,500	-6,775
18	331,430	28,725	35,500	-6,775	-452	26,275	35,500	-9,225
19	360,155	28,725	35,500	-6,775	28,273	28,725	35,500	-6,775
20	380,960	20,805	35,500	-14,695	54,998	26,725	35,500	-8,775

The cashflow table shows the expenses, income, cashflow and cumulative cashflow per year in relation to time. The assessed time period was 20 years. The column *Expenses [\$]* displays the expenses and reinvestments associated with units operation each year, the column *Income [\$]* displays the annual total gross income generated by the units, the column *Cashflow [\$]* (total net revenue annually, roughly speaking) is a sum of the expenses and income. The *Cumulative Cashflow [\$]* column displays the current financial state of the investment, as it takes into account the capital cost and annual cashflow.

Based on the table above cashflow diagrams were obtained (shown in *Figure 35* and *Figure 36* for variant A and variant B respectively). These cashflow diagrams give a good idea about the financial viability of both units. It is apparent from the cashflow diagrams that variant A has lower initial investment cost, while having slightly higher annual cashflow (revenue) than variant B. Therefore, variant A pays itself back quicker (and the cumulative cashflow turns into positive numbers) and accumulates more cashflow by the end of the assessment period. In comparison, variant B has a larger initial investment cost and slightly lower annual cashflow. Therefore, the payback period is longer than variant A.

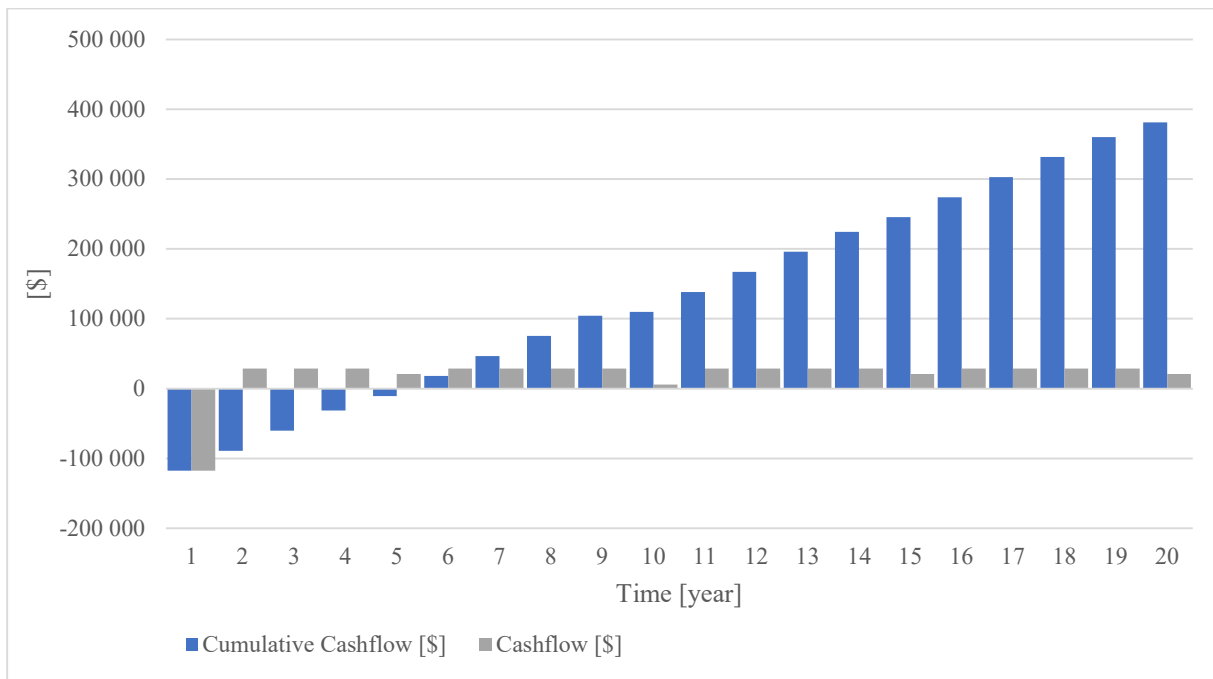


Figure 35 Cashflow diagram of variant A

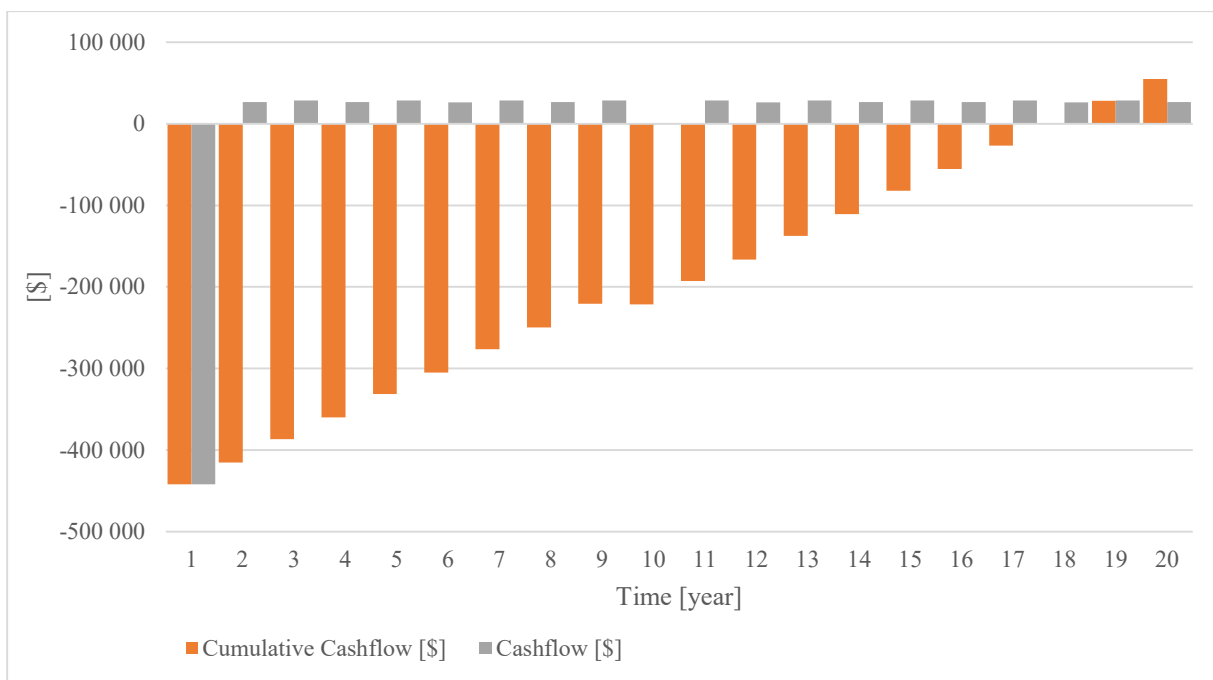


Figure 36 Cashflow diagram of variant B

The exact payback period was calculated to be 5.6 years in the case of variant A and 18.8 years in the case of variant B. The payback period of variant B is approx. 336% longer than the payback period of variant A. Since there is just a small difference (approx. \$84) between the average annual revenues of both units, it is likely that the large capital cost of variant B (mainly the MVC section and PV system section) is the main reason behind the difference between the payback periods.

The total cumulative cashflow after the assessment period (20 years) is \$380,960 for variant A and \$54,998 for variant B. From these numbers it is apparent that variant A is more economically viable and offers up to 260% ROI after the assessment period. In comparison the

ROI of variant B is 11.7%, which deems this variant unprofitable over the assessment period based on used calculations and estimates. The overview of economic parameters considered in this analysis is shown in *Table 15*.

Table 15 Overview of calculated economic parameters

Unit variant	Return on investment	Cumulative cashflow after 20 years	Payback period	Capital Cost	Average Annual Revenue ¹⁵
A	260.0%	\$380,960	5.6 years	\$146,550	\$26,376
B	11.7%	\$54,998	17.9 years	\$470,848	\$26,262

From the economic perspective, the more *financially viable* desalination unit is *variant A – reverse osmosis unit*. The capital cost of variant A is approx. 69% lower than variant B and the operating cost of variant A is higher by approx. 0.3%. Another advantage of variant A is also the option to change the price of water and adapt to different market conditions.

One way of improving the economic parameters and making the investment into such desalination unit attractive is to check and sign up for incentive programs authorized by local governments. For example, the overall amount of renewable energy subsidies paid by the EU has reached about €120 billion in 2020 [67]. These subsidies can decrease the total capital cost, therefore decrease the payback period and increase the ROI.

5.3 Basic Design & Economic Analysis Conclusion

In this section, the results of the design section and the techno-economic study are presented and discussed, and one designed variant will be chosen as the final variant and selected for the environmental impact assessment.

Two different small autonomous desalination units have been designed, one with reverse osmosis technology and one with mechanical vapor compression technology combined with nanofiltration pretreatment technology. Techno-economic study was conducted on both variants, which evaluated the OPEX and CAPEX of both units as well as their payback periods and returns on investment.

Variant A desalinates water by reverse osmosis technology with a total calculated electric power input of 10 kW and specific power consumption of 5.6 kWh/m³. The unit is supplied by a PV field with an electric power output of approx. 209 kW_p that consists of 36 panels that spread out on 95 m² of surface area. The total capital cost was estimated to be \$146,550 and the annual revenue was estimated to be \$26,376. The payback period was calculated to be 5.6 years and the return on investment after 20 years of operation is approx. 260%.

Variant B desalinates water by mechanical vapor compression technology with nanofiltration pretreatment with a total calculated electric power input of 23 kW and specific power consumption of 13.8 kWh/m³. The unit is supplied by a PV field with an electric power output of approx. 470 kW_p that consists of 81 panels that spread out on 213.8 m² of surface area. The total capital cost was estimated to be \$470,848 and the annual revenue was estimated to be \$26,262. The payback period was calculated to be 17.9 years and the return on investment after 20 years of operation is approx. 11.7%.

¹⁵ Does not consider the initial investment cost.

Based on the technical properties and calculated economic parameters of both variants the unit selected for the environmental impact assessment is *variant A – reverse osmosis desalination unit*. The overall scheme of the proposed unit is illustrated in *Appendix 9*. The desalination equipment (PV panels are not included) should be compact and should be able to fit inside a shipping container. The PV panels can be placed around the unit and mounted by concrete blocks, which enables easier construction, assembly and disassembly. If the PV panels were collected, it would be possible to transport the entire unit efficiently. There is a potential for PV system optimization, since the used calculation method did not consider any specific location nor exact power consumption. If the PV system was implemented in a remote settlement, it would be possible to use them as an electricity source for the settlement. Another advantage of the higher number of panels is that it mitigates the impact of peak power output decline, which typically occurs in PV panels over time.

5.4 Environmental Impact Assessment Results

As stated in the methodology chapter, the objective of the environmental impact assessment is to evaluate the manufacturing and operation of the designed reverse osmosis desalination unit. The boundaries of the assessment include manufacturing of the materials and energy consumption of the designed unit per 1000 m³ of desalinated water (the functional unit).

After an extensive literature search and estimations, the life cycle inventory list (in *Table 16*) has been created in order to primarily evaluate the EIs (stated in the assessments methodology) of the unit's manufacturing (the secondary purpose is to conduct the assessment of the energy production). The inventory lists important devices and equipment and their composition of materials with weights. As there are reinvestments and purchases of new equipment expected in its lifetime (also see chapter 5.2.1), these additional materials are included in the inventory list. Moreover, the total weights of materials were converted to relation to 1000 m³ of product¹⁶, which is the functional unit of this assessment. Since the location of the unit's components manufacturing is unknown, the global market (GLO) was selected as a provider of all materials in the Ecoinvent database. When the global market option was not available, the European market was selected (RER).

As far as the material compositions of the equipment is concerned, the largest portion of the weight is thermally pre-stressed glass, which makes 4.7 kg/1000 m³ of product, followed by steel (including stainless steel and regular steel), which makes total 2.9 kg/1000 m³ of product, assuming that the lifetime of the system is 20 years. Other used materials are various metals, heavy metals and different types of plastics.

The material assessment results are graphically illustrated in *Figure 37* and *Figure 38*, after calculating the impacts of different sections of the unit and the total impact per 1000 m³ of product using the CML method. The calculated values of the ozone layer depletion potential (ODP) impact were very low (in the order of 10⁻⁴ kg CFC-11 eq) across all sections, therefore it is not displayed. Overall, the section with the highest values of negative environmental impacts is the battery section.

¹⁶ The conversion has been done by dividing the total weight of material by the total amount of water produced during the unit's lifecycle and then multiplying it by 1000.

Table 16 Life cycle inventory of RO desalination unit

Section	Device	Material	Total Weight [kg]	Specific Weight [kg/1000 m ³]	Reference
Reverse Osmosis	RO Membranes (4x40")	fiberglass with polyester resin	43.2	0.3	[68], Appendix 1
		polyester (PET) with polysulfone (PSF) layer and polyamide (PA) layer	86.4	0.5	
		polypropylene (PP)	25.2	0.2	
		polyester (PET)	32.4	0.2	
		acrylonitrile butadiene styrene (ABS)	86.4	0.5	
		polyurethane glue	28.8	0.2	
	HPP & Electric Motor	stainless steel	306.0	2.0	[69], Appendix 2
		cast iron	18.0	0.1	
		copper	18.0	0.1	
		iron	18.0	0.1	
Energy Recovery	ER Motor	stainless steel	16.3	0.1	estimated, Appendix 3
		copper	0.9	0.01	
Post-treatment	Water Storage Tank	polyvinyl chloride (PVC)	232.0	1.5	[69]
		fiber reinforced plastic	58.0	0.4	
PV System	PV panels	thermally pre-stressed glass	743.0	4.7	[70], Appendix 6
		semi-tempered glass	123.8	0.8	
		aluminum	222.9	1.4	
		monocrystalline silicon	49.5	0.3	
		silver	0.6	0.004	
		polyvinyl fluoride	18.6	0.1	
		EVA adhesive layer	79.9	0.5	
	Inverters	aluminum alloy	9.4	0.1	[71]
		copper	37.1	0.2	
		steel	66.0	0.4	
		electronic components	12.2	0.1	
		packaging	16.8	0.1	
		polymers	2.5	0.02	
	Battery	lithium	110.9	0.7	[72], Appendix 8
		graphite	64.7	0.4	
		copper	30.8	0.2	
		electrolyte (LiPF ₆)	33.9	0.2	
		polypropylene (PP)	6.2	0.04	
steel		61.6	0.4		

As apparent from Figure 37, the battery section has the highest toxicity impacts (marine aquatic ecotoxicity, freshwater toxicity, human toxicity and terrestrial toxicity) of all sections. This is mainly due to the extraction of lithium and copper, which are generally known to have high toxicity impacts [73] [74].



Figure 37 LCA results materials - sections

The battery section accounts for 34-39% of the total unit’s toxicity impacts. As far as the global warming potential (GWP) is concerned, the materials of the PV panels section and the battery section account for 37% and 43% respectively, making up total 80% of the unit’s total CO₂ emissions equivalent. Moreover, both sections account for 75% of the total unit’s abiotic depletion (fossil fuel). This is mainly because of lithium extraction for the batteries and silicon extraction for the PV panels. The extractions of both elements have been known to be energy-intensive processes [73] [75]. Overall, the PV system has significantly higher environmental impact than the other processes. The environmental impacts of the sections combined – summarized environmental impacts of the designed desalination unit’s materials – are shown in *Figure 38*.

The biggest contributor to abiotic depletion is the inverters section, since it contains copper components and electronics. In the case of abiotic depletion (fossil fuels), the most impactful sections are the PV panels and the battery. The levels of fossil fuels depletion correspond to their GWP mentioned above. As far as other impacts are concerned, the largest contributor is the battery section in all cases.

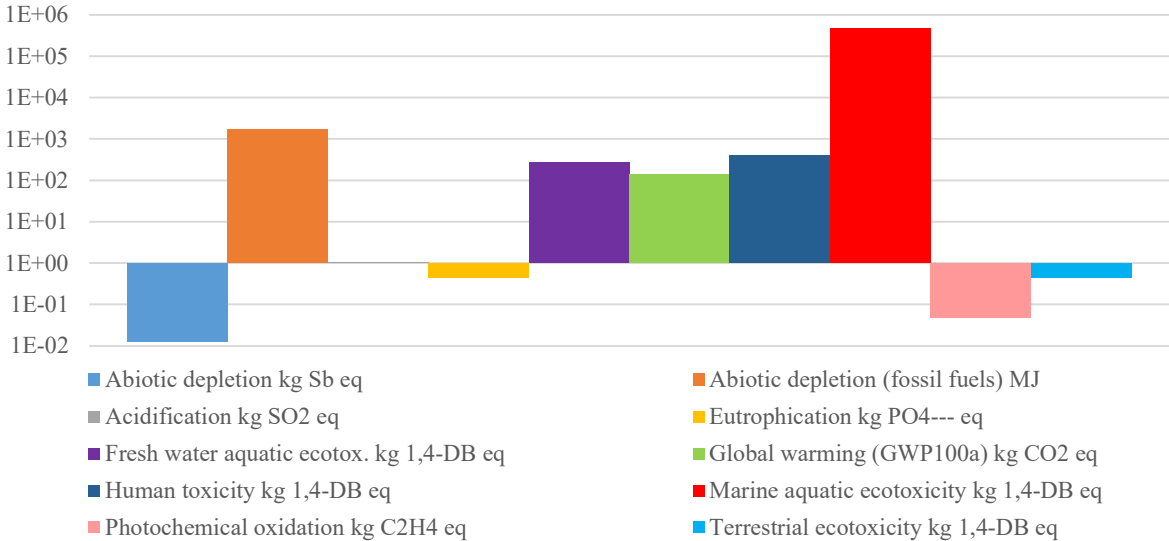


Figure 38 LCA material manufacturing results – total impacts

The second part of the assessment investigated the impacts of the unit’s energy consumption. The main input was the calculated specific electric energy consumption of 5.6 kWh/m³, which makes 5.6 MWh/1000 m³ after conversion to the functional unit. Overall, to conduct this part of the assessment, the same CML method was used as in the previous part. Specifically, the main investigated impact was the global warming potential (GWP). In this part of the assessment, the comparison between the PV electricity source, the European electricity grid supply and the Czech electricity grid supply was included, to provide context.

The calculated results validate the assumption that the PV system is a way less negatively impactful energy source than the energy supply from both grid systems. Compared to the PV system, the impacts of both electricity grids were multiple times higher in some cases – the comparison of impacts is shown in *Figure 39*, the total impacts of the PV energy production are shown in *Figure 40*. The biggest contrast could be seen between the eutrophication potentials of the Czech electricity grid supply and the PV system. The Czech electricity grid had 61 times higher impact on EP than the PV system. As far as the key impact in this study (the GWP) is concerned, the European electricity grid supply generates 11 times and the Czech

electricity grid generates 24 times the amount of CO₂ equivalents than the PV system per one functional unit. A big portion of electricity produced in the Czech Republic comes from fossil fuels – mostly coal plants (43.9%) and coal has a high carbon footprint [64]. The European electricity market contains more renewable energy sources (approximately 22.3%), whereas the share of renewable energy sources on the Czech market is lower (approximately 5.6%) [64] [76]. These facts explain the differences between both electricity markets and the PV system eventually.

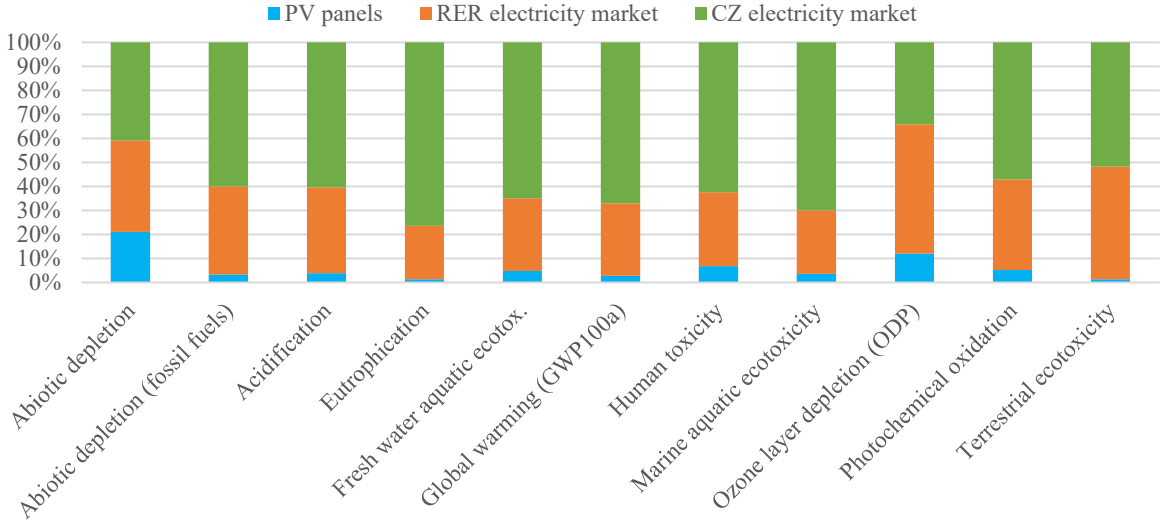


Figure 39 Environmental impacts of energy production - three sources comparison

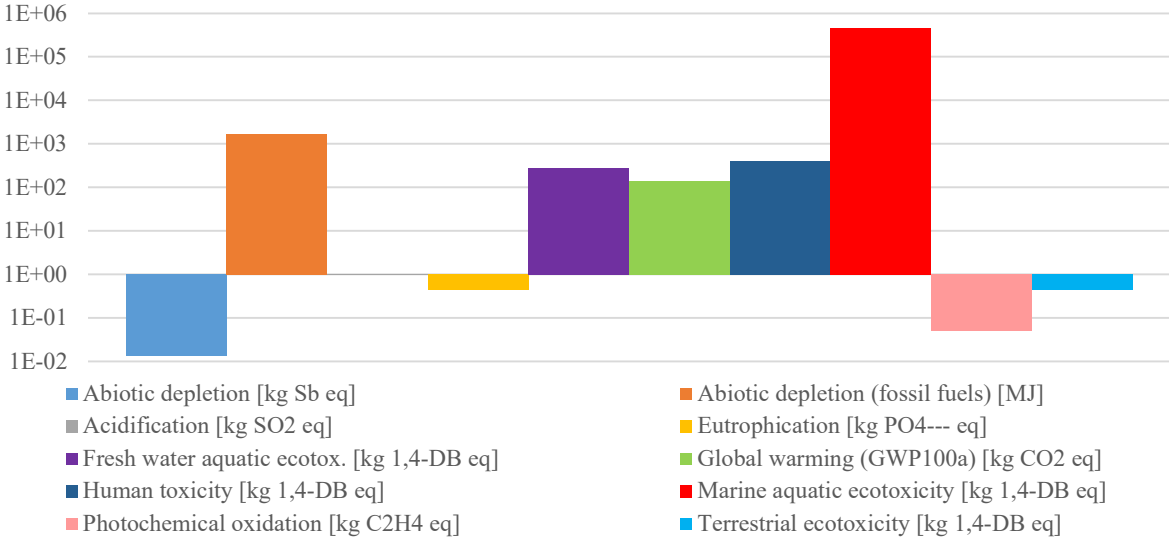


Figure 40 LCA photovoltaic energy production – total impacts

In conclusion, the evaluated impacts of material manufacturing range between 41-54% of the total unit's impacts – the percentages are illustrated in *Figure 41*. The global warming potential impact of the entire desalination unit is identified as 355 kg CO₂eq/1000m³ of desalinated water, with 42% (117 kg CO₂eq/1000m³ in absolute units) contributed by material manufacturing and 58% (196 kg CO₂eq/1000m³ in absolute units) contributed by energy production. After conversion¹⁷, the amount of kg CO₂ equivalents produced by the photovoltaic energy production is 35 g CO₂eq/kWh, which is comparable to the GHG emissions by PV panels listed in other sources [77] [78].

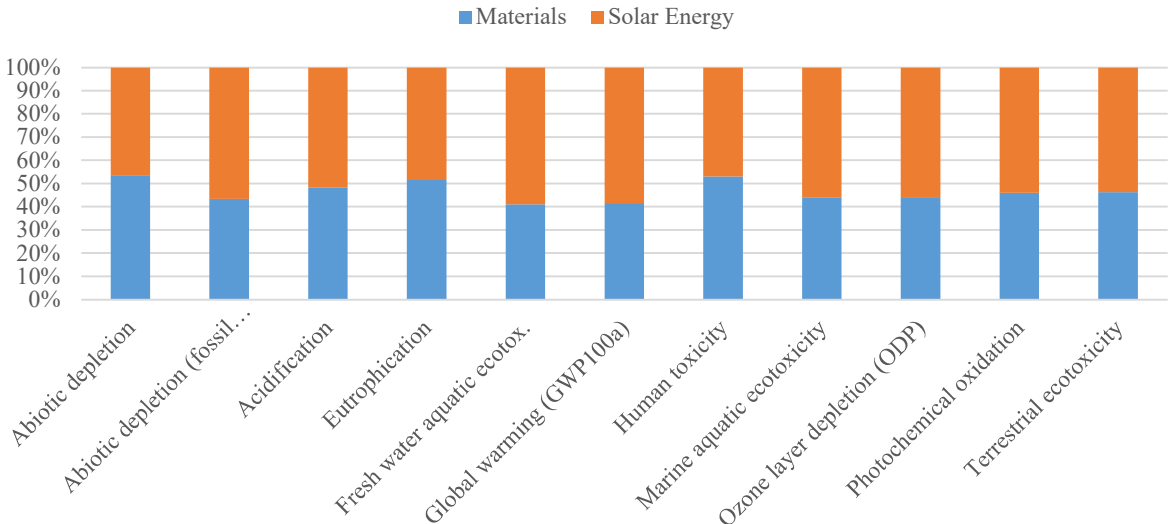


Figure 41 Environmental impacts of the unit – materials and energy comparison

¹⁷ The mass of kg CO₂ eq divided by 5564 kWh/1000 m³ (specific electricity consumption) and multiplied by 1000.

6 Conclusions

Desalination is an approach of producing drinking water in areas with long-term water scarcity and access to seawater. Despite its numerous, it is crucial to acknowledge and address the technological, economic and environmental drawbacks of the process. The main challenge is to strike a balance between the benefits and drawbacks arising from its high energy consumption, investment cost and waste production in the form of brine. However, as water scarcity continues to grow as a widespread issue and the reliance on desalination increases, it becomes imperative to mitigate and manage the environmental impacts of this technology.

The main objectives of this thesis were to design a small autonomous desalination unit which is powered by solar energy and conduct a feasibility assessment on this unit. One of the main outcomes of this thesis is the extension of knowledge about the environmental impact of desalination powered by photovoltaic energy. Another practical outcome is the functional small-scale unit, which can serve as a basis for a detailed design for a similarly designed unit, suitable for drinking water production in remote communities.

Based on the state-of-the-art of desalination technologies, two units utilizing two different desalination technologies were designed along with their corresponding photovoltaic systems. The first unit utilizes reverse osmosis (membrane process), which provides low energy consumption and low investment cost while maintaining acceptable water quality levels. The second unit utilizes mechanical vapor compression (thermal process), which provides high water quality and easy maintenance. Techno-economic study has been conducted on both units. The designed reverse osmosis unit has a lower specific energy consumption of 5.6 kWh/m³ and is powered by 36 solar panels, compared to 13.8 kWh/m³ powered by 81 solar panels of the designed mechanical vapor compression unit. The investment cost of the reverse osmosis unit is \$146,550, compared to \$470,848 for the mechanical vapor compression unit. Based on the energy consumption and economic parameters, the reverse osmosis unit was deemed a preferable option and was selected for further environmental impact assessment.

The software openLCA software equipped with the Ecoinvent 3.8 database was used to conduct the environmental impact assessment. The main purpose of the evaluation is to analyze the impacts of the extraction of materials used to manufacture the unit's equipment and evaluate the impact of its energy consumption. To provide context for the energy consumption evaluation, a comparison to other energy sources (European electricity market and Czech electricity market) was performed. The method used in the assessment was the CML-IA baseline method, where 11 environmental impacts were considered. As per the assessment results, the largest contributor to negative environmental impacts is the unit's battery and PV panels. They contain a relatively high amount of extracted metals, minerals and other chemicals. The impact of the unit's energy consumption in the case of PV system electricity production is significantly lower than production from the European or the Czech electricity markets. Global warming potential was the primarily investigated impact. It was found that the GWP impact of PV panel electricity production is 11 times lower compared to the European electricity market and 24 times lower compared to the Czech electricity market, which proves that utilizing photovoltaic panels to supply small desalination plants can be a sustainable way of producing drinking water with lower harm to the environment.

However, the conducted design focused only on the main desalination technology and its photovoltaic system. Moreover, the photovoltaic system was designed in a conservative manner so it might require optimization to reduce its size. Additionally, the environmental impact assessment took into account only the energy production part of the unit's operation.

Given these drawbacks, these are the follow-up suggestions on further research investigations:

- execute a detailed design of the pretreatment and post-treatment sections,
- optimize the size of the PV system,
- consider the pretreatment and post-treatment chemicals in the environmental impact assessment,
- investigate the environmental impacts of seawater intake and brine production,
- compare the parameters of the designed unit with a unit utilizing an emerging desalination technology.

The future research should be built on the designed unit and should investigate the environmental impacts that are less covered in scientific literature. Even though small autonomous desalination units offer an attractive solution to water scarcity, the unwanted negative impact on the environment of their operation should be carefully assessed and considered before building such units.

List of Symbols & Abbreviations

Nomenclature	
ABS	acrylonitrile butadiene styrene
AP	acidification potential
BHE	brine heat exchanger
CA	cellulose acetate
Ca ²⁺	calcium
CAPEX	capital expenditures
CDI	capacitive deionization
CED	cumulative energy demand
CO ₂	carbon dioxide
CPV	concentrator photovoltaics
CSP	concentrated solar power
DAR	depletion of abiotic resources
E&C	evaporation & condensation
ED	electrodialysis
EI	environmental impact
EIA	environmental impact assessment
EP	eutrophication potential
ERD	energy recovery device
ETP	ecotoxicity potential
EU	European Union
EVA	ethylene-vinyl acetate
FO	forward osmosis
FWU	freshwater use
GHG	greenhouse gas
GWP	global warming potential
HE	heat exchanger
HP	high pressure
HPP	high-pressure pump
HTP	human toxicity potential
HY	hydration
IXR	ion exchange resin
LCA	life-cycle assessment
LiPF ₆	lithium hexafluorophosphate
MED	multi-effect distillation
MES	multi-effect stack evaporator
Mg ²⁺	magnesium
MSF	multi-stage flash distillation
MVC	mechanical vapor compression
NaCl	sodium chloride
NF	nanofiltration
O&M	operation & maintenance
OPEX	operating expenditures
PE	population equivalent
PET	polyester
pH	potential hydrogen
PHE	distillate heat exchanger
PHO	photochemical oxidation
PV	photovoltaic
RES	renewable energy desalination
RO	reverse osmosis
RPX	rotary pressure exchanger
TBT	top brine temperature
TDS	total dissolved
TFC	thin-film composite
TVC	thermal vapor compression
USA	United States of America
VC	vapor compression
VF	vacuum freezing
WHO	World Health Organization

Symbol	Meaning	Unit
A	surface area	m ²
AC	accumulated cashflow	\$
C	cost	\$
CC	capital cost	\$
CF	cashflow	\$
c	specific heat capacity	kJ/(kg·K)
E	energy	kJ, kWh
h	specific enthalpy	kJ/kg
L	latent heat	kJ/kg
M	mass, mass flow	kg, kg/h
N	number	-
ODA	operating days annually	days
OT	operating time	hours
p	pressure	MPa, bar
P	performance, energy input	kW
ROI	return on investment	%
RR	recovery ratio	%
SR	salt rejection ratio	%
T	temperature	°C, K
TSI	total solar irradiation	kWh/m ²
U	overall heat transfer coefficient	kW/m ² K
UP	solar panel unit price	\$
V	volume, volumetric flow	m ³ , m ³ /h
W	performance, energy output	kW
X	salt concentration	g/kg, ppm
ΔT _{lm}	log. mean temperature difference	K
η	efficiency	%
ρ	density	kg/m ³

List of Figures

Figure 1 World map of blue water scarcity (Period: 1996-2005) [1].....	15
Figure 2 The timeline of desalination technologies [12].....	17
Figure 3 Customer-type breakdown on the basis of global desalination capacity [17]	18
Figure 4 Global distribution of operational desalination plants [16]	18
Figure 5 Classification of Desalination Technologies - adopted from [12].....	20
Figure 6 Graph of technology breakdown of installed global desalination - data from [27]...	21
Figure 7 Graph of the relationship between number of evaporation stages and capital costs .	22
Figure 8 Scheme of the MED process [12].....	23
Figure 9 Scheme of the through-flow MSF process [12].....	25
Figure 10 The temperature profile of through-flow MSF process [18]	25
Figure 11 Scheme of the recycling MSF process [12].....	26
Figure 12 Temperature profile of a recycling MSF process [18].....	26
Figure 13 Scheme of the MVC process [12].....	27
Figure 14 Scheme of the TVC process [12].....	28
Figure 15 The principle of osmotic pressure [12].....	29
Figure 16 Scheme of the RO desalination process [12]	30
Figure 17 Plate-and-Frame membrane configuration [34].....	31
Figure 18 Tubular membrane module [33]	31
Figure 19 Hollow Fiber membrane configuration [33].....	31
Figure 20 Spiral-wound membrane module [33]	32
Figure 21 Rotary Pressure Exchanger scheme [12]	32
Figure 22 The working principle and scheme of nanofiltration technology [12]	34
Figure 23 Graphs of trends and history in desalination research [18]	35
Figure 24 Combinations of RES with Desalination Technologies – adopted from [12]	36
Figure 25 Thesis Methodology	39
Figure 26 Variant A scheme.....	42
Figure 27 Single element membrane AMI M-S4040A (taken from Appendix 1).....	43
Figure 28 Danfoss APP (W) 5.1 high pressure pump [48]	44
Figure 29 Installation of the APM motor and the APP pump (reference to Appendix 3)	45
Figure 30 Variant B scheme.....	46
Figure 31 Grundfos CRN 5-16 A-FGJ-A-E-HQQE pump [52].....	49
Figure 32 PV panel Q.PEAK DUO XL-G11S 580 (edited from Appendix 6).....	52
Figure 33 SE100K inverter by SolarEdge [55]	54
Figure 34 Environmental Assessment Boundaries.....	57
Figure 35 Cashflow diagram of variant A.....	67
Figure 36 Cashflow diagram of variant B.....	67
Figure 37 LCA results materials - sections	71
Figure 38 LCA material manufacturing results – total impacts	72
Figure 39 Environmental impacts of energy production - three sources comparison.....	73
Figure 40 LCA photovoltaic energy production – total impacts.....	73
Figure 41 Environmental impacts of the unit – materials and energy comparison.....	74

List of Appendices

- Appendix 1 AMI M-S4040A Datasheet
- Appendix 2 Danfoss APP High Pressure Pump Datasheet Pages
- Appendix 3 Danfoss APM Energy Recovery Motor Datasheet Pages
- Appendix 4 Grundfos Pump Curves Tool Results
- Appendix 5 Brine Tables Page
- Appendix 6 QCells Q.PEAK DUO XL-G11 PV Panel Datasheet
- Appendix 7 SolarEdge Inverter Datasheet Page
- Appendix 8 BYD Battery-Box Datasheet Page
- Appendix 9 Scheme of Variant A: RO Desalination Unit

List of References

- [1] M. M. Mekonnen and A. Y. Hoekstra, “Four billion people facing severe water scarcity,” *Sci. Adv.*, vol. 2, no. 2, p. e1500323, Feb. 2016, doi: 10.1126/sciadv.1500323.
- [2] R. Hochstrat, T. Wintgens, C. Kazner, T. Melin, and J. Gebel, “Options for water scarcity and drought management—the role of desalination,” *Desalination and Water Treatment*, vol. 18, no. 1–3, pp. 96–102, Jun. 2010, doi: 10.5004/dwt.2010.1347.
- [3] DG Environment, European Commission, “Water Scarcity & Droughts In-Depth Assessment.” Jun. 2007.
- [4] C. He *et al.*, “Future global urban water scarcity and potential solutions,” *Nat Commun*, vol. 12, no. 1, p. 4667, Aug. 2021, doi: 10.1038/s41467-021-25026-3.
- [5] A. Y. Hoekstra and M. M. Mekonnen, “The water footprint of humanity,” *Proc. Natl. Acad. Sci. U.S.A.*, vol. 109, no. 9, pp. 3232–3237, Feb. 2012, doi: 10.1073/pnas.1109936109.
- [6] F. Jaramillo and G. Destouni, “Local flow regulation and irrigation raise global human water consumption and footprint,” *Science*, vol. 350, no. 6265, pp. 1248–1251, Dec. 2015, doi: 10.1126/science.aad1010.
- [7] L. Rosa, D. D. Chiarelli, C. Tu, M. C. Rulli, and P. D’Odorico, “Global unsustainable virtual water flows in agricultural trade,” *Environ. Res. Lett.*, vol. 14, no. 11, p. 114001, Nov. 2019, doi: 10.1088/1748-9326/ab4bfc.
- [8] M. Petruzzello, “water scarcity,” *Encyclopedia Britannica*, Jan. 23, 2023. <https://www.britannica.com/topic/water-scarcity>
- [9] D. Zetland, *The end of abundance: economic solutions to water scarcity*. Amsterdam ; Mission Viejo: Aguanomics Press, 2011.
- [10] D. Garrick *et al.*, “Scalable solutions to freshwater scarcity: Advancing theories of change to incentivise sustainable water use,” *Water Security*, vol. 9, p. 100055, Apr. 2020, doi: 10.1016/j.wasec.2019.100055.
- [11] O. K. Buros, *The ABCs of Desalting*, Second Edition. Topsfield, Massachusetts, USA: International Desalination Association.
- [12] D. Curto, V. Franzitta, and A. Guercio, “A Review of the Water Desalination Technologies,” *Applied Sciences*, vol. 11, no. 2, p. 670, Jan. 2021, doi: 10.3390/app11020670.
- [13] W. Weir, *The Weir Group: the history of a Scottish engineering legend, 1872 - 2008*. London: Profile Books, 2008.
- [14] N. Lior, *Advances in water desalination*. in *Advances in Water Desalination*, no. v. 1. Hoboken, N.J: Wiley, 2012.
- [15] GWI, *IDA Desalination Yearbook 2008-2009*. London: Global Water Intelligence, 2009.

- [16] E. Jones, M. Qadir, M. T. H. van Vliet, V. Smakhtin, and S. Kang, “The state of desalination and brine production: A global outlook,” *Science of The Total Environment*, vol. 657, pp. 1343–1356, Mar. 2019, doi: 10.1016/j.scitotenv.2018.12.076.
- [17] H. A. Arafat and Eds., *Desalination sustainability: a technical, socioeconomic, and environmental approach*. Amsterdam, Netherlands: Elsevier, 2017.
- [18] H. Zheng, *Solar energy desalination technology*. Amsterdam, Netherlands: Elsevier, 2017.
- [19] S. Kalogirou, “Survey of solar desalination systems and system selection,” *Energy*, vol. 22, no. 1, pp. 69–81, Jan. 1997, doi: 10.1016/S0360-5442(96)00100-4.
- [20] A. Subramani, M. Badruzzaman, J. Oppenheimer, and J. G. Jacangelo, “Energy minimization strategies and renewable energy utilization for desalination: A review,” *Water Research*, vol. 45, no. 5, pp. 1907–1920, Feb. 2011, doi: 10.1016/j.watres.2010.12.032.
- [21] D. Kim, G. L. Amy, and T. Karanfil, “Disinfection by-product formation during seawater desalination: A review,” *Water Research*, vol. 81, pp. 343–355, Sep. 2015, doi: 10.1016/j.watres.2015.05.040.
- [22] A. M. K. El-Ghonemy, “Performance test of a sea water multi-stage flash distillation plant: Case study,” *Alexandria Engineering Journal*, vol. 57, no. 4, pp. 2401–2413, Dec. 2018, doi: 10.1016/j.aej.2017.08.019.
- [23] A. Alkaisi, R. Mossad, and A. Sharifian-Barforoush, “A Review of the Water Desalination Systems Integrated with Renewable Energy,” *Energy Procedia*, vol. 110, pp. 268–274, Mar. 2017, doi: 10.1016/j.egypro.2017.03.138.
- [24] Z. Zimerman, “Development of large capacity high efficiency mechanical vapor compression (MVC) units,” *Desalination*, vol. 96, no. 1–3, pp. 51–58, Jun. 1994, doi: 10.1016/0011-9164(94)85156-5.
- [25] G. Wetterau, Ed., *Desalination of seawater: AWWA manual M61*, 1st ed. Denver, CO: American Water Works Association, 2011.
- [26] M. Talaeipour, J. Nouri, A. H. Hassani, and A. H. Mahvi, “An investigation of desalination by nanofiltration, reverse osmosis and integrated (hybrid NF/RO) membranes employed in brackish water treatment,” *J Environ Health Sci Engineer*, vol. 15, no. 1, p. 18, Dec. 2017, doi: 10.1186/s40201-017-0279-x.
- [27] *DesalData*, 2016. <http://desaldata.com/>
- [28] A. Bennett, “Cost effective desalination: Innovation continues to lower desalination costs,” *Filtration + Separation*, vol. 48, no. 4, pp. 24–27, Jul. 2011, doi: 10.1016/S0015-1882(11)70164-1.
- [29] M. Al-Shammiri and M. Safar, “Multi-effect distillation plants: state of the art,” *Desalination*, vol. 126, no. 1–3, pp. 45–59, Nov. 1999, doi: 10.1016/S0011-9164(99)00154-X.

- [30] M. Shatat and S. B. Riffat, "Water desalination technologies utilizing conventional and renewable energy sources," *International Journal of Low-Carbon Technologies*, vol. 9, no. 1, pp. 1–19, Mar. 2014, doi: 10.1093/ijlct/cts025.
- [31] S. A. Kalogirou, "Solar Desalination Systems," in *Solar Energy Engineering*, Elsevier, 2014, pp. 431–479. doi: 10.1016/B978-0-12-397270-5.00008-X.
- [32] A. Al-Karaghoul and L. L. Kazmerski, "Energy consumption and water production cost of conventional and renewable-energy-powered desalination processes," *Renewable and Sustainable Energy Reviews*, vol. 24, pp. 343–356, Aug. 2013, doi: 10.1016/j.rser.2012.12.064.
- [33] M. Qasim, M. Badrelzaman, N. N. Darwish, N. A. Darwish, and N. Hilal, "Reverse osmosis desalination: A state-of-the-art review," *Desalination*, vol. 459, pp. 59–104, Jun. 2019, doi: 10.1016/j.desal.2019.02.008.
- [34] P. Pal, J. Sikder, S. Roy, and L. Giorno, "Process intensification in lactic acid production: A review of membrane based processes," *Chemical Engineering and Processing: Process Intensification*, vol. 48, no. 11–12, pp. 1549–1559, Nov. 2009, doi: 10.1016/j.cep.2009.09.003.
- [35] J. Martin and D. Eisberg, "Brackish Water Desalination - Energy and Cost Consideration," *International Desalination Assoc. World Congr. Desalin. Water Reuse*, vol. 2007, no. 22, pp. 99–131.
- [36] V. V. Volkov, B. V. Mchedlishvili, V. I. Roldugin, S. S. Ivanchev, and A. B. Yaroslavtsev, "Membranes and nanotechnologies," *Nanotechnol Russia*, vol. 3, no. 11–12, pp. 656–687, Dec. 2008, doi: 10.1134/S1995078008110025.
- [37] M. K. Wafi, N. Hussain, O. El-Sharief Abdalla, M. D. Al-Far, N. A. Al-Hajaj, and K. F. Alzonnikah, "Nanofiltration as a cost-saving desalination process," *SN Appl. Sci.*, vol. 1, no. 7, p. 751, Jul. 2019, doi: 10.1007/s42452-019-0775-y.
- [38] M. Turek *et al.*, "Improving the Performance of a Salt Production Plant by Using Nanofiltration as a Pretreatment," *Membranes*, vol. 12, no. 12, p. 1191, Nov. 2022, doi: 10.3390/membranes12121191.
- [39] J. Bundschuh, M. Kaczmarczyk, N. Ghaffour, and B. Tomaszewska, "State-of-the-art of renewable energy sources used in water desalination: Present and future prospects," *Desalination*, vol. 508, p. 115035, Jul. 2021, doi: 10.1016/j.desal.2021.115035.
- [40] M. Asaka, "Water Desalination Using Renewable Energy." IEA-ETSAP and IRENA, Mar. 2012.
- [41] E. Delyannis, "Historic background of desalination and renewable energies," *Solar Energy*, vol. 75, no. 5, pp. 357–366, Nov. 2003, doi: 10.1016/j.solener.2003.08.002.
- [42] W. W. Boesch, "World's first solar powered reverse osmosis desalination plant," *Desalination*, vol. 41, no. 2, pp. 233–237, May 1982, doi: 10.1016/S0011-9164(00)88726-3.

- [43] O. Alnajdi, Y. Wu, and J. Kaiser Calautit, "Toward a Sustainable Decentralized Water Supply: Review of Adsorption Desorption Desalination (ADD) and Current Technologies: Saudi Arabia (SA) as a Case Study," *Water*, vol. 12, no. 4, p. 1111, Apr. 2020, doi: 10.3390/w12041111.
- [44] K. Lee and W. Jepson, "Environmental impact of desalination: A systematic review of Life Cycle Assessment," *Desalination*, vol. 509, p. 115066, Aug. 2021, doi: 10.1016/j.desal.2021.115066.
- [45] M. P. Shahabi, A. McHugh, M. Anda, and G. Ho, "Environmental life cycle assessment of seawater reverse osmosis desalination plant powered by renewable energy," *Renewable Energy*, vol. 67, pp. 53–58, Jul. 2014, doi: 10.1016/j.renene.2013.11.050.
- [46] S. Kalogirou, "Seawater desalination using renewable energy sources," *Progress in Energy and Combustion Science*, vol. 31, no. 3, pp. 242–281, 2005, doi: 10.1016/j.peccs.2005.03.001.
- [47] F. Vince, F. Marechal, E. Aoustin, and P. Bréant, "Multi-objective optimization of RO desalination plants," *Desalination*, vol. 222, no. 1–3, pp. 96–118, Mar. 2008, doi: 10.1016/j.desal.2007.02.064.
- [48] Lenntech, "Danfoss pump APP 5.1 ATEX High Pressure Pump," *Lenntech*. <https://www.lenntech.com/products/Danfoss-pump/180B3105/APP-5.1-ATEX-High-Pressure-Pump/index.html>
- [49] H. S. Aybar, "Analysis of a mechanical vapor compression desalination system," *Desalination*, vol. 142, no. 2, pp. 181–186, Feb. 2002, doi: 10.1016/S0011-9164(01)00437-4.
- [50] M. A. Farahat, H. E. S. Fath, I. I. El-Sharkawy, S. Ookawara, and M. Ahmed, "Energy/exergy analysis of solar driven mechanical vapor compression desalination system with nano-filtration pretreatment," *Desalination*, vol. 509, p. 115078, Aug. 2021, doi: 10.1016/j.desal.2021.115078.
- [51] N. Hilal, H. Al-Zoubi, A. W. Mohammad, and N. A. Darwish, "Nanofiltration of highly concentrated salt solutions up to seawater salinity," *Desalination*, vol. 184, no. 1–3, pp. 315–326, Nov. 2005, doi: 10.1016/j.desal.2005.02.062.
- [52] Grundfos Holding A/S, "CRN 5-16 A-FGJ-A-E-HQQE," *GRUNDFOS*. <https://product-selection.grundfos.com/products/cr-cre-cri-crie-crn-crne-crt-crte/crn/crn-5-16-96517195?tab=variant-curves&pumpsystemid=2089408247>
- [53] G. L. Dittman, "Calculation of Brine Properties." Lawrence Livermore Laboratory, Feb. 16, 1977.
- [54] ESMAP 2019, "Global Solar Atlas 2.0 Technical Report," Washington, DC: World Bank.
- [55] SunWatts, "100kW SolarEdge Three Phase Inverter with Synergy Technology 277/480V," *sunwatts*, 2023. <https://sunwatts.com/100kw-solaredge-three-phase-inverter-with-synergy-technology-277-480v/>

- [56] WaterAnywhere, “4"x40" | 1950 GPD | 99.6% Salt Rejection | Seawater RO Membrane | Applied Membranes,” *wateranywhere*, 2021. <https://wateranywhere.com/4-x40-1950-gpd-99-6-salt-rejection-seawater-ro-membrane-applied-membranes/>
- [57] Manufacturers Edge, Inc., “99917098,” *PumpCatalog.com*, 2023. <https://www.pumpcatalog.com/grundfos/cr-multistage-pumps/99917098/>
- [58] WaterAnywhere, “4"x40" | 97% Salt Rejection | 2,000 GPD | FilmTec NF90 Element,” *wateranywhere*, 2021. <https://wateranywhere.com/4-x40-97-salt-rejection-2-000-gpd-filmtec-nf90-element/>
- [59] DC GAP LTD, “Q-Cells QPEAK DUO XL G11.7 570Wp,” *DC GAP LTD*, 2022. <https://www.dc-gap.com/product/q-cells-qpeak-duo-xl-g11-7/>
- [60] Tandem Solar Systems, “Hanwha Q-Cells QPEAKDUO XL-G11/BFG 580W,” *Tandem Solar Systems*, 2020. <https://tandem-solar-systems.com/product/hanwha-q-cells-qpeakduo-xl-g11bfg-580w/>
- [61] mg-solar-shop, “mg solar,” *mg solar*, 2023. <https://www.mg-solar-shop.com>
- [62] D. Akgul, M. Çakmakcı, N. Kayaalp, and I. Koyuncu, “Cost analysis of seawater desalination with reverse osmosis in Turkey,” *Desalination*, vol. 220, no. 1–3, pp. 123–131, Mar. 2008, doi: 10.1016/j.desal.2007.01.027.
- [63] V. N. X. Que, D. V. Tuan, N. N. Huy, and V. L. Phu, “Design and performance of small-scale reverse osmosis desalination for brackish water powered by photovoltaic units: a review,” *IOP Conf. Ser.: Earth Environ. Sci.*, vol. 652, no. 1, p. 012024, Feb. 2021, doi: 10.1088/1755-1315/652/1/012024.
- [64] OTE, a.s., “Zbytkový energetický mix,” *OTE*, 2022. <https://www.ote-cr.cz/cs/statistika/zbytkovy-energeticky-mix>
- [65] G. Raluy, L. Serra, and J. Uche, “Life cycle assessment of MSF, MED and RO desalination technologies,” *Energy*, vol. 31, no. 13, pp. 2361–2372, Oct. 2006, doi: 10.1016/j.energy.2006.02.005.
- [66] H. Ettouney, “Design of single-effect mechanical vapor compression,” *Desalination*, vol. 190, no. 1–3, pp. 1–15, Apr. 2006, doi: 10.1016/j.desal.2005.08.003.
- [67] European Commission, Directorate-General for Energy, Badouard, T., Bon Mardion, J., Bovy, P. et al., “Study on energy subsidies and other government interventions in the European Union - Final Report: 2022 edition.” Publications Office of the European Union, 2022. [Online]. Available: <https://data.europa.eu/doi/10.2833/304199>
- [68] W. Lawler, J. Alvarez-Gaitan, G. Leslie, and P. Le-Clech, “Comparative life cycle assessment of end-of-life options for reverse osmosis membranes,” *Desalination*, vol. 357, pp. 45–54, Feb. 2015, doi: 10.1016/j.desal.2014.10.013.
- [69] H. Cherif, G. Champenois, and J. Belhadj, “Environmental life cycle analysis of a water pumping and desalination process powered by intermittent renewable energy sources,” *Renewable and Sustainable Energy Reviews*, vol. 59, pp. 1504–1513, Jun. 2016, doi: 10.1016/j.rser.2016.01.094.

- [70] Y. Xu, J. Li, Q. Tan, A. L. Peters, and C. Yang, “Global status of recycling waste solar panels: A review,” *Waste Management*, vol. 75, pp. 450–458, May 2018, doi: 10.1016/j.wasman.2018.01.036.
- [71] M. Herrando, D. Elduque, C. Javierre, and N. Fueyo, “Life Cycle Assessment of solar energy systems for the provision of heating, cooling and electricity in buildings: A comparative analysis,” *Energy Conversion and Management*, vol. 257, p. 115402, Apr. 2022, doi: 10.1016/j.enconman.2022.115402.
- [72] D. Landi, M. Marconi, and G. Pietroni, “Comparative life cycle assessment of two different battery technologies: lithium iron phosphate and sodium-sulfur,” *Procedia CIRP*, vol. 105, pp. 482–488, 2022, doi: 10.1016/j.procir.2022.02.080.
- [73] R. B. Kaunda, “Potential environmental impacts of lithium mining,” *Journal of Energy & Natural Resources Law*, vol. 38, no. 3, pp. 237–244, Jul. 2020, doi: 10.1080/02646811.2020.1754596.
- [74] D. Dong, L. van Oers, A. Tukker, and E. van der Voet, “Assessing the future environmental impacts of copper production in China: Implications of the energy transition,” *Journal of Cleaner Production*, vol. 274, p. 122825, Nov. 2020, doi: 10.1016/j.jclepro.2020.122825.
- [75] V. Muteri *et al.*, “Review on Life Cycle Assessment of Solar Photovoltaic Panels,” *Energies*, vol. 13, no. 1, p. 252, Jan. 2020, doi: 10.3390/en13010252.
- [76] “Wind and solar were EU’s top electricity source in 2022 for first time ever,” *Carbon Brief*, 2023. <https://www.carbonbrief.org/wind-and-solar-were-eus-top-electricity-source-in-2022-for-first-time-ever/>
- [77] Sam Wigness, “What is the Carbon Footprint of Solar Panels?,” *solar.com*, Feb. 07, 2023. <https://www.solar.com/learn/what-is-the-carbon-footprint-of-solar-panels/?fbclid=IwAR2x2T1t6sfIcFDFATBpJ0mjExobw8EtKtUVi-D6AdD1smSRNXHo9Ygp544>
- [78] A. Louwen, W. G. J. H. M. van Sark, A. P. C. Faaij, and R. E. I. Schropp, “Re-assessment of net energy production and greenhouse gas emissions avoidance after 40 years of photovoltaics development,” *Nat Commun*, vol. 7, no. 1, p. 13728, Dec. 2016, doi: 10.1038/ncomms13728.

Appendix 1 AMI M-S4040A Datasheet

AMI[®] MEMBRANES

Seawater Desalination RO Membrane Elements

AMI high rejection and high productivity seawater reverse osmosis membranes are specially designed for marine applications. AMI SWRO membranes are ideal for seawater desalination in shipboard applications, watermakers, land-based desalinators and sea-based desalinators.



PERFORMANCE SPECIFICATIONS

Model No.	Permeate Flow Rate		Size (Dia. " × Length")	Single Element Recovery (%)	Minimum Salt Rejection (%)	Stabilized Salt Rejection (%)
	gpd	m ³ /day				
M-S2514A	150	0.57	2.5 × 14	2	99.4	99.6
M-S2521A	300	1.14	2.5 × 21	4	99.4	99.6
M-S2540A	700	2.65	2.5 × 40	8	99.4	99.6
M-S4014A	350	1.32	4.0 × 14	2	99.4	99.6
M-S4021A	800	3.03	4.0 × 21	4	99.4	99.6
M-S4040A	1950	7.38	4.0 × 40	8	99.4	99.6

Note: Performance specifications based on 32,000 mg/l sodium chloride, 800 psi (5.5 MPa) applied pressure, 77°F (25°C) feed water temperature, pH 8 and the recovery listed in the table above. Element permeate flow may vary ± 20%.

RECOMMENDED OPERATING CONDITIONS

◆ Maximum Operating Pressure	1,000 psig (6.9MPa)	◆ Maximum Feed Flow Rate	
◆ Maximum Operating Temperature	113°F (45°C)	○ 2.5" Dia. Elements	6 gpm
◆ Maximum Feed water SDI (15 min)	5	○ 4" Dia. Elements	16 gpm
◆ Chlorine Tolerance	0	◆ Feed water pH Range (Continuous)	2-11
◆ Maximum Pressure Drop:	15psig (1 bar)	◆ Feed water pH Range (Cleaning – 30 min.)	1-13



MEMBRANE ELEMENT DIMENSIONS

Model No.	L		I		D	
	inches	centimeters	inches	centimeters	inches	centimeters
M-S2514A	14	35.6	11.62	30	2.5	6.4
M-S2521A	21	53.3	19	48	2.5	6.4
M-S2540A	40	101.6	38	96	2.5	6.4
M-S4014A	14	35.6	12	30	3.9	9.9
M-S4021A	21	53.3	19	48	3.9	9.9
M-S4040A	40	101.6	38	96	3.9	9.9

EM[®] EFFLUED MEMBRANES INC.[®] EFFLUED[®] ARE TRADEMARKS OF APPLIED MEMBRANES, INC. © 2022

APPLIED
MEMBRANES INC.[®]

(760) 727-3711 www.appliedmembranes.com sales@appliedmembranes.com

Appendix 2 Danfoss APP High Pressure Pump Datasheet Pages



Data sheet

APP 0.6-43 / APP (W) 5.1-10.2 pumps

4.3 APP (W) 5.1-10.2

Pump size		APP (W) 5.1	APP (W) 6.5	APP (W) 7.2	APP (W) 8.2	APP (W) 10.2
Code number APP		180B3005	180B3006	180B3007	180B3008	180B3010
Code number APP W		180B3075	180B3076	180B3077	180B3078	180B3080
Geometric displacement	cm ³ /rev.	50.2	63.3	70.3	80.4	100.5
	in ³ /rev.	3.06	3.86	4.29	4.91	6.13
Pressure						
Max. outlet ¹⁾ pressure continuous	barg	80	80	80	80	80
	psig	1160	1160	1160	1160	1160
Min. outlet ¹⁾ pressure	barg	20	20	20	20	20
	psig	290	290	290	290	290
Inlet pressure ¹⁾ continuous	barg	0.5 - 5	0.5 - 5	0.5 - 5	0.5 - 5	0.5 - 5
	psig	7.3 - 72.5	7.3 - 72.5	7.3 - 72.5	7.3 - 72.5	7.3 - 72.5
Max. inlet pressure peak	barg	5	5	5	5	5
	psig	72.5	72.5	72.5	72.5	72.5
Speed						
Min. speed continuous	rpm	700	700	700	700	700
Max. speed ²⁾ continuous	rpm	1800	1800	1800	1800	1800
Typical flow - Flow curves available in Item 5						
1000 rpm at max. pressure	m ³ /h	2.79	3.57	4.01	4.62	5.83
1500 rpm at max. pressure	m ³ /h	4.19	5.36	6.01	6.93	8.75
1200 rpm at max. pressure	gpm	14.75	18.87	21.16	24.39	30.82
1800 rpm at max. pressure	gpm	22.13	28.31	31.74	36.59	46.23
Typical motor size						
1800 rpm at max. pressure	kW	15.0	18.5	22.0	22.0	30.0
1200 rpm at max. pressure	hp	20.0	20.0	20.0	20.0	25.0
Torque at max. outlet pressure	Nm	70.27	88.61	98.41	112.55	140.69
	lb-ft	51.83	65.36	72.58	83.01	103.77
Media ³⁾ temperature	°C	2 - 50	2 - 50	2 - 50	2 - 50	2 - 50
	°F	35.6 - 122	35.6 - 122	35.6 - 122	35.6 - 122	35.6 - 122
Ambient temperature	°C	0 - 50	0 - 50	0 - 50	0 - 50	0 - 50
	°F	32 - 122	32 - 122	32 - 122	32 - 122	32 - 122
Sound ⁴⁾ pressure level	dB(A)	78	78	78	78	78
Weight	kg	30	30	30	30	30
	lb	66	66	66	66	66

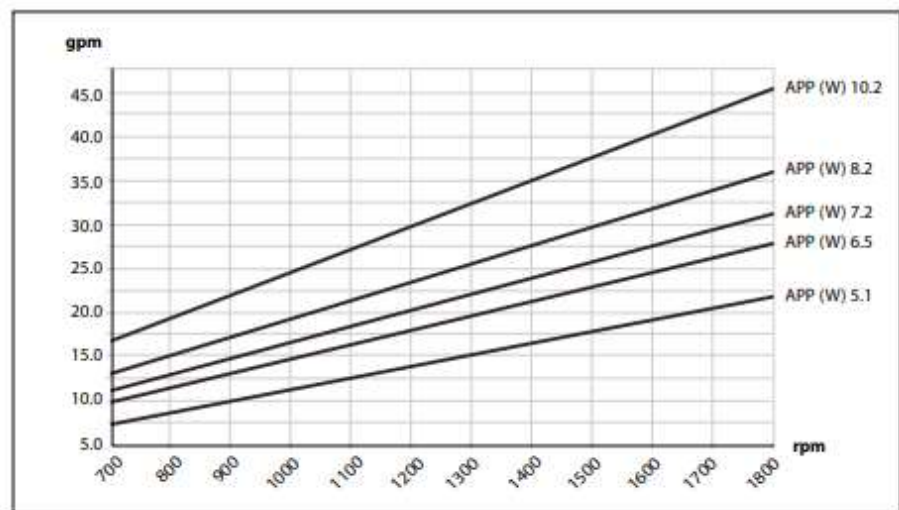
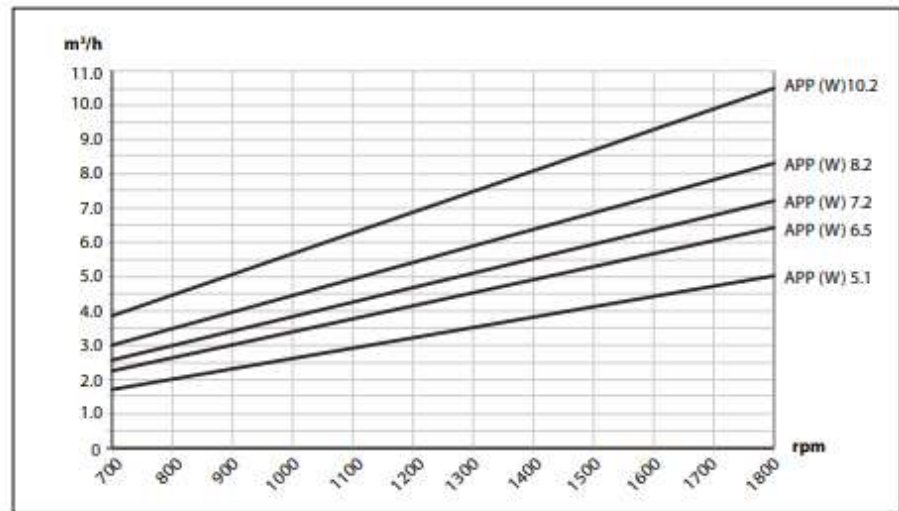
¹⁾ For lower and higher pressure, please contact Danfoss.

²⁾ For speeds above 1500 rpm the pump must be boosted at a pressure of 1-5 barg (14.5 - 72.5 psig).

³⁾ Dependent on the NaCl concentration.

⁴⁾ Measurements according to EN ISO 3744:2010 / dB(A)[L_{WA,1m}] values are calculated. Measured at max pressure and rpm for a motor pump unit.

5.3 APP (W) 5.1-10.2 flow curves at 80 barg (1160 psig)





Data sheet | APM 0.8 – 2.9 motors

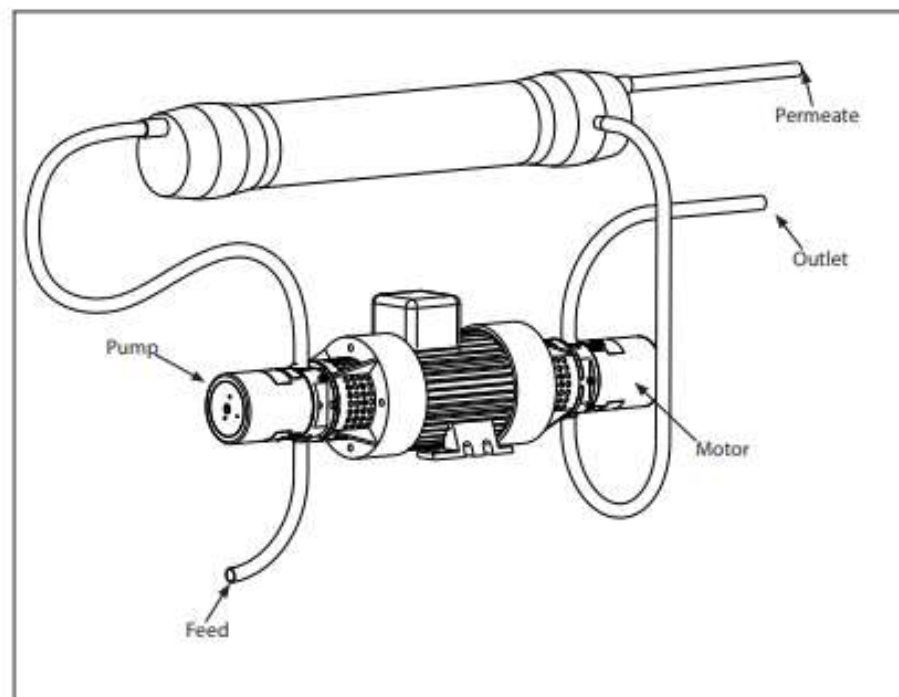
3.2 APM 1.8 – 2.9

Motor size		APM 1.8	APM 2.0	APM 2.5	AMP 2.9
Code number APM CCW		180F1100	180F1101	180F1102	180F1103
Geometric displacement	cm ³ /rev.	9.31	10.0	12.5	15.3
	in ³ /rev.	0.57	0.61	0.76	0.93
Pressure					
Max. inlet pressure continuous	barg	80	80	80	80
	psig	1160	1160	1160	1160
Min. inlet pressure continuous	barg	10	10	10	10
	psig	145	145	145	145
Outlet pressure	barg	0.5 – 5	0.5 – 5	0.5 – 5	0.5 – 5
	psig	7.3 – 72.5	7.3 – 72.5	7.3 – 72.5	7.3 – 72.5
Speed					
Min. speed	rpm	700	700	700	700
Max. speed continuous	rpm	3450	3450	3450	3000
Typical performance					
Max. waterflow	m ³ /h	2.03	2.18	2.69	2.83
	l/min	33.9	36.4	44.8	47.2
	gpm	9.0	9.6	11.8	12.5
Max. power at max. speed cont. and max. pressure	kW	3.9	4.2	5.3	5.6
	HP	5.2	5.7	7.1	7.6
Max. torque at max. pressure	Nm	10.8	11.7	14.7	18.0
	lbf-ft	8.0	8.6	10.8	13.2
Technical specifications					
Sound pressure level	dB(A)	77	77	77	81
Media temperature	°C	2 – 50	2 – 50	2 – 50	2 – 50
	°F	35.6 – 122	35.6 – 122	35.6 – 122	35.6 – 122
Ambient temperature	°C	0 – 50	0 – 50	0 – 50	0 – 50
	°F	32 – 122	32 – 122	32 – 122	32 – 122
Weight (dry)	kg	8.6	8.6	8.6	8.6
	lb	19	19	19	19

11. Preferred system design

APM is used for energy recovery unit which consists of an APP pump and an APM motor, both connected to a double shafted electric motor. Energy recovery is obtained when high-pressure brine from the membranes is fed to the APM that converts the energy in the pressurized brine to mechanical energy to be reused by the electric motor. As the APM has a fixed volumetric displacement, the recovery rate will be fixed.

System example



Appendix 4 Grundfos Pump Curves Tool Results

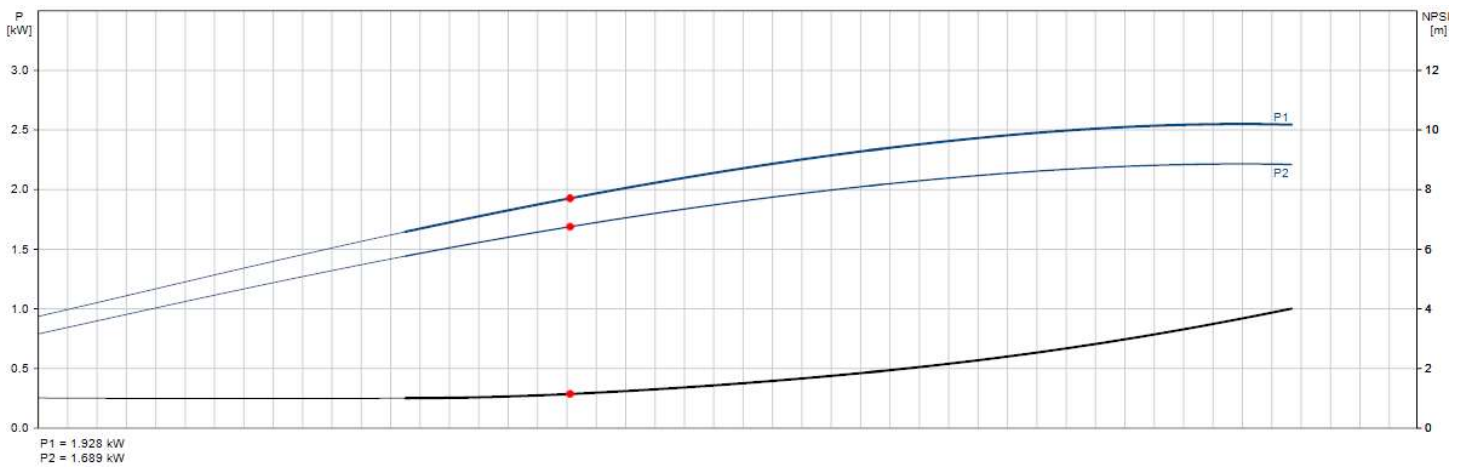
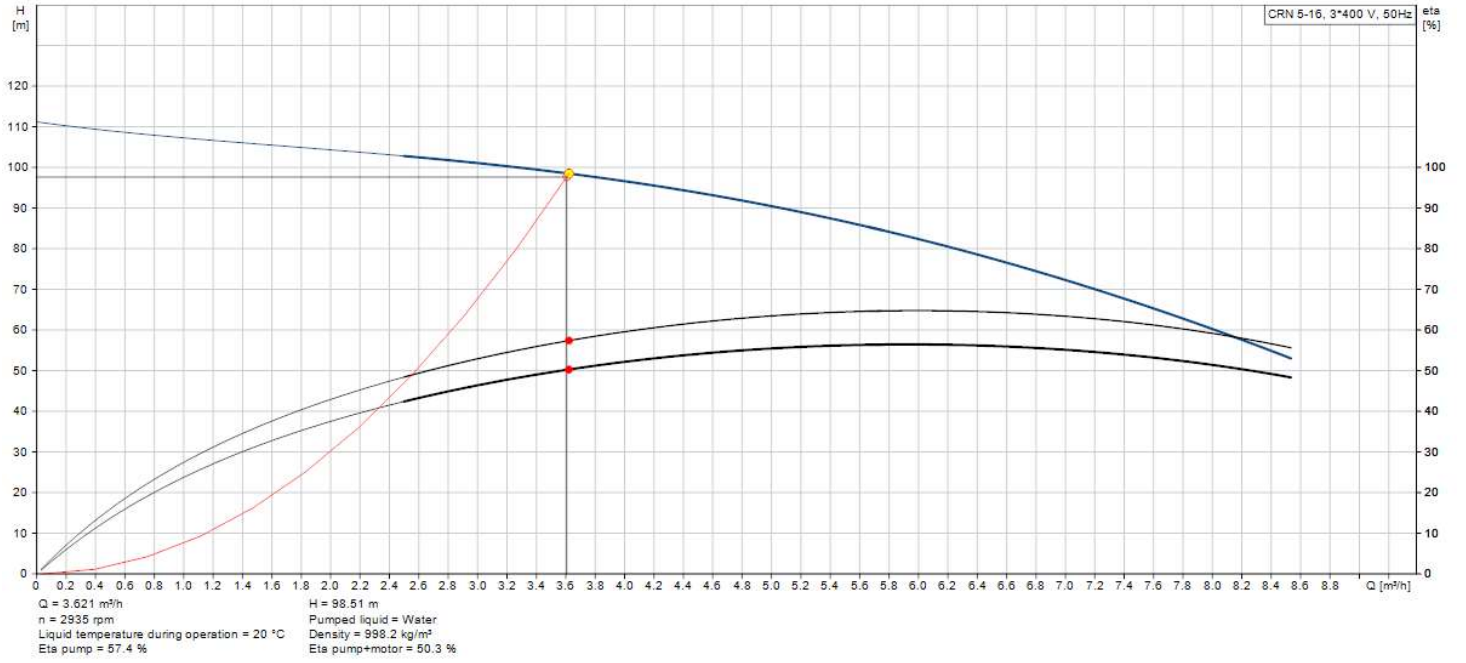


TABLE 4

COMPARISON OF BRINE PROPERTIES AT SEVERAL SALT PERCENTAGES
AND SELECTED TEMPERATURES

Weight Percent Salt	T, °F	Saturation Pressure, PSIA			Liquid Density, LBM/FT ³			Sat. Liquid Enthalpy, BTU/LBM					Sat. Liquid Entropy, BTU/LBM-°R	
		Ref. 2	Ref. 3	PSATB(T)	Ref. 2	Ref. 3	RHOB(T)	Ref. 2	Ref. 4	Ref. 5	HB(T)	Ref. 4	SB(T)	
5	200	11.3	11.6	11.2	62.2	62.3	64.0	154	162	161	158	.2831	.2712	
	400	241.7	240.8	239.6	56.2	56.1	55.3	335	355	360	365	.5477	.5413	
	600	-	1496.8	1495.1	-	45.9	46.8	-	-	592	590	-	.7745	
10	200	10.9	11.2	10.8	64.5	64.5	65.9	141	156	155	153	.2739	.2619	
	400	235.4	232.1	231.0	58.7	58.6	58.2	301	340	345	345	.5163	.5156	
	600	-	1438.8	1441.1	-	49.6	50.4	-	-	567	557	-	.7319	
15	200	10.4	10.2	10.3	67.0	66.5	67.9	132	151	148	150	.2659	.2569	
	400	221.7	221.9	221.1	61.3	61.1	60.9	277	322	330	331	.4950	.4954	
	600	-	1373.5	1379.4	-	53.2	54.0	-	-	541	525	-	.6959	
20	200	9.8	10.2	9.8	69.5	69.1	69.8	126	147	141	145	.2582	.2505	
	400	210.8	210.3	209.5	63.8	63.7	63.4	265	312	315	315	.4758	.4761	
	600	-	1303.9	1306.8	-	56.8	57.0	-	-	516	499	-	.6638	
25	200	9.3	9.7	9.2	72.0	71.6	71.8	124	142	134	140	.2511	.2452	
	400	198.1	197.3	196.4	66.6	66.1	65.8	256	300	300	303	.4591	.4599	
	600	-	1232.8	1225.1	-	60.2	59.9	-	-	491	476	-	.6369	

Q.PEAK DUO XL-G11 SERIES



570 - 585 Wp | 156 Cells
21.4 % Maximum Module Efficiency

MODEL: Q.PEAK DUO XL-G11.3/BFG



Bifacial energy yield gain of up to 20 %

Bifacial Q.ANTUM solar cells make efficient use of light shining on the module rear-side for radically improved LCOE.



Low electricity generation costs

Q.ANTUM DUO Z combines cutting edge cell separation and innovative wiring with Q.ANTUM Technology for higher yield per surface area, lower BOS costs, higher power classes, and an efficiency rate of up to 21.4%.



A reliable investment

Double glass module design enables extended lifetime with 12-year product warranty and improved 30-year performance warranty¹.



Enduring high performance

Long-term yield security with Anti LeTID and Anti PID Technology², Hot-Spot Protect.



Frame for versatile mounting options

High-tech aluminum alloy frame protects from damage, enables use of a wide range of mounting structures and is certified regarding IEC for high snow (5400 Pa) and wind loads (2400 Pa).



Innovative all-weather technology

Optimal yields, whatever the weather with excellent low-light and temperature behavior.

¹ See data sheet on rear for further information.

² APT test conditions according to IEC/TS 62904-1:2015 method B (~1500V, 168h) including post-treatment according to IEC 6215-1: Ed. 2.0 (CD)

The ideal solution for:



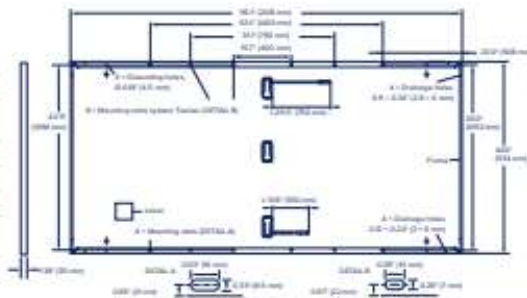
Ground mounted solar panels



Q.PEAK DUO XL-G11 SERIES

Mechanical Specification

Format	55.1in x 44.7in x 1.38in (including frame) (2416mm x 1134mm x 35mm)
Weight	75.8lbs (34.4kg)
Front Cover	0.08in (2mm) thermally pre-stressed glass with anti-reflection technology
Back Cover	0.08in (2mm) semi-tempered glass
Frame	Anodized aluminum
Cell	5 x 26 monocrystalline Q.ANTUM solar half cells
Junction box	2.09-3.98 x 1.26-2.36 x 0.59-0.71in (53-101mm x 32-60mm x 15-18mm), Protection class IP67, with bypass diodes
Cable	4mm ² Solar cable, (+) >29.5in (750mm), (-) >13.8in (350mm)
Connector	Stäubli MC4; Stäubli MC4-Evo2; - IPE8



Electrical Characteristics

POWER CLASS	570	575	580	585
-------------	-----	-----	-----	-----

MINIMUM PERFORMANCE AT STANDARD TEST CONDITIONS, STC¹ (POWER TOLERANCE +5W/-0W)

			B570		B575		B580		B585	
			Minimum	BSTC ²	Minimum	BSTC ²	Minimum	BSTC ²	Minimum	BSTC ²
Power at MPP ¹	P_{MPP} [W]	570	623.5	575	629.0	580	634.4	585	639.9	
Short Circuit Current ¹	I_{SC} [A]	13.50	14.77	13.52	14.80	13.55	14.83	13.57	14.86	
Open Circuit Voltage ¹	V_{OC} [V]	53.50	53.69	53.53	53.72	53.56	53.75	53.59	53.78	
Current at MPP	I_{MPP} [A]	12.83	14.03	12.87	14.09	12.92	14.14	12.97	14.19	
Voltage at MPP	V_{MPP} [V]	44.44	44.43	44.66	44.65	44.88	44.87	45.10	45.09	
Efficiency ¹	η [%]	>20.8		>21.0		>21.2		>21.4		

Efficiency of P_{MPP} and I_{SC} : 70% ± 5% • Bifaciality given for rear side irradiation on top of STC (front side) • According to IEC 60904-2

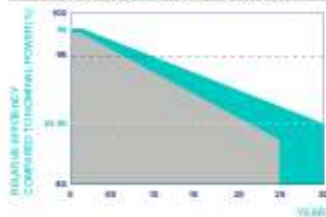
¹ Measurement tolerances P_{MPP} ± 3%; I_{SC} , V_{OC} ± 5% at STC: 1000 W/m², ² at BSTC: 1000 W/m² + ϕ = 135 W/m², ϕ = 70% ± 5%, 25 ± 2°C, AM 1.5 according to IEC 60904-3

MINIMUM PERFORMANCE AT NORMAL OPERATING CONDITIONS, NMOT²

		570	575	580	585
Power at MPP	P_{MPP} [W]	429.1	432.9	436.6	440.4
Short Circuit Current	I_{SC} [A]	10.87	10.89	10.91	10.93
Open Circuit Voltage	V_{OC} [V]	50.60	50.63	50.66	50.68
Current at MPP	I_{MPP} [A]	10.09	10.14	10.18	10.22
Voltage at MPP	V_{MPP} [V]	42.51	42.71	42.89	43.08

² 800 W/m², NMOT, spectrum AM 1.5

Qcells PERFORMANCE WARRANTY

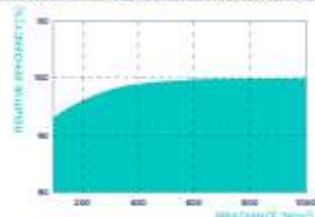


At least 98% of nominal power during first year. Thereafter max. 0.45% degradation per year. At least 93.95% of nominal power up to 10 years. At least 84.95% of nominal power up to 30 years.

All data within measurement tolerances. Full warranties in accordance with the warranty terms of the Qcells sales organisation of your respective country.

*Standard terms of guarantee for the 5 PV companies with the highest production capacity in 2021 (February 2021)

PERFORMANCE AT LOW IRRADIANCE



Typical module performance under low irradiance conditions in comparison to STC conditions (25°C, 1000W/m²)

TEMPERATURE COEFFICIENTS

Temperature Coefficient of I_{SC}	α [%/K]	+0.04	Temperature Coefficient of V_{OC}	β [%/K]	-0.27
Temperature Coefficient of P_{MPP}	γ [%/K]	-0.34	Nominal Module Operating Temperature	NMOT (°F)	109 ± 5.4 (43 ± 3°C)

Properties for System Design

Maximum System Voltage	V_{MS} [V]	1500	PV module classification	Class II
Maximum Series Fuse Rating	[A DC]	25	Fire Rating based on ANSI / UL 61730	TYPE 2 ¹
Max. Design Load, Push/Pull ²	[lbs/ft ²] / [kg/m ²]	75 (3500 Pa) / 33 (1600 Pa)	Permitted Module Temperature on Continuous Duty	-40°F up to +185°F (-40°C up to +85°C)
Max. Test Load, Push/Pull ³	[lbs/ft ²] / [kg/m ²]	113 (5400 Pa) / 50 (2400 Pa)		

¹ See Installation Manual

² New Type is similar to Type 3 but with metallic frame

Qualifications and Certificates

UL 61730, CE-compliant, IEC 61215-2016, IEC 61730-2016, U.S. Patent No. 9,893,315 (solar cells)



Qcells pursues minimizing paper output in consideration of the global environment.

Note: Installation instructions must be followed. Contact our technical service for further information on approved installation of this product.
 Technical & Sales Assistance: 430 Spectrum Center Drive, Suite 1603, Irvine, CA 92618, USA | TEL: +1 949 748 59 95 | EMAIL: help-enquiry@qcells.com | WEB: www.qcells.com

qcells

Three Phase Inverter with Synergy Technology

For 220V/230V Line to Line Grids

SE50K / SE66.6K / SE90K / SE100K

Applicable to Inverter with Part Number	SExxK-xxx01xxx				
	SE50K	SE66.6K	SE90K	SE100K	
OUTPUT					
Rated AC Active Output Power	29000	38450	51900	57700	W
Maximum AC Apparent Output Power	29000	38450	51900	57700	VA
AC Output Voltage — Line to Line / Line to Neutral (Nominal)	220 / 127 ; 230 / 133				Vac
AC Output Voltage — Line to Line Range	176 - 253 / 184 - 264.5				Vac
AC Frequency	50/60 ± 5%				Hz
Maximum Continuous Output Current (per Phase)	72.5	96.5	130.5	145	Aac
AC Output Line Connections	3W + PE (Corner grounded not supported), 4W + PE				
Supported Grids	WYE: TN-C, TN-S, TN-C-S, TT, IT; Delta: IT				
Maximum Residual Current Injection ⁽¹⁾	200		300		mA
Utility Monitoring, Islanding Protection, Configurable Power Factor, Country Configurable Thresholds	Yes				
Total Harmonic Distortion	≤ 3				
Power Factor Range	+/-0.2 to 1				
INPUT					
Maximum DC Power (Module STC) Inverter / Synergy Unit	50750 / 25375	67280 / 33640	90825 / 30275	100975 / 33650	W
Transformer-less, Ungrounded	Yes				
Maximum Input Voltage DC+ to DC-	600				
Operating Voltage Range	370 - 600				
Maximum Input Current	2 x 36.25	2 x 48.25	3 x 43.5	3 x 48.25	Adc
Reverse-Polarity Protection	Yes				
Ground-Fault Isolation Detection	167kΩ Sensitivity per Synergy Unit ⁽²⁾				
Maximum Inverter Efficiency	98.3				
European Weighted Efficiency	98				
Nighttime Power Consumption	< 8		< 12		W
ADDITIONAL FEATURES					
Supported Communication Interfaces ⁽³⁾	2 x RS485, Ethernet, Wi-Fi (optional), Cellular (optional)				
Smart Energy Management	Export Limitation				
Inverter Commissioning	With the SetApp mobile application using built-in Wi-Fi access point for local connection				
Arc Fault Protection	Built-in, User Configurable (According to UL1699B)				
Rapid Shutdown	Optional (automatic upon AC Grid Disconnect)				
PID Rectifier	Nighttime, built-in				
RS485 Surge Protection (ports 1 + 2)	Type II, field replaceable, integrated				
DC Surge Protection	Type II, field replaceable, integrated				
AC Surge Protection	Type II, field replaceable, optional				
DC Fuses (Single Pole)	25A, optional				
DC Disconnect Switch	Optional				
STANDARD COMPLIANCE					
Safety	IEC-62109-1, IEC-62109-2, AS3100				
Grid Connection Standards ⁽⁴⁾	EN50549-1, EN50549-2, VDE-AR-N 4105, VDE-AR-N 4110, VDE V 0126-1-1, CEI 0-21, CEI 0-16, TOR Erzeuger Typ A+B, G99 Type A+B, G99 (NI) Type A+B, VFR 2019				
Emissions	IEC61000-6-2, IEC61000-6-3 Class A, IEC61000-3-11, IEC61000-3-12				
RoHS	Yes				

(1) If an external RCD is required, its trip value must be ≥ 200mA for SE50K/SE66.6K, ≥ 300mA for SE90K, SE100K

(2) Where permitted by local regulations







(3) For specifications of the optional communication options, visit <https://www.solaredge.com/products/communication> or the Resource Library webpage:

<https://www.solaredge.com/resource-library>, to download the relevant product datasheet

(4) For all standards and certificates download, refer to Certifications category on the Resource Library webpage: <https://www.solaredge.com/resource-library>

Appendix 8 BYD Battery-Box Datasheet Page

TECHNICAL PARAMETERS PREMIUM LVS

						
	LVS 4.0	LVS 8.0	LVS 12.0	LVS 16.0	LVS 20.0	LVS 24.0
Battery Module	LVS (4 kWh, 51.2 V, 45 kg)					
Number of Modules	1	2	3	4	5	6
Usable Energy [1]	4 kWh	8 kWh	12 kWh	16 kWh	20 kWh	24 kWh
Max Cont. Output Current [2]	65 A	130 A	195 A	250 A	250 A	250 A
Peak Output Current [2]	90 A, 5 s	180 A, 5 s	270 A, 5 s	360 A, 5 s	360 A, 5 s	350 A, 5 s
Dimensions (H/W/D)	478 x 650 x 298 mm	711 x 650 x 298 mm	944 x 650 x 298 mm	1177 x 650 x 298 mm	1410 x 550 x 298 mm	1643 x 650 x 298 mm
Weight:	64 kg	109 kg	154 kg	199 kg	244 kg	289 kg
Nominal Voltage	51.2 V					
Operating Voltage	40-57,6 V					
Operating Temperature	-10 °C to +50°C					
Battery Cell Technology	Lithium iron Phosphate (cobalt-free)					
Communication	CAN / RS485					
Enclosure Protection Rating	IP55					
Round-Trip Efficiency	≥95%					
Scalability [3]	Max. 64 Modules in Parallel (256 kWh)				Single Tower Only	
Certification	VDE2510-50 / IEC62619 / CE / CEC / UN38.3					
Applications	ON Grid / ON Grid + Backup / OFF Grid					
Warranty [4]	10 Years					
Compatible Inverters	Refer to BYD Battery-Box Premium LVS Minimum Configuration List.					
Rated DC power	3.3kW	6.7kW	10.0kW	12.8kW	12.8kW	12.8kW
Short Circuit Current	2300A					

[1] DC Usable Energy, Test conditions: 100% DOD, 0.2C charge & discharge at +25 °C. System Usable Energy may vary with different inverter brands.

[2] Charge derating will occur between -10 °C and +5 °C.

[3] Parallel tower function only available for 1 to 4 battery modules per tower. LVS 20.0 and LVS 24.0 can only be used as a single tower.

[4] Conditions apply. Refer to BYD Battery-Box Premium Limited Warranty Letter.



BYD Company Limited
www.bydbatterybox.com
Global Sales: batteryboxgrp@byd.com
Global Service: bbboxservice@byd.com

Battery-Box EU Service Partner
EFT-Systems GmbH
www.eft-systems.de
service@eft-systems.de

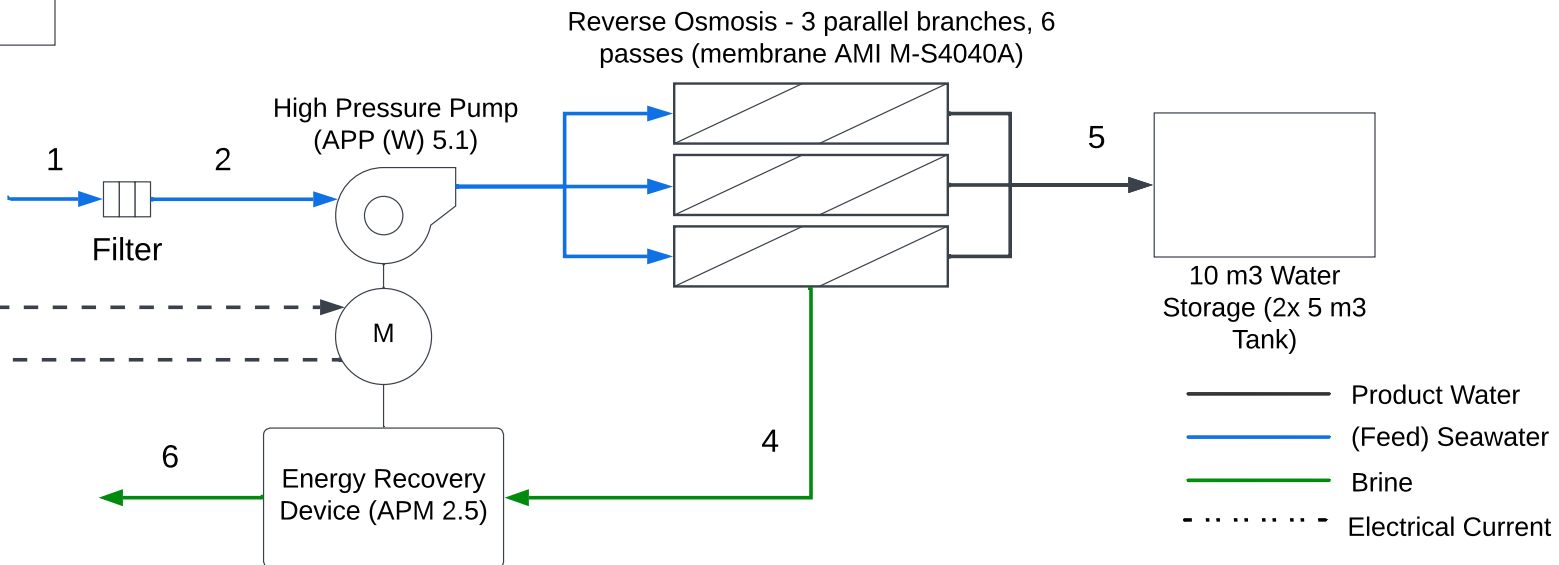
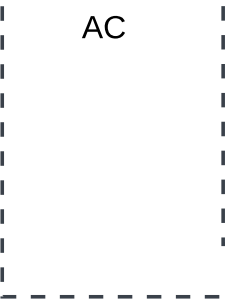
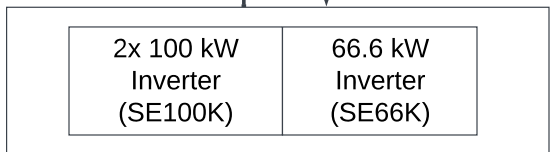
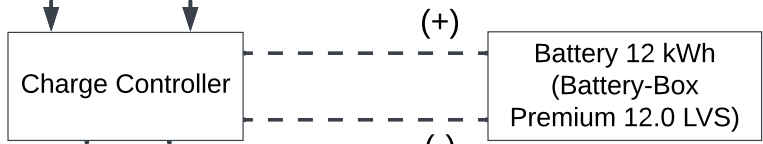
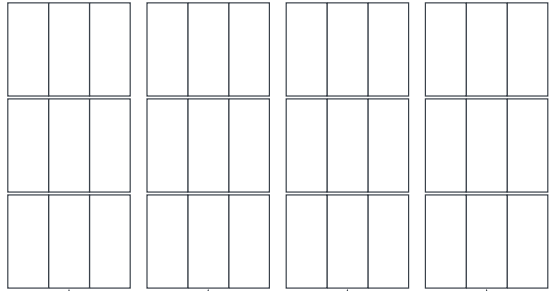
Battery-Box AU Service Partner
Alps Power Pty Ltd
www.alpspower.com.au
service@alpspower.com.au

Battery-Box US Service Partner
EFT-Systems GmbH
www.eft-systems.de/us
USservice@eft-systems.de

v2.0



208.8 kWp PV Field
36x PV panel (Q.PEAK DUO XL-G11S 580 kWp)



- Product Water
- (Feed) Seawater
- Brine
- - - - - Electrical Current

Material Balance				
Stream	M [kg/h]	V [m ³ /h]	Xc [g/kg]	X [ppm]
1	4,213.0	4.12	35.00	35,000
2	4,213.0	4.12	35.00	35,000
3	4,213.0	4.12	35.00	35,000
4	2,375.4	2.27	61.84	61,844
5	1,837.6	1.85	0.30	300
6	2,375.4	2.27	61.84	61,844

Energy Requirements			
Device (equipment)	Electrical Power Input [kW]	Energy Consumption [MWh/day]	Energy Consumption [MWh/year]
High Pressure Pump	15	0.180	63.9
Energy Recovery Device	-5.3	-0.064	-22.578
Other	0.3	0.004	1.278
Total	10	0.12	42.6

PV System			
peak power output	208.8	kWp	
number of panels	36	-	
field surface area	95.0	m ²	
inverter power output	269.2	kW	
battery capacity	12	kWh	

Project:	Design of Autonomous Desalination Unit
Project Type:	Master's Thesis
Drawing Name:	Appendix 9 Scheme of Variant A: RO Desalination Unit
Author:	Bc. Michael Kijanica
Date:	26.05.2023